

Cosmological perturbation theory for baryons and dark matter I: one-loop corrections in the RPT framework

Gábor Somogyi^{1,2,*} and Robert E. Smith^{2,†}

¹*Deutsches Elektronensynchrotron DESY, Platanenallee 6, D-15738 Zeuthen, Germany*

²*Institute for Theoretical Physics, University of Zurich, CH-8037 Zurich, Switzerland*

(Dated: February 22, 2019)

We generalize the “renormalized” perturbation theory (RPT) formalism of Crocce and Scoccimarro [1] to deal with multiple fluids in the Universe and here we present the complete calculations up to the one-loop level in the RPT. We apply this approach to the problem of following the non-linear evolution of baryon and cold dark matter (CDM) perturbations, evolving from the distinct sets of initial conditions, from the high redshift post-recombination Universe right through to the present day. In current theoretical and numerical models of structure formation, it is standard practice to treat baryons and CDM as an effective single matter fluid – the so called dark matter only modeling. In this approximation, one uses a weighed sum of late time baryon and CDM transfer functions to set initial mass fluctuations. In this paper we explore whether this approach can be employed for high precision modeling of structure formation. We show that, even if we only follow the linear evolution, there is a large-scale scale-dependent bias between baryons and CDM for the currently favored WMAP5 Λ CDM model. This time evolving bias is significant ($> 1\%$) until the present day, when it is driven towards unity through gravitational relaxation processes. Using the RPT formalism we test this approximation in the non-linear regime. We show that the non-linear CDM power spectrum in the 2-component fluid differs from that obtained from an effective mean-mass 1-component fluid by $\sim 3\%$ on scales of order $k \sim 0.05 h \text{ Mpc}^{-1}$ at $z = 10$, and by $\sim 0.5\%$ at $z = 0$. However, for the case of the non-linear evolution of the baryons the situation is worse and we find that the power spectrum is suppressed, relative to the total matter, by $\sim 15\%$ on scales $k \sim 0.05 h \text{ Mpc}^{-1}$ at $z = 10$, and by $\sim 3 - 5\%$ at $z = 0$. Importantly, besides the suppression of the spectrum, the Baryonic Acoustic Oscillation (BAO) features are amplified for baryon and slightly damped for CDM spectra. If we compare the total matter power spectra in the 2- and 1-component fluid approaches, then we find excellent agreement, with deviations being $< 0.5\%$ throughout the evolution. Consequences: high precision modeling of the large-scale distribution of baryons in the Universe can not be achieved through an effective mean-mass 1-component fluid approximation; detection significance of BAO will be amplified in probes that study baryonic matter, relative to probes that study the CDM or total mass only. The CDM distribution can be modeled accurately at late times and the total matter at all times. This is good news for probes that are sensitive to the total mass, such as gravitational weak lensing as existing modeling techniques are good enough. Lastly, we identify an analytic approximation that greatly simplifies the evaluation of the full PT expressions, and it is better than $< 1\%$ over the full range of scales and times considered.

I. INTRODUCTION

In the current paradigm for structure formation in the Universe, it is supposed that there was an initial period of inflation, during which, quantum fluctuations were generated and inflated up to super-horizon scales; producing a near scale-invariant and near Gaussian set of primordial potential fluctuations. At the end of inflation the Universe is reheated, and particles and radiation are synthesized. In this hot early phase, cold thermal relics are also produced, these particles interact gravitationally and possibly through the weak interaction – dubbed Cold Dark Matter (CDM). Prior to recombination photons are coupled to electrons through Thompson scattering, and in turn electrons to baryonic nuclei through the Coulomb interaction. Baryon fluctuations are pressure supported on scales smaller than the sound horizon scale. Subsequent to recombination photons free-stream out of perturbations and baryons cool into the CDM potential wells. Structure formation then proceeds in a hierarchical way with small objects collapsing first and then merging to form larger objects. Eventually, sufficiently dense gas wells are accumulated and galaxies form. At late times the Universe switches from a decelerating phase of expansion to an accelerated phase. This is attributed to the non-zero constant energy-density of the vacuum. This paradigm has been dubbed: Λ CDM [2, 3, 4].

*Electronic address: Gabor.Somogyi@desy.de

†Electronic address: res@physik.unizh.ch

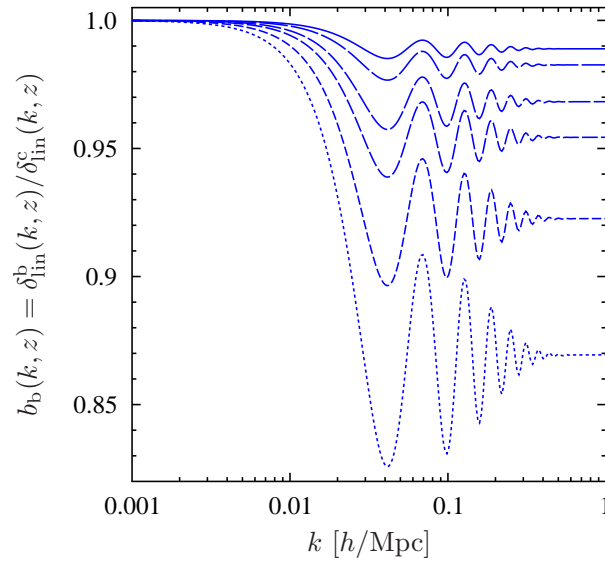


FIG. 1: Baryon bias as a function of inverse spatial scale, where we have defined the baryon bias $b_b(k, z) \equiv \delta_{\text{lin}}^b(k, z) / \delta_{\text{lin}}^c(k, z)$. Solid through to dashed lines show results for redshifts $z = \{0, 1.0, 3.0, 5.0, 10.0, 20.0\}$.

The present day energy-density budget for the Λ CDM model is distributed into several components, which in units of the critical density are: vacuum energy $\Omega_{\Lambda,0} \approx 0.73$, matter $\Omega_{m,0} \approx 0.27$, neutrinos $\Omega_{\nu,0} \lesssim 10^{-2}$ and radiation $\Omega_{r,0} \approx 5 \times 10^{-4}$. The matter distribution can be subdivided further into contributions from CDM and baryons, with present day values $\Omega_c \approx 0.225$ and $\Omega_b \approx 0.045$. The detailed physics for the evolution of the radiation, CDM, baryon and neutrino fluctuations ($\delta^r, \delta^c, \delta^b, \delta^\nu$), from the early Universe through to recombination can be obtained by solving the Einstein–Boltzmann equations. These are a set of coupled non-linear partial differential equations, however while the fluctuations are small they may be linearized and solved [for a review see 5, 6]. At later times these fluctuations enter a phase of non-linear growth. Their evolution during this period can no longer be described accurately using the linear Einstein–Boltzmann theory and must be followed using higher order perturbation theory (hereafter PT) techniques [7] or more directly through N -body simulations [8].

The cross-over from the linear to the non-linear theory is, in general, not straightforward. Most of the theoretical and numerical approaches to this latter task were developed during the previous two decades, during which time the Standard CDM model was favored: essentially Einstein-de Sitter spacetime, $\Omega_m = 1$, with energy-density dominated by CDM $\gtrsim 97\%$, and baryons contributing $\lesssim 3\%$ to the total matter. For this case it is natural to assume that the CDM fluctuations dominate the gravitational potentials at nearly all times, with baryons playing little role in the formation of large-scale structure [see for example 9, 10, 11]. Thus, one simply requires a transfer function for the CDM distribution at some late time, to model the evolution of both components.

In the latter part of the 1990s, cosmological tests pointed towards the Λ CDM paradigm, and it was recognized that baryons should play some role in shaping the transfer function of matter fluctuations [5, 12, 13, 14]. However, rather than attempting to follow the CDM and baryons as separate fluids evolving from distinct sets of initial conditions, a simpler approximate scheme was adopted. This scheme is currently standard practice for all studies of structure formation in the Universe [15, 16, 17, 18]. It can be summarized as follows:

1. Fix the cosmological model, specifying Ω_c and Ω_b , and hence the fraction of baryons, f^b . Solve for the evolution of all perturbed species using the linearized coupled Einstein–Boltzmann equations. Obtain transfer functions at $z = 0$, where CDM and baryons are fully relaxed: i.e. $T^c(k, z = 0) \approx T^b(k, z = 0)$, where T^c and T^b are the transfer functions of the CDM and baryons, respectively.
2. Use the transfer functions to generate the linear matter power spectrum, normalized to the present day: i.e. $P_{\delta\delta}(\mathbf{k}, z = 0) \approx [(1 - f^b)T^c(k, z = 0) + f^b T^b(k, z = 0)]^2 A k^n \approx [T^c(k, z = 0)]^2 A k^n$, where the total matter fluctuation is $\delta = (1 - f^b)\delta^c + f^b \delta^b$.
3. Scale this power spectrum back to the initial time z_i , using the linear growth factor for the total matter fluctuation δ , which obtains from solving the equations of motion for a single fluid.
4. Generate the initial CDM density field and assume that the baryons are perfect tracers of the CDM.

5. Evolve this effective CDM+baryon fluid under gravity using full non-linear equations of motion, either as a single fluid for dark matter only, or as a 2-component fluid if hydrodynamics are also to be followed.

This effective description for the formation of structure becomes poor as the baryon fraction $f^b = \Omega_b/\Omega_m$ approaches $\sim O(1)$, and for the currently favored WMAP5 cosmology $f^b \approx 0.17$. In fact, in linear theory the gravitational relaxation between baryonic and dark matter components is only achieved at the level of $< 1\%$ by $z = 0$. Moreover, as can be seen in Fig. 1 there is a non-trivial scale-dependent bias between baryons and dark matter that exists right through to the present day. Failing, to take these biases into account may lead to non-negligible systematic errors in studies that attempt to obtain cosmological constraints from Large-Scale Structure (LSS) tests. With the next generation of LSS tests aiming to achieving 1% precision in measurements of the matter power spectrum [19, 20], it seems timely to investigate whether such modeling assumptions may impact inferences. Where we expect such systematic effects to play an important role is for studies based on baryonic physics such as: using 21cm emission from neutral hydrogen to trace mass density at the epoch of reionization $z_{\text{reion}} \approx 10$ [21, 22, 23, 24]; and studies of the Lyman alpha forest to probe the matter power spectrum [25].

In this, the first in a series of papers, we test whether this effective procedure can indeed be employed to follow, at high precision, the non-linear growth of structure formation in baryon and CDM fluids, from recombination right through to the present day. We do this by generalizing the matrix based “renormalized” perturbation theory (RPT) [45] techniques of Crocce and Scoccimarro [1, 26, 27] to an arbitrary number of gravitating fluids. In this paper we content our selves with calculating the observables up to the one-loop level in the theory. In a future paper we consider the resummation to arbitrary orders (Somogyi & Smith 2009, in preparation).

Recently, [28] gave a treatment of CDM plus baryons, using non-linear PT techniques. The work presented by these authors differs from that presented here in a number of fundamental ways. Firstly, these authors have assumed that, on large scales, baryons and CDM fluctuations evolve with the same initial conditions and that the only physical difference between the two fluids arises on small scales, where galaxy formation processes are able to provide some pressure support. They model this with a fixed comoving-scale Jeans criterion. In this work we are not so much interested in following how small-scale baryonic collapse feeds back on the mass distribution, but are more interested in following the very large-scale baryon and CDM fluctuations, initialized with their correct post-recombination spatial distributions, into the non-linear regime. Secondly, their work was developed within standard PT, the problems associated with this formalism are well documented [7]. Here, we develop the more successful RPT approach [1]. In passing, we note that a number of additional complimentary approaches and extensions to single-fluid RPT have recently been developed [29, 30, 31, 32, 33]. In addition, there has recently been progress on realistic modeling of massive neutrinos and CDM [34, 35, 36, 37, 38, 39], for simplicity we shall assume that neutrinos play a negligible role.

The paper is broken down as follows: In §II we set up the theoretical formalism: presenting the coupled equations of motion for the N -component fluid. Then we show how, when written in matrix form, the equations may be solved at linear order. We discuss generalized initial conditions, and then discuss the specific case of baryons and CDM. In §III we develop the non-linear PT expansion for the solutions, and show that they may be constructed to arbitrary order using a set of Feynman rules. In §IV we discuss the two-point statistics of the fields, which we take as our lowest order observables. In §V we give specific details of how we calculate the one-loop corrections in our theory. In §VI we present results for various quantities of interest. In §VII we give details of an approximate RPT scheme, which matches the exact calculation to within $< 1\%$, for all times of interest and on all scales where the perturbation theory is valid. Finally, in §VIII we draw our conclusions.

II. EQUATIONS OF MOTION

A. Standard form

For an N -component fluid in a uniformly expanding spacetime, the relevant equations of motion are, conservation of mass, momentum, and the Poisson equation. These may be written ($i = 1, \dots, N$ labels the i -th component) [7]:

$$\frac{\partial \delta_i(\mathbf{x}, \tau)}{\partial \tau} + \nabla \cdot [(1 + \delta_i(\mathbf{x}, \tau)) \mathbf{v}_i(\mathbf{x}, \tau)] = 0, \quad (1)$$

$$\frac{\partial \mathbf{v}_i(\mathbf{x}, \tau)}{\partial \tau} + \mathcal{H}(\tau) \mathbf{v}_i(\mathbf{x}, \tau) + (\mathbf{v}_i(\mathbf{x}, \tau) \cdot \nabla) \mathbf{v}_i(\mathbf{x}, \tau) = -\nabla \Phi(\mathbf{x}, \tau); \quad (2)$$

$$\nabla^2 \Phi(\mathbf{x}, \tau) = 4\pi G a^2 \sum_{i=1}^N \bar{\rho}_i(\tau) \delta_i(\mathbf{x}, \tau) = \frac{3}{2} \Omega_m(\tau) \mathcal{H}^2(\tau) \sum_{i=1}^N w_i \delta_i(\mathbf{x}, \tau). \quad (3)$$

where τ is conformal time $d\tau \equiv dt/a$, with a the scale factor. Here we have introduced the density perturbations in each component as $\delta_i(\mathbf{x}, \tau) \equiv \rho_i(\mathbf{x}, \tau)/\bar{\rho}_i - 1 = \rho_i(\mathbf{x}, \tau)/w_i \bar{\rho}_m - 1$, where ρ_i and $\bar{\rho}_i$ are the density and mean density.

$\mathbf{v}_i(\mathbf{x}, \tau)$ is the peculiar velocity. $\mathcal{H}(\tau) = d \ln a / d\tau$ is the conformal Hubble parameter, related to the usual Hubble parameter, $H \equiv \dot{a}/a$, through $\mathcal{H}(\tau) = aH$. The $w_i \equiv \Omega_i/\Omega_m$ are the fractional contributions of each fluid species to the total matter density. They are constant in time, and normalized

$$\sum_{i=1}^N w_i = 1. \quad (4)$$

In the above we have also expressed the mean energy-density in each species in units of the critical density,

$$\Omega_i(\tau) \equiv \frac{\bar{\rho}_i(\tau)}{\rho_{\text{crit}}(\tau)} = \frac{8\pi G \bar{\rho}_i(\tau)}{3a^2 \mathcal{H}^2(\tau)}, \quad (5)$$

and with subscript 0 denoting present day quantities, $\Omega_{i,0} = \Omega_i(\tau = \tau_0)$. Finally, the Hubble and density parameters of each species are related through the Friedmann equation, which can be written:

$$\mathcal{H}^2(\tau) = a^{-2} \mathcal{H}_0^2 [\Omega_{m,0} a^{-3} + \Omega_{\Lambda,0} + \Omega_{K,0} a^{-2}] ; \quad \Omega_{K,0} \equiv 1 - \Omega_{m,0} - \Omega_{\Lambda,0}. \quad (6)$$

Taking the divergence of Eq. (2) and using Eq. (3) to eliminate Φ , we obtain

$$\begin{aligned} \frac{\partial \Theta_i(\mathbf{x}, \tau)}{\partial \tau} + \mathcal{H}(\tau) \Theta_i(\mathbf{x}, \tau) + \sum_{j,k} [\partial_j (\mathbf{v}_i)_k(\mathbf{x}, \tau)] [\partial_k (\mathbf{v}_i)_j(\mathbf{x}, \tau)] + (\mathbf{v}_i(\mathbf{x}, \tau) \cdot \nabla) \Theta_i(\mathbf{x}, \tau) \\ = -\frac{3}{2} \Omega_m(\tau) \mathcal{H}^2(\tau) \sum_{j=1}^N w_j \delta_j(\mathbf{x}, \tau), \end{aligned} \quad (7)$$

where we have set $\nabla \cdot \mathbf{v}(\mathbf{x}, \tau) = \Theta(\mathbf{x}, \tau)$ and j and k denote vector components. Next, we go to Fourier space. For a quantity $A(\mathbf{x}, \tau)$, we define the Fourier transform, $\tilde{A}(\mathbf{k}, \tau)$ and its inverse, as follows

$$A(\mathbf{x}, \tau) = \int d^3 \mathbf{k} e^{i\mathbf{k} \cdot \mathbf{x}} \tilde{A}(\mathbf{k}, \tau) \quad \Leftrightarrow \quad \tilde{A}(\mathbf{k}, \tau) = \int \frac{d^3 \mathbf{x}}{(2\pi)^3} e^{-i\mathbf{k} \cdot \mathbf{x}} A(\mathbf{x}, \tau). \quad (8)$$

Assuming $\mathbf{v}_i(\mathbf{x}, \tau)$ to be irrotational, there exists a scalar field $u_i(\mathbf{x}, \tau)$, such that $\mathbf{v}_i(\mathbf{x}, \tau) = -\nabla u_i(\mathbf{x}, \tau)$ and thus

$$\tilde{\mathbf{v}}_i(\mathbf{k}, \tau) = -i\mathbf{k} \tilde{u}_i(\mathbf{k}, \tau), \quad \tilde{\Theta}_i(\mathbf{k}, \tau) = \mathbf{k}^2 \tilde{u}_i(\mathbf{k}, \tau) \quad \Rightarrow \quad \tilde{\mathbf{v}}_i(\mathbf{k}, \tau) = -i\mathbf{k} \frac{\tilde{\Theta}_i(\mathbf{k}, \tau)}{\mathbf{k}^2}. \quad (9)$$

On inserting this relation into the equations of motion we find:

$$\frac{\partial \tilde{\delta}_i(\mathbf{k}, \tau)}{\partial \tau} + \tilde{\Theta}_i(\mathbf{k}, \tau) + \int d^3 \mathbf{k}_1 d^3 \mathbf{k}_2 \delta^D(\mathbf{k} - \mathbf{k}_1 - \mathbf{k}_2) \left(1 + \frac{\mathbf{k}_1 \cdot \mathbf{k}_2}{\mathbf{k}_2^2} \right) \tilde{\delta}_i(\mathbf{k}_1, \tau) \tilde{\Theta}_i(\mathbf{k}_2, \tau) = 0; \quad (10)$$

$$\begin{aligned} \frac{\partial \tilde{\Theta}_i(\mathbf{k}, \tau)}{\partial \tau} + \mathcal{H}(\tau) \tilde{\Theta}_i(\mathbf{k}, \tau) + \frac{3}{2} \Omega_m(\tau) \mathcal{H}^2(\tau) \sum_{j=1}^N w_j \tilde{\delta}_j(\mathbf{k}, \tau) \\ + \int d^3 \mathbf{k}_1 d^3 \mathbf{k}_2 \delta^D(\mathbf{k} - \mathbf{k}_1 - \mathbf{k}_2) \left[\frac{(\mathbf{k}_1 + \mathbf{k}_2)^2 \mathbf{k}_1 \cdot \mathbf{k}_2}{2\mathbf{k}_1^2 \mathbf{k}_2^2} \right] \tilde{\Theta}_i(\mathbf{k}_1, \tau) \tilde{\Theta}_i(\mathbf{k}_2, \tau) = 0. \end{aligned} \quad (11)$$

Finally, we introduce the variable $\tilde{\theta}_i(\mathbf{k}, \tau) \equiv -\tilde{\Theta}_i(\mathbf{k}, \tau)/\mathcal{H}(\tau)$ and change the “time” variable to $\eta = \ln a(\tau)$. Using

$$\frac{d}{d\tau} = \frac{d}{d\eta} \frac{d\eta}{d\tau} = \frac{d}{d\eta} \frac{d \ln a}{d\tau} = \mathcal{H} \frac{d}{d\eta}, \quad (12)$$

and where $d\mathcal{H}/d\tau = -\mathcal{H}^2[\Omega_m/2 - \Omega_\Lambda]$, (see Appendix A), we obtain:

$$\frac{\partial \tilde{\delta}_i(\mathbf{k}, \eta)}{\partial \eta} - \tilde{\theta}_i(\mathbf{k}, \eta) = \int d^3 \mathbf{k}_1 d^3 \mathbf{k}_2 \delta^D(\mathbf{k} - \mathbf{k}_1 - \mathbf{k}_2) \alpha(\mathbf{k}_2, \mathbf{k}_1) \tilde{\delta}_i(\mathbf{k}_1, \eta) \tilde{\theta}_i(\mathbf{k}_2, \eta); \quad (13)$$

$$\begin{aligned} \frac{\partial \tilde{\theta}_i(\mathbf{k}, \eta)}{\partial \eta} + \tilde{\theta}_i(\mathbf{k}, \eta) \left[1 - \frac{\Omega_m(\eta)}{2} + \Omega_\Lambda(\eta) \right] - \frac{3}{2} \Omega_m(\eta) \sum_{j=1}^N w_j \tilde{\delta}_j(\mathbf{k}, \eta) \\ = \int d^3 \mathbf{k}_1 d^3 \mathbf{k}_2 \delta^D(\mathbf{k} - \mathbf{k}_1 - \mathbf{k}_2) \beta(\mathbf{k}_1, \mathbf{k}_2) \tilde{\theta}_i(\mathbf{k}_1, \eta) \tilde{\theta}_i(\mathbf{k}_2, \eta), \end{aligned} \quad (14)$$

where in the above expressions we introduced the mode-coupling functions:

$$\alpha(\mathbf{k}_1, \mathbf{k}_2) = 1 + \frac{\mathbf{k}_1 \cdot \mathbf{k}_2}{\mathbf{k}_1^2}, \quad \beta(\mathbf{k}_1, \mathbf{k}_2) = \frac{(\mathbf{k}_1 + \mathbf{k}_2)^2 \mathbf{k}_1 \cdot \mathbf{k}_2}{2\mathbf{k}_1^2 \mathbf{k}_2^2}. \quad (15)$$

B. Matrix form

Following [1] we now rewrite the equations of motion in matrix form. To do this, we first introduce a $2N$ -component “vector” of fields Ψ_a , the transpose of which is given by

$$\Psi_a^T(\mathbf{k}, \eta) = \left[\tilde{\delta}_1(\mathbf{k}, \eta), \tilde{\theta}_1(\mathbf{k}, \eta), \dots, \tilde{\delta}_N(\mathbf{k}, \eta), \tilde{\theta}_N(\mathbf{k}, \eta) \right], \quad (16)$$

where the index $a = 1, 2, \dots, 2N$. With this notation, the equations of motion, Eqs (13) and (14), can be written in the compact form (repeated indices are summed over)

$$\partial_\eta \Psi_a(\mathbf{k}, \eta) + \Omega_{ab} \Psi_b(\mathbf{k}, \eta) = \int d^3 \mathbf{k}_1 d^3 \mathbf{k}_2 \gamma_{abc}^{(s)}(\mathbf{k}, \mathbf{k}_1, \mathbf{k}_2) \Psi_b(\mathbf{k}_1, \eta) \Psi_c(\mathbf{k}_2, \eta). \quad (17)$$

We shall also introduce the additional compactification that repeated k -vectors are to be integrated over, hence we may rewrite Eq. (17) as

$$\rightarrow \partial_\eta \Psi_a(\mathbf{k}, \eta) + \Omega_{ab} \Psi_b(\mathbf{k}, \eta) = \gamma_{abc}^{(s)}(\mathbf{k}, \mathbf{k}_1, \mathbf{k}_2) \Psi_b(\mathbf{k}_1, \eta) \Psi_c(\mathbf{k}_2, \eta). \quad (18)$$

The $2N \times 2N$ matrix Ω_{ab} appearing in Eq. (17) reads

$$\Omega_{ab} = \begin{bmatrix} 0 & -1 & 0 & 0 & 0 & 0 & 0 & \dots & 0 & 0 \\ -\frac{3}{2}\Omega_m w_1 & [1 - \frac{\Omega_m}{2} + \Omega_\Lambda] & -\frac{3}{2}\Omega_m w_2 & 0 & -\frac{3}{2}\Omega_m w_3 & 0 & \dots & -\frac{3}{2}\Omega_m w_N & 0 & 0 \\ 0 & 0 & 0 & -1 & 0 & 0 & \dots & 0 & 0 & 0 \\ -\frac{3}{2}\Omega_m w_1 & 0 & -\frac{3}{2}\Omega_m w_2 & [1 - \frac{\Omega_m}{2} + \Omega_\Lambda] & -\frac{3}{2}\Omega_m w_3 & 0 & \dots & -\frac{3}{2}\Omega_m w_N & 0 & 0 \\ \vdots & \vdots & \vdots & \vdots & \vdots & \vdots & \vdots & \vdots & \vdots & \vdots \\ 0 & 0 & 0 & 0 & 0 & 0 & \dots & 0 & -1 & 0 \\ -\frac{3}{2}\Omega_m w_1 & 0 & -\frac{3}{2}\Omega_m w_2 & 0 & -\frac{3}{2}\Omega_m w_3 & 0 & \dots & -\frac{3}{2}\Omega_m w_N & [1 - \frac{\Omega_m}{2} + \Omega_\Lambda] & 0 \end{bmatrix}, \quad (19)$$

where for the cases of $N = 1$ and $N = 2$ we simply take the top left 2×2 and 4×4 sub-matrices, respectively.

The symmetrized vertex matrix may be written for general N as,

$$\begin{aligned} \gamma_{(2j-1)(2j-1)(2j)}^{(s)}(\mathbf{k}, \mathbf{k}_1, \mathbf{k}_2) &= \frac{\alpha(\mathbf{k}_2, \mathbf{k}_1)}{2} \delta^D(\mathbf{k} - \mathbf{k}_1 - \mathbf{k}_2) \\ \gamma_{(2j-1)(2j)(2j-1)}^{(s)}(\mathbf{k}, \mathbf{k}_1, \mathbf{k}_2) &= \frac{\alpha(\mathbf{k}_1, \mathbf{k}_2)}{2} \delta^D(\mathbf{k} - \mathbf{k}_1 - \mathbf{k}_2) \\ \gamma_{(2j)(2j)(2j)}^{(s)}(\mathbf{k}, \mathbf{k}_1, \mathbf{k}_2) &= \beta(\mathbf{k}_1, \mathbf{k}_2) \delta^D(\mathbf{k} - \mathbf{k}_1 - \mathbf{k}_2), \end{aligned} \quad (20)$$

where $j = 1, 2, \dots, N$, and all other matrix elements are zero. For the sake of clarity, let us write explicitly the vertex matrix for $N = 1$ and $N = 2$:

- For $N = 1$ the vertex matrix reads:

$$\bar{\gamma}_{1bc}^{(s)}(\mathbf{k}_1, \mathbf{k}_2) = \begin{bmatrix} 0 & \alpha(\mathbf{k}_2, \mathbf{k}_1)/2 \\ \alpha(\mathbf{k}_1, \mathbf{k}_2)/2 & 0 \end{bmatrix}, \quad \bar{\gamma}_{2bc}^{(s)}(\mathbf{k}_1, \mathbf{k}_2) = \begin{bmatrix} 0 & 0 \\ 0 & \beta(\mathbf{k}_1, \mathbf{k}_2) \end{bmatrix}. \quad (21)$$

- For $N = 2$ the vertex matrix reads:

$$\begin{aligned} \bar{\gamma}_{1bc}^{(s)}(\mathbf{k}_1, \mathbf{k}_2) &= \begin{bmatrix} 0 & \alpha(\mathbf{k}_2, \mathbf{k}_1)/2 & 0 & 0 \\ \alpha(\mathbf{k}_1, \mathbf{k}_2)/2 & 0 & 0 & 0 \\ 0 & 0 & 0 & 0 \\ 0 & 0 & 0 & 0 \end{bmatrix}, & \bar{\gamma}_{2bc}^{(s)}(\mathbf{k}_1, \mathbf{k}_2) &= \begin{bmatrix} 0 & 0 & 0 & 0 \\ 0 & \beta(\mathbf{k}_1, \mathbf{k}_2) & 0 & 0 \\ 0 & 0 & 0 & 0 \\ 0 & 0 & 0 & 0 \end{bmatrix}, \\ \bar{\gamma}_{3bc}^{(s)}(\mathbf{k}_1, \mathbf{k}_2) &= \begin{bmatrix} 0 & 0 & 0 & 0 \\ 0 & 0 & 0 & 0 \\ 0 & 0 & 0 & \alpha(\mathbf{k}_2, \mathbf{k}_1)/2 \\ 0 & 0 & \alpha(\mathbf{k}_1, \mathbf{k}_2)/2 & 0 \end{bmatrix}, & \bar{\gamma}_{4bc}^{(s)}(\mathbf{k}_1, \mathbf{k}_2) &= \begin{bmatrix} 0 & 0 & 0 & 0 \\ 0 & 0 & 0 & 0 \\ 0 & 0 & 0 & 0 \\ 0 & 0 & 0 & \beta(\mathbf{k}_1, \mathbf{k}_2) \end{bmatrix}. \end{aligned} \quad (22)$$

In the above we defined $\bar{\gamma}^{(s)}$ to be the vertex matrix *without* the delta function for momentum conservation, i.e. $\gamma_{abc}^{(s)}(\mathbf{k}, \mathbf{k}_1, \mathbf{k}_2) = \bar{\gamma}_{abc}^{(s)}(\mathbf{k}_1, \mathbf{k}_2) \delta^D(\mathbf{k} - \mathbf{k}_1 - \mathbf{k}_2)$.

C. Solving for the propagator

The main advantage of writing Eq. (17) in this compact form is, as was pointed out in [1], that an implicit integral solution can be obtained by Laplace transforming in the variable η . This approach, however, requires that we set the background cosmological model to be Einstein–de Sitter: i.e. $\{\Omega_m(\eta) = 1, \Omega_\Lambda(\eta) = 0\}$ (we shall discuss generalizations to other cosmological models in §IID). This means that the matrix Ω_{ab} is independent of time, hence

$$\sigma_{ab}^{-1}(s)\Psi_b(\mathbf{k}, s) = \phi_a^{(0)}(\mathbf{k}) + \gamma_{abc}^{(s)}(\mathbf{k}, \mathbf{k}_1, \mathbf{k}_2) \oint \frac{ds_1}{2\pi i} \Psi_b(\mathbf{k}, s_1) \Psi_b(\mathbf{k}, s - s_1) , \quad (23)$$

where $\phi_a^{(0)}(\mathbf{k}) \equiv \Psi_a(\mathbf{k}, \eta = 0)$ denotes the initial conditions, set when the growth factor is one and $\sigma_{ab}^{-1}(s) = s\delta_{ab} + \Omega_{ab}$. Multiplying by the matrix $\sigma_{ab}(s)$ and performing the inverse Laplace transform gives the formal solution [1],

$$\Psi_a(\mathbf{k}, a) = g_{ab}(\eta)\phi_b^{(0)}(\mathbf{k}) + \int_0^\eta d\eta' g_{ab}(\eta - \eta') \gamma_{bcd}^{(s)}(\mathbf{k}, \mathbf{k}_1, \mathbf{k}_2) \Psi_c(\mathbf{k}_1, \eta') \Psi_d(\mathbf{k}_1, \eta') , \quad (24)$$

where $g_{ab}(\eta)$ is the *linear propagator* given by

$$g_{ab}(\eta) = \mathcal{L}^{-1} [\sigma_{ab}(s), s, \eta] , \quad (25)$$

where $\mathcal{L}^{-1}[f(s), s, \eta]$ denotes the inverse Laplace transform of the function $f(s)$ from the variable s to the variable η . In Appendix F, we prove that the linear propagator has the general form ($j, k = 1, 2, \dots, N$)

$$\begin{aligned} g_{(2j-1)(2k-1)} &= \frac{1}{5} \left(3e^\eta - 5 + 2e^{-3\eta/2} \right) w_k + \delta_{jk} , \\ g_{(2j)(2k-1)} &= \frac{3}{5} \left(e^\eta - e^{-3\eta/2} \right) w_k , \\ g_{(2j-1)(2k)} &= \frac{2}{5} \left(e^\eta - 5 + 5e^{-\eta/2} - e^{-3\eta/2} \right) w_k + (2 - 2e^{-\eta/2}) \delta_{jk} , \\ g_{(2j)(2k)} &= \frac{1}{5} \left(2e^\eta - 5e^{-\eta/2} + 3e^{-3\eta/2} \right) w_k + e^{-\eta/2} \delta_{jk} , \end{aligned} \quad (26)$$

for $\eta \geq 0$, and $g_{ab}(\eta) = 0$ for $\eta < 0$ due to causality, and furthermore $g_{ab}(\eta) \rightarrow \delta_{ab}^K$ as $\eta \rightarrow 0^+$. Clearly we can write the propagator as

$$g_{ab}(\eta) = \sum_l e^{l\eta} g_{ab,l} , \quad (27)$$

where the summation runs over the set $l \in \{1, 0, -1/2, -3/2\}$ and the $g_{ab,l}$ are constant matrices. Explicitly we find:

- For $N = 1$, we have $w_1 = 1$ and the propagator reads:

$$g_{ab}(\eta) = \frac{1}{5} \begin{bmatrix} 3e^\eta + 2e^{-3\eta/2} & 2e^\eta - 2e^{-3\eta/2} \\ 3e^\eta - 3e^{-3\eta/2} & 2e^\eta + 3e^{-3\eta/2} \end{bmatrix} = \frac{e^\eta}{5} \begin{bmatrix} 3 & 2 \\ 3 & 2 \end{bmatrix} - \frac{e^{-3\eta/2}}{5} \begin{bmatrix} -2 & 2 \\ 3 & -3 \end{bmatrix} , \quad (28)$$

in agreement with the usual expression [1], where there are two solutions for the time evolution of the modes: a growing $D_+ \propto e^\eta$ and a decaying mode $D_- \propto e^{-3\eta/2}$. Thus for $N = 1$ *only*, $g_{ab,0} = g_{ab,-1/2} = 0$ and

$$g_{ab,1} = \frac{1}{5} \begin{bmatrix} 3 & 2 \\ 3 & 2 \end{bmatrix} , \quad g_{ab,-3/2} = \frac{1}{5} \begin{bmatrix} 2 & -2 \\ -3 & 3 \end{bmatrix} . \quad (29)$$

- For $N = 2$, the propagator takes the general form of Eq. (27), with all the $g_{ab,l}$ non-zero:

$$\begin{aligned} g_{ab,1} &= \frac{1}{5} \begin{bmatrix} 3w_1 & 2w_1 & 3w_2 & 2w_2 \\ 3w_1 & 2w_1 & 3w_2 & 2w_2 \\ 3w_1 & 2w_1 & 3w_2 & 2w_2 \\ 3w_1 & 2w_1 & 3w_2 & 2w_2 \end{bmatrix} , & g_{ab,0} &= \begin{bmatrix} 1 - w_1 & 2(1 - w_1) & -w_2 & -2w_2 \\ 0 & 0 & 0 & 0 \\ -w_1 & -2w_1 & 1 - w_2 & 2(1 - w_2) \\ 0 & 0 & 0 & 0 \end{bmatrix} , \\ g_{ab,-1/2} &= \begin{bmatrix} 0 & -2(1 - w_1) & 0 & 2w_2 \\ 0 & 1 - w_1 & 0 & -w_2 \\ 0 & 2w_1 & 0 & -2(1 - w_2) \\ 0 & -w_1 & 0 & 1 - w_2 \end{bmatrix} , & g_{ab,-3/2} &= \frac{1}{5} \begin{bmatrix} 2w_1 & -2w_1 & 2w_2 & -2w_2 \\ -3w_1 & 3w_1 & -3w_2 & 3w_2 \\ 2w_1 & -2w_1 & 2w_2 & -2w_2 \\ -3w_1 & 3w_1 & -3w_2 & 3w_2 \end{bmatrix} . \end{aligned} \quad (30)$$

Interestingly, we now see that there are more solutions for the time evolution of the modes, and besides the usual growing and decaying modes, there is an additional decaying mode $g_{ab} \propto e^{-\eta/2}$, and a static mode $g_{ab} \propto \text{const.}$ In Appendix E we give an explicit expression for the linear propagator for the specific case of $N = 3$. The interesting point to note in going from $N = 2$ to $N = 3$, is that, whilst the eigenvectors do change, no new eigenvalues are generated and this holds for general N . This explicitly follows from Eq. (26).

D. Extension to general cosmological models

An approximate treatment of the dependence of the PT and RPT kernels on cosmology was discussed by [26, 40], and we shall adopt the same approach here. The necessary changes to be made are that we use a new time variable,

$$\eta \equiv \log D_+(\tau) , \quad (31)$$

where $D_+(\tau)$ is the linear growth factor for the appropriate cosmology. Also, instead of working with the solution vector of the form Eq. (16), we work with vectors

$$\Psi_a^T(\mathbf{k}, \eta) = \left[\tilde{\delta}_1(\mathbf{k}, \eta), \tilde{\theta}_1(\mathbf{k}, \eta)/f(\eta), \dots, \tilde{\delta}_N(\mathbf{k}, \eta), \tilde{\theta}_N(\mathbf{k}, \eta)/f(\eta) \right] , \quad (32)$$

where $f(\eta) \equiv d \log D_+ / d \log a$ is the logarithmic growth factor for peculiar velocity fields. On performing these transformations Eq. (17) remains structurally the same, except for the elements of the matrix Ω_{ab} , which gain time dependence. This means that it is no longer straightforward to perform the Laplace transforms and so we do not obtain Eq. (24). However, as was argued by [26], most of the cosmological dependence is encoded in $D_+(\eta)$, and so to a very good approximation we may simply take $\Omega_{ab}(\Omega_m, \Omega_\Lambda) \rightarrow \Omega_{ab}(\Omega_m = 1, \Omega_\Lambda = 0)$, and keep Eq. (24). We shall use this approximation throughout the remainder of this paper.

E. Initial conditions

We must now specify the initial conditions for the $2N$ variables. For cosmological structure formation the most relevant case is when, for each fluid component, $\tilde{\delta}_i(\mathbf{k}, \eta = 0)$ and $\tilde{\theta}_i(\mathbf{k}, \eta = 0)$ ($i = 1, 2, \dots, N$) are proportional to the same random field. However, the initial random field can differ from component to component. In this case we can write

$$\left[\phi_a^{(0)}(\mathbf{k}) \right]^T = \left[u_1 \delta_1^{(0)}(\mathbf{k}), u_2 \delta_1^{(0)}(\mathbf{k}), \dots, u_{2N-1} \delta_N^{(0)}(\mathbf{k}), u_{2N} \delta_N^{(0)}(\mathbf{k}), \right] , \quad (33)$$

where the u_a , ($a = 1, 2, \dots, 2N$) are simply numerical coefficients.

For the case of the $N = 1$ component fluid, “pure growing” mode initial conditions can be obtained by setting $u_a = u_a^{(1)} \equiv (1, 1)$, and “pure decaying” mode ones by setting $u_a = u_a^{(2)} \equiv (2/3, -1)$. These are the eigenvectors of the matrix g_{ab} . In going to the more complex case of the $N = 2$ multi-fluid, there are, unfortunately, no such simple choices for the u_a components to obtain pure “growing mode” or pure “decaying modes” at all k -modes, unless all of the $\delta_i^{(0)}(\mathbf{k})$ are equivalent. To see why this is so, consider the eigenvectors of the linear propagator g_{ab} , these are:

$$u_a^{(1)} = \begin{pmatrix} 1 \\ 1 \\ 1 \\ 1 \end{pmatrix} ; u_a^{(2)} = \begin{pmatrix} 2/3 \\ -1 \\ 2/3 \\ -1 \end{pmatrix} ; u_a^{(3,1)} = \begin{pmatrix} w_2 \\ 0 \\ -w_1 \\ 0 \end{pmatrix} ; u_a^{(4,1)} = \begin{pmatrix} 2w_2 \\ -w_2 \\ -2w_1 \\ w_1 \end{pmatrix} . \quad (34)$$

On dotting g_{ab} with $u^{(1)}$ we find $g_{ab} u_b^{(1)} = e^\eta u_a^{(1)}$, and we have a pure growing mode solution. However, to propagate the initial modes we require g_{ab} dotted with $\phi_b^{(0)}(\mathbf{k})$. If we do this and set $u_a = u_a^{(1)}$ then we find:

$$g_{ab}(\eta) \phi_b^{(0)}(\mathbf{k}) = \sum_b g_{ab}(\eta) u_b^{(1)} \delta_b^{(0)}(\mathbf{k}) = e^\eta u_a^{(1)} \delta^{(0)}(\mathbf{k}) = e^\eta \phi_a^{(0)}(\mathbf{k}) , \quad (35)$$

if and only if $\delta_b^{(0)}(\mathbf{k}) = \delta^{(0)}(\mathbf{k})$ for all b . However, this situation is not physically interesting since, in the absence of any process such as pressure support, there would be no discernible difference between treating the N -component fluid as an effective 1-component fluid.

The more interesting physical case will be the situation where each fluid component evolves from a distinct set of initial conditions, i.e. $\delta_i^{(0)} \neq \delta_j^{(0)}$, with $(i \neq j)$. What then are the appropriate choices for the u_a ? The distinct initial conditions that are of interest are: the dark matter, baryon, neutrino and photon, perturbations present in the post-recombination Universe. As described earlier the dynamics of these species are generally followed from the post-inflationary universe and through the recombination era using the coupled, linearized Einstein–Boltzmann equations [see for example 5]. In this case the fluctuations in k -space are all proportional to the same random field, which is related to the primordial curvature perturbation, but with some k -dependent transfer function that takes into account the physical processes that affects each species. We shall use CMBFAST [6] for following the time evolution of the perturbations up to some large redshift say $z = 100$ as the initial condition for our non-linear computation; and the information on the different components is given as a set of transfer functions, which we denote $T_i(k)$. Thus for the N -component fluid, we shall express our initial conditions, more specifically as:

$$\left[\phi_a^{(0)}(\mathbf{k}) \right]^T = [u_1 T_1(k), u_2 T_1(k), \dots, u_{2N-1} T_N(k), u_{2N} T_N(k)] \delta_0(\mathbf{k}). \quad (36)$$

Importantly for the standard Λ CDM framework of adiabatic near scale-invariant fluctuations, all of the $T_i(k) \rightarrow 1$ as $k \rightarrow 0$. Hence, on large scales if we choose $u_a = u_a^{(1)}$, then $\phi_a^{(0)}(\mathbf{k})$ is an eigenvector of the linear propagator and so we have pure growing mode initial conditions. On smaller scales there will, however, be some mixing of growing and decaying modes in the initial conditions.

F. Application to a CDM and baryon fluid

As a demonstration of the formalism, we now consider the specific case of the linear evolution under gravity of a two-component fluid of CDM and baryons. In this calculation we set the initial cosmological model to be that identified from the WMAP5 analysis [4]: $\{\Omega_c = 0.2275, \Omega_b = 0.0456, \Omega_\Lambda = 0.7268, h = 0.705, n_s = 0.96, \sigma_8 = 0.812\}$; and assume negligible contribution from neutrinos. Thus, we have $\{w_1 = \Omega_c/\Omega_m = (1 - f^b), w_2 = \Omega_b/\Omega_m = f^b\}$. We use CMBFAST [6] to generate CDM and baryon transfer functions at the initial redshift $z_i = 100$: hence $T_1(k) = T^c(k, z = 100) \equiv T^c(k)$ and $T_2(k) = T^b(k, z = 100) \equiv T^b(k)$.

The implicit solution for $\Psi_a(\mathbf{k}, \eta)$, Eq. (24), can be linearized, and the zeroth order term can be written: $\Psi_a^{(0)}(\mathbf{k}, \eta) = g_{ab}(\eta) \phi_b^{(0)}(\mathbf{k})$ (c.f. Eq. (42)). Following our discussions in §I and §II E, we are interested in the case where the initial conditions are those of the post-recombination era Universe. Prior to this time, electrons and photons are tightly coupled through Thompson scattering, and photons drag electrons and baryons out of the potential wells. Thus at the end of recombination, baryons and dark matter are spatially displaced from one another (c.f. Fig. 1). In a somewhat simplified view, once the scattering processes are switched off, the evolution of the fluids can be captured by the two perturbations relaxing under gravity and so the evolving fields are simply some linear combination of the initial fields, with appropriate weight factors.

Fig. 2 graphically demonstrates this. Here we show the ratio of the initial CDM (left panel) and baryon (right panel) perturbations evolving under the action of the linear propagator $g_{ab}(\eta)$, divided through by the amplitude of the initial primordial density perturbation that sourced them. For large-scale growing mode initial conditions ($u_a = u_a^{(1)}$), then we have:

$$\begin{aligned} \delta_{\text{lin}}^c(\mathbf{k}, \eta)/\delta_0(k) &= \Psi_1^{(0)}(\mathbf{k}, \eta)/\delta_0(k) = [g_{11}(\eta) + g_{12}(\eta)] T^c(k) + [g_{13}(\eta) + g_{14}(\eta)] T^b(k) ; \\ &= \left[(1 - f^b)e^\eta + 3f^b(1 - 2e^{-\eta/2}) \right] T^c(k) + f^b \left[e^\eta - 3 + 2e^{-\eta/2} \right] T^b(k) ; \end{aligned} \quad (37)$$

$$\begin{aligned} \delta_{\text{lin}}^b(\mathbf{k}, \eta)/\delta_0(k) &= \Psi_3^{(0)}(\mathbf{k}, \eta)/\delta_0(k) = [g_{31}(\eta) + g_{32}(\eta)] T^c(k) + [g_{33}(\eta) + g_{34}(\eta)] T^b(k) ; \\ &= (1 - f^b) \left[e^\eta - 3 + 2e^{-\eta/2} \right] T^c(k) + \left[f^b e^\eta + (1 - f^b)(3 - 2e^{-\eta/2}) \right] T^b(k). \end{aligned} \quad (38)$$

In the limit of small and large η these relations simplify to:

$$\delta_{\text{lin}}^c(\mathbf{k}, \eta)/\delta_0(k) \approx \begin{cases} T^c(k) & (\eta \ll 1) \\ e^\eta [(1 - f^b)T^c(k) + f^b T^b(k)] & (\eta \gg 1) \end{cases} ; \quad (39)$$

$$\delta_{\text{lin}}^b(\mathbf{k}, \eta)/\delta_0(k) \approx \begin{cases} T^b(k) & (\eta \ll 1) \\ e^\eta [(1 - f^b)T^c(k) + f^b T^b(k)] & (\eta \gg 1) \end{cases} , \quad (40)$$

where the $\eta \gg 1$ relations, show that the fields evolve to an equilibrium state.

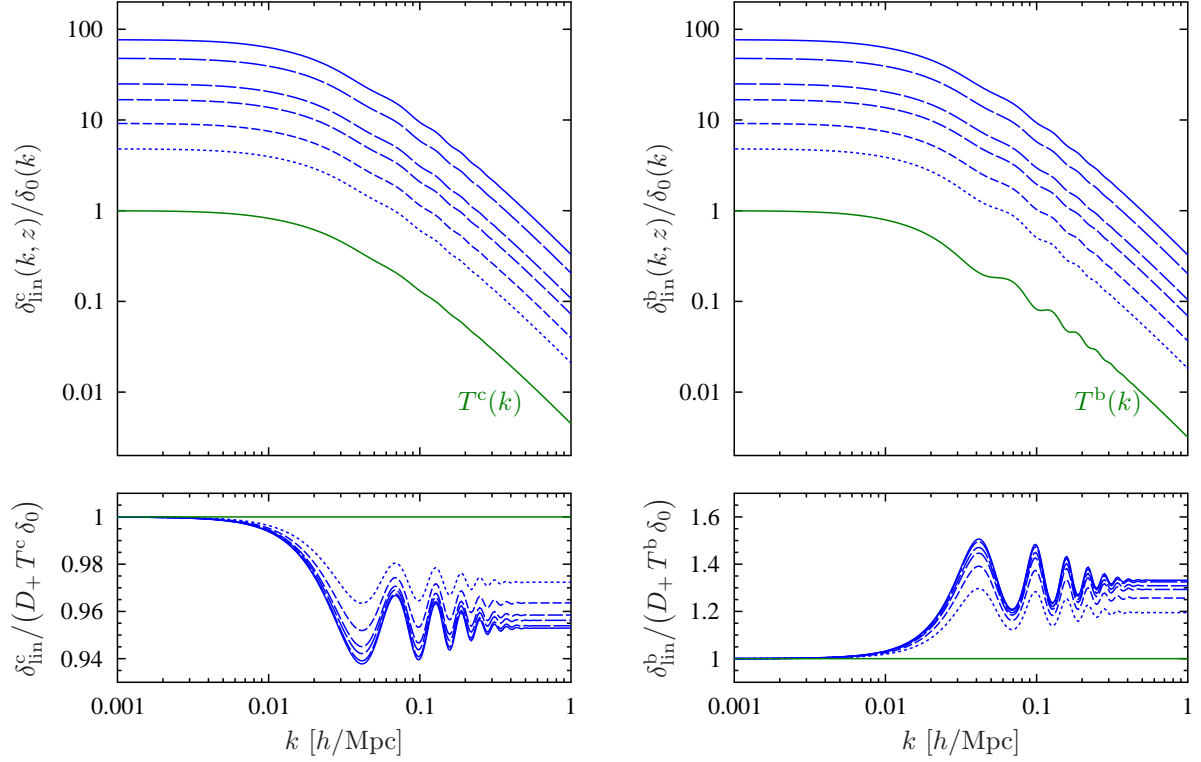


FIG. 2: Evolution of the initial density perturbations for the CDM and baryons under the linear propagator, relative to the primordial density perturbation, as a function of spatial wavenumber and redshift. *Top left and right panels:* evolution of the CDM perturbations δ^c , and baryons, δ^b , respectively. Going from top to bottom, the blue solid through to dashed lines show results for redshifts $z = \{0, 1.0, 3.0, 5.0, 10.0, 20.0\}$. The solid green line at the bottom shows the initial mode. *Bottom left and right panels:* ratio of the linearly evolved CDM and baryon perturbations to the initial perturbations evolved under the standard linear growth factor for matter perturbations. Line styles are as for above.

On inspecting Fig. 2, we note that on large scales at the initial time (green solid lines) the two perturbations are perfectly correlated with the primordial fluctuation. On smaller scales we see that both the CDM and baryon modes are damped, and this is due to the Mészáros effect [see 41, 42]. Also the waves have an oscillating structure as a function of k , these are the Baryon Acoustic Oscillations (BAO) [for a discussion see 13, 14]. We also note that the BAO are almost absent in the dark matter distribution at $z_i = 100$, whereas for the baryons they are strongly present.

As the system evolves linearly under gravity, we now see that on large scales ($k < 0.01 h \text{ Mpc}^{-1}$) both solutions scale with time in accordance with the standard linear growth factor for the total matter perturbation on large scales: i.e., $\delta^m(\mathbf{k}, \eta) = \lim_{k \rightarrow 0} [w_1 \delta^c(\mathbf{k}, \eta) + w_2 \delta^b(\mathbf{k}, \eta)] = D_+(\eta) \delta^m(\mathbf{k}, \eta_0)$, which we obtain using the model of [43] with $\Omega_m = \Omega_c + \Omega_b$. On smaller scales ($k > 0.01 h \text{ Mpc}^{-1}$) the fluctuations grow with time, but now we note that the BAO features present in the baryon modes become damped, whilst those in the CDM grow. This can be seen more clearly by dividing each mode by $D_+(\eta) \delta^{(0)}(k) = D_+(\eta) T(k) \delta_0(k)$, for each component and this is what is plotted in the bottom panels of Fig. 2. Again, in the large scale limit, all $T_i(k) \rightarrow 1$, and so $g_{1b}(\eta) u_b^{(1)} \rightarrow D_+(\eta)$. Hence $\delta_{\text{lin}}^c(k, \eta) / [D_+(\eta) T^c(k) \delta_0(k)] \rightarrow 1$, and likewise for the baryons. Thus we see that the amplitude of the BAO in the CDM are indeed increasing, and those in the baryons are decaying.

Note that for the CDM distribution, by $z = 5$ the BAO are almost fully in place with $< 1\%$ changes to the oscillation amplitude as the distribution is evolved to $z = 0$. However between $z = 10$ and 5 there is a significant difference and one must be careful to account for these changes when modeling BAO at high redshift. We now draw attention to the important fact that the baryon distributions display more significant changes, there being an almost 50% difference between the initial and final distributions on large-scales. As noted this will lead to significant baryon bias for statistical probes that are sensitive primarily to the distribution of baryons in the Universe and not the dark matter. In the following sections, we explore how non-linear evolution changes these results.

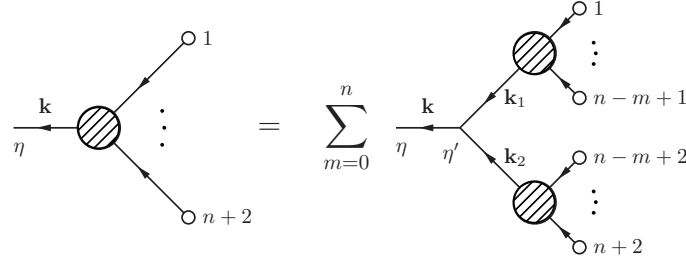


FIG. 3: Graphical representation of Eq. (45). The blob on the left hand side corresponds to $\Psi^{(n+1)}$ (which clearly involves $n+2$ initial conditions), while the two blobs on the right hand side correspond to $\Psi^{(n-m)}$ and $\Psi^{(m)}$ (involving $n-m+1$ and $m+1$ initial conditions) respectively. The trivalent vertex denotes the vertex matrix $\gamma^{(s)}$.

III. PERTURBATION THEORY

A. Solutions

Following [1] we look for power series solutions to the equations of motion, Eq. (17)

$$\Psi_a(\mathbf{k}, \eta) = \sum_{j=0}^{\infty} \Psi_a^{(j)}(\mathbf{k}, \eta) \quad (41)$$

(in our notation the linear solution is $\Psi^{(0)}$ as opposed to the more usual $\Psi^{(1)}$). On inserting the above expression into the general solution of Eq. (24), we find that

$$\Psi_a^{(0)}(\mathbf{k}, \eta) = g_{ab}(\eta) \phi_b^{(0)}(\mathbf{k}); \quad (42)$$

$$\Psi_a^{(1)}(\mathbf{k}, \eta) = \int_0^\eta d\eta' g_{ab}(\eta - \eta') \gamma_{bcd}^{(s)}(\mathbf{k}, \mathbf{k}_1, \mathbf{k}_2) \Psi_c^{(0)}(\mathbf{k}_1, \eta') \Psi_d^{(0)}(\mathbf{k}_2, \eta'); \quad (43)$$

$$\Psi_a^{(2)}(\mathbf{k}, \eta) = 2 \int_0^\eta d\eta' g_{ab}(\eta - \eta') \gamma_{bcd}^{(s)}(\mathbf{k}, \mathbf{k}_1, \mathbf{k}_2) \Psi_c^{(0)}(\mathbf{k}_1, \eta') \Psi_d^{(1)}(\mathbf{k}_2, \eta'); \quad (44)$$

$$\vdots \quad \vdots \quad \vdots \quad \vdots \quad \vdots$$

$$\Psi_a^{(n+1)}(\mathbf{k}, \eta) = \int_0^\eta d\eta' g_{ab}(\eta - \eta') \gamma_{bcd}^{(s)}(\mathbf{k}, \mathbf{k}_1, \mathbf{k}_2) \sum_{m=0}^n \Psi_c^{(n-m)}(\mathbf{k}_1, \eta') \Psi_d^{(m)}(\mathbf{k}_2, \eta'). \quad (45)$$

Fig. 3 shows a graphical representation of Eq. (45).

We may develop these solutions further by inserting into the above expressions the linear propagator $g_{ab}(\eta)$ given by Eq. (27). Thus, for the linear evolution of the initial waves, we have:

$$\Psi_a^{(0)}(\mathbf{k}, \eta) = \sum_l e^{l\eta} g_{ab,l} \phi_b^{(0)}(\mathbf{k}). \quad (46)$$

Similarly, for the first order solution we have

$$\begin{aligned} \Psi_a^{(1)}(\mathbf{k}, \eta) &= \int_0^\eta d\eta' g_{ab}(\eta - \eta') \gamma_{bcd}^{(s)}(\mathbf{k}, \mathbf{k}_1, \mathbf{k}_2) g_{cc'}(\eta') \phi_{c'}(\mathbf{k}_1) g_{dd'}(\eta') \phi_{d'}(\mathbf{k}_2); \\ &= \int_0^\eta d\eta' \sum_l e^{l(\eta - \eta')} g_{ab,l} \gamma_{bcd}^{(s)}(\mathbf{k}, \mathbf{k}_1, \mathbf{k}_2) \sum_m e^{m\eta'} g_{cc',m} \phi_{c'}^{(0)}(\mathbf{k}_1) \sum_n e^{n\eta'} g_{dd',n} \phi_{d'}^{(0)}(\mathbf{k}_2); \\ &= \int_0^\eta d\eta' \sum_{l,m,n} e^{l\eta + (m+n-l)\eta'} g_{ab,l} \gamma_{bcd}^{(s)}(\mathbf{k}, \mathbf{k}_1, \mathbf{k}_2) g_{cc',m} g_{dd',n} \phi_{c'}^{(0)}(\mathbf{k}_1) \phi_{d'}^{(0)}(\mathbf{k}_2); \\ &= \sum_{l,m,n} e^{l\eta} I_1(m+n-l; \eta) g_{ab,l} \tilde{\gamma}_{bcd}^{(s)}(\mathbf{k}_1, \mathbf{k} - \mathbf{k}_1) g_{cc',m} g_{dd',n} \phi_{c'}^{(0)}(\mathbf{k}_1) \phi_{d'}^{(0)}(\mathbf{k} - \mathbf{k}_1), \end{aligned} \quad (47)$$

where in the last line we have introduced the function:

$$I_1(l; \eta) = \int_0^\eta d\eta' e^{l\eta'} = \begin{cases} (e^{l\eta} - 1)/l & l \neq 0 \\ \eta & l = 0 \end{cases}, \quad (48)$$

and performed the \mathbf{k}_2 integral using the Dirac delta function implicit in $\gamma_{bcd}^{(s)}(\mathbf{k}, \mathbf{k}_1, \mathbf{k}_2)$.

In what follows we shall also need to make use of the 2nd order solution for the fields and after a similar procedure as above we find:

$$\begin{aligned} \Psi_a^{(2)}(\mathbf{k}, \eta) &= 2 \sum_{l,m} \sum_{p,q,r} e^{l\eta} I_2(m+p-l, q+r-p; \eta) g_{ab,l} \bar{\gamma}_{bcd}^{(s)}(\mathbf{k}_1, \mathbf{k} - \mathbf{k}_1) g_{cc',m} \\ &\times g_{df,p} \bar{\gamma}_{fgh}^{(s)}(\mathbf{k}_2, \mathbf{k} - \mathbf{k}_1 - \mathbf{k}_2) g_{gg',q} g_{hh',r} \phi_{c'}^{(0)}(\mathbf{k}_1) \phi_{g'}^{(0)}(\mathbf{k}_2) \phi_{h'}^{(0)}(\mathbf{k} - \mathbf{k}_1 - \mathbf{k}_2). \end{aligned} \quad (49)$$

In the above we have introduced a further auxiliary function,

$$I_2(l_2, l_1; \eta) = \int_0^\eta d\eta' e^{l_2\eta'} I_1(l_1; \eta') = \begin{cases} [l_2 e^{(l_1+l_2)\eta} - (l_1 + l_2) e^{l_2\eta} + l_1] / [l_1 l_2 (l_1 + l_2)] & (l_1 \neq 0, l_2 \neq 0) \\ [e^{l_1\eta} - 1 - l_1\eta] / l_1^2 & (l_1 \neq 0, l_2 = 0) \\ [e^{l_2\eta} (l_2\eta - 1) + 1] / l_2^2 & (l_1 = 0, l_2 \neq 0) \\ \eta^2 / 2 & (l_1 = 0, l_2 = 0) \end{cases}. \quad (50)$$

B. Feynman rules for the PT solutions

As was shown by [1] there is a simple interpretation for the solutions $\Psi_a^{(n)}(\mathbf{k})$ given by Eqs (42)–(45). The first equation in the hierarchy denotes an initial condition $\phi_a^{(0)}$, evolved under the linear propagator g_{ab} . The second denotes the non-linear coupling between two initial waves of incoming momentum \mathbf{k}_1 and \mathbf{k}_2 through the interaction vertex $\gamma_{abc}^{(s)}(\mathbf{k}, \mathbf{k}_1, \mathbf{k}_2)$, to produce an outgoing wave of momentum $\mathbf{k} = \mathbf{k}_1 + \mathbf{k}_2$, which is one order higher in the PT series and evolving under the action of g_{ab} . For the next equation in the series we see that the solution structure is now repeated, and this recurs for all higher order terms. Thus a convenient graphical representation for the solutions is obtained by “iterating” the graph in Fig. 3, until on the right-hand-side we are left with diagrams involving only trivalent vertices and no “blobs”. Associated to this graphical representation is a simple set of *Feynman rules* for obtaining the n -th order solution, $\Psi^{(n)}(\mathbf{k}, \eta)$; these may be stated as follows:

1. Draw all *topologically distinct, connected tree diagrams* containing n vertices and a directed line coming into the diagram from the right for each of $n + 1$ initial conditions, and a directed line going to the left out of the diagram for the final wave. Draw any number of directed internal lines running from one vertex to another, as required to give each vertex exactly two incoming and one outgoing attached line. It is most straightforward to label the direction of the lines by drawing arrows on them.
2. Assign each vertex its own time variable, s_j , and each line its own momentum, \mathbf{k}_j , such that momentum is conserved at each vertex, with the momenta considered to flow in the direction of the arrows. For the single outgoing line, assign the momentum \mathbf{k} and final time η .
3. Identify the various pieces of each diagram with the mathematical expressions as shown in Fig. 4.
4. Integrate over all intermediate times s_j , each between $[0, \eta]$. Integrate over all the independent wavevectors with the measure $d^3\mathbf{k}_j$. (Note that the momenta of all internal lines and a single incoming line are fixed by momentum conservation, thus there will be n independent momenta to integrate over.) Sum over all internal field indices b, c , etc.
5. Each diagram carries a factor of 2^r if there are precisely r vertices that are not symmetric with respect to interchanging their two incoming waves.
6. The value of $\Psi_a^{(n)}(\mathbf{k}, \eta)$ is given by the sum over the values of these diagrams.

Fig. 5 shows all diagrams up to $n = 3$, together with their symmetry factors calculated as in Step 5 above. As an example of the use of the Feynman rules, the expressions corresponding to the first two diagrams can be written,

$$\Psi_a^{(0)}(\mathbf{k}, \eta) = g_{ab}(\eta) \phi_b^{(0)}(\mathbf{k}), \quad (51)$$

$$\Psi_a^{(1)}(\mathbf{k}, \eta) = \int_0^\eta ds_1 g_{ab}(\eta - s_1) \int d^3\mathbf{k}_1 \bar{\gamma}_{bcd}^{(s)}(\mathbf{k}_1, \mathbf{k} - \mathbf{k}_1) g_{cc'}(s_1) \phi_{c'}^{(0)}(\mathbf{k}_1) g_{dd'}(s_1) \phi_{d'}^{(0)}(\mathbf{k} - \mathbf{k}_1), \quad (52)$$

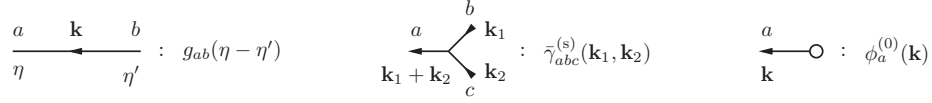


FIG. 4: Diagrammatic representation of the basic mathematical building blocks of the solutions. *Left panel:* the linear propagator $g_{ab}(\eta - \eta')$. *Middle panel:* the interaction vertex $\bar{\gamma}_{abc}^{(s)}(\mathbf{k}_1, \mathbf{k}_2)$. The sticks are not part of the vertex and are present only to show the correct number of incoming and outgoing lines. *Right panel:* the initial field $\phi_a^{(0)}(\mathbf{k})$, denoted by the empty dot. The stick with the arrow serves only to show that an initial condition must always be connected to a diagram with a line going into the diagram, i.e. oriented away from the initial condition itself.

which are nothing but Eqs (46) and (47) (after performing the s_1 integral in Eq. (52)). Similarly, evaluating the third diagram, we obtain Eq. (49), and so on.

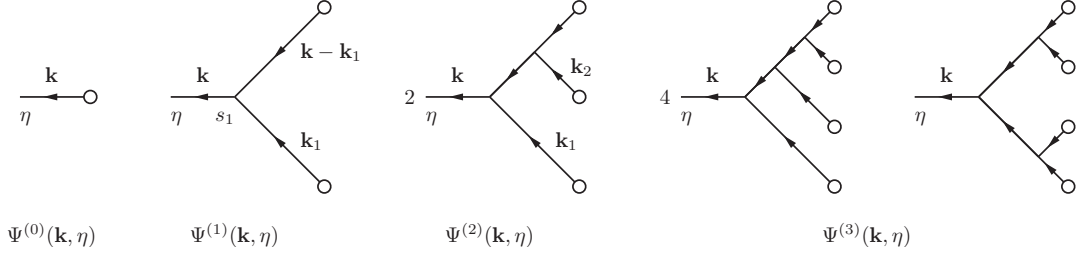


FIG. 5: Graphical representation of the topologically distinct Feynman diagrams for the perturbation theory up to third order. From left to right we show, $\Psi_a^{(n)}(\mathbf{k})$, for $n \in \{0, 1, 2, 3\}$, with the last two diagrams contributing to $n = 3$.

IV. STATISTICS

A. Two-point covariance matrix of density and velocity modes

In cosmology rather than modeling $\Psi_a(\mathbf{k})$ at a particular point, we are more interested in computing statistical averages of various products of the fields at different points in space. We shall represent these statistical averages as: $\langle \dots \rangle$. For mean zero fields, we must have $\langle \Psi_a(\mathbf{k}) \rangle = 0$. Thus the lowest order statistic of interest to us is the two-point correlation function, or power spectrum, of $\Psi_a(\mathbf{k})$, which can be defined:

$$\langle \Psi_a(\mathbf{k}, \eta) \Psi_b(\mathbf{k}', \eta) \rangle = P_{ab}(\mathbf{k}, \eta) \delta^D(\mathbf{k} + \mathbf{k}'). \quad (53)$$

B. Two-point covariance matrix of initial fields

Throughout we will assume that the initial conditions are Gaussian. Consequently the statistical properties of the fields $\phi_a^{(0)}(\mathbf{k})$ are then completely characterized by the two-point covariance matrix:

$$\langle \phi_a^{(0)}(\mathbf{k}) \phi_b^{(0)}(\mathbf{k}') \rangle \equiv \mathcal{P}_{ab}^{(0)}(k) \delta^D(\mathbf{k} + \mathbf{k}'). \quad (54)$$

For the case of a CDM and baryon fluid this matrix takes the explicit form:

$$\mathcal{P}_{ab}^{(0)}(k) = \begin{bmatrix} u_1^2 [T^c(k)]^2 & u_1 u_2 [T^c(k)]^2 & u_1 u_3 T^c(k) T^b(k) & u_1 u_4 T^c(k) T^b(k) \\ u_1 u_2 [T^c(k)]^2 & u_2^2 [T^c(k)]^2 & u_2 u_3 T^c(k) T^b(k) & u_2 u_4 T^c(k) T^b(k) \\ u_1 u_3 T^c(k) T^b(k) & u_2 u_3 T^c(k) T^b(k) & u_3^2 [T^b(k)]^2 & u_3 u_4 [T^b(k)]^2 \\ u_1 u_4 T^c(k) T^b(k) & u_2 u_4 T^c(k) T^b(k) & u_3 u_4 [T^b(k)]^2 & u_4^2 [T^b(k)]^2 \end{bmatrix} \mathcal{P}_0(k), \quad (55)$$

where we defined $\mathcal{P}_0(k) \delta^D(\mathbf{k} + \mathbf{k}') = \langle \delta_0(\mathbf{k}) \delta_0(\mathbf{k}') \rangle$, to be the power spectrum of primordial density fluctuations: i.e. $\mathcal{P}_0 \propto k^n$, with $n = 1$ for the usual Harrison-Zel'dovich spectrum. The two-point correlation matrix of the

initial fields may be expressed more compactly if we choose large-scale growing mode initial conditions, $(u_a = u_a^{(1)} = (1, 1, 1, 1))$, whereupon

$$\mathcal{P}_{ab}^{(0)}(k) = T_a(k)T_b(k)\mathcal{P}_0(k) , \quad (56)$$

with $[T_a(k)]^T \equiv [T^c(k), T^c(k), T^b(k), T^b(k)]$.

For Gaussian initial conditions all of the multi-point correlators of the initial $\phi_a^{(0)}(\mathbf{k})$ can be computed using Wick's theorem: all higher order correlators involving an odd number of fields vanish, while for an even number, there are $(2n - 1)!!$ contributions corresponding to the number of different pairings of the $2n$ fields:

$$\left\langle \phi_{a_1}^{(0)}(\mathbf{k}_1) \dots \phi_{a_{2n}}^{(0)}(\mathbf{k}_{2n}) \right\rangle = \sum_{\text{all pair associations}} \prod_{\text{p pairs of } (i,j)} \left\langle \phi_{a_i}^{(0)}(\mathbf{k}_i) \phi_{a_j}^{(0)}(\mathbf{k}_j) \right\rangle . \quad (57)$$

For later use, we now also introduce a diagrammatic representation of the initial power spectrum matrix, see Fig. 6.

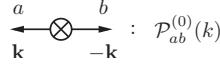


FIG. 6: Diagrammatic representation of the initial power spectrum matrix. The averaged pair of initial fields is denoted by the crossed dot, with the sticks and arrows serving only to show that each initial power spectrum will have two outgoing lines attached in any diagram.

C. The non-linear propagator

As the non-linear interactions are turned on, the evolution of the initial field breaks away from the simple scaling, $\Psi_a(\mathbf{k}, \eta) = g_{ab}(\eta)\phi_b^{(0)}(\mathbf{k})$. The deviations can be thought of as, *erasing the memory of the mode to its initial conditions*. This concept can be made more concrete, through introducing the non-linear propagator [1, 26]:

$$G_{ab}(\mathbf{k}, \eta)\delta^D(\mathbf{k} - \mathbf{k}') \equiv \left\langle \frac{\delta\Psi_a(\mathbf{k}, \eta)[\phi^{(0)}]}{\delta\phi_b^{(0)}(\mathbf{k}')} \right\rangle . \quad (58)$$

This means that we take the functional derivative of the full solution $\Psi_a(\mathbf{k}, \eta)$ with respect to the initial condition $\phi_b^{(0)}(\mathbf{k}')$, and then perform the ensemble average. Note that the non-linear propagator G_{ab} is defined with the momentum conserving delta function factored out. The expectation is taken since, again, it is the average evolution of the mode away from its initial conditions that we are interested in.

In perturbation theory, the full solution is given as in Eq. (41), and thus

$$G_{ab}(\mathbf{k}, \eta) = \sum_{l=0}^{\infty} \delta G_{ab}^{(l)}(\mathbf{k}, \eta) , \quad (59)$$

where

$$\delta G_{ab}^{(l)}(\mathbf{k}, \eta)\delta^D(\mathbf{k} - \mathbf{k}') = \left\langle \frac{\delta\Psi_a^{(2l)}(\mathbf{k}, \eta)[\phi^{(0)}]}{\delta\phi_b^{(0)}(\mathbf{k}')} \right\rangle . \quad (60)$$

Notice that in the above equation we only consider contributions to the propagator that come from terms in the expansion of $\Psi_a(\mathbf{k}, \eta)$ with an odd number of initial conditions, i.e. only terms $\Psi_a^{(j)}(\mathbf{k}, \eta)$ with j an even number contribute. This owes to the fact that, for non-linear fields involving an even number of initial conditions, after performing the functional differentiation we are left with products that involve an isolated initial field, which vanishes on taking the expectation: $\langle \phi_a^{(0)}(\mathbf{k}) \rangle = 0$. Recall that we take $j = 0$ as the first term in the perturbative series for Ψ_a . Thus the total non-linear propagator up to one-loop level can be written:

$$G_{ab}^{(1)}(\mathbf{k}, \eta) = g_{ab}(\eta) + \delta G_{ab}^{(1)}(\mathbf{k}, \eta) , \quad (61)$$

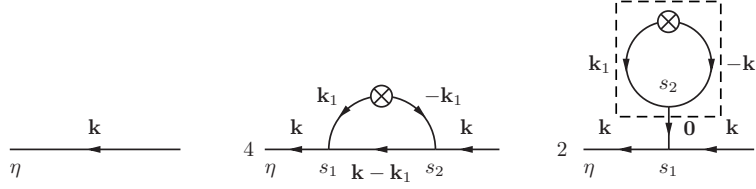


FIG. 7: The diagrams for the one-loop non-linear propagator $G^{(1)}(\mathbf{k}, \eta)$. The first diagram represents Eq. (27); the second Eq. (62); and the last diagram contains a tadpole (marked with the dashed box) and thus evaluates to zero.

where we used the fact that $\delta G_{ab}^{(0)}(\mathbf{k}, \eta) = g_{ab}(\eta)$, and where [26],

$$\begin{aligned} \delta G_{ab}^{(1)}(\mathbf{k}, \eta) &= 4 \int_0^\eta d\eta' \int_0^\eta d\eta'' g_{ab'}(\eta - \eta') \int d^3\mathbf{k}_1 \bar{\gamma}_{b'cd}^{(s)}(\mathbf{k}_1, \mathbf{k} - \mathbf{k}_1) g_{de}(\eta' - \eta'') \\ &\quad \times \bar{\gamma}_{efg}^{(s)}(-\mathbf{k}_1, \mathbf{k}) g_{cc'}(\eta') g_{ff'}(\eta'') g_{gb}(\eta'')(\mathbf{k}_1) \mathcal{P}_{c'f'}^{(0)}(k_1) . \end{aligned} \quad (62)$$

In Appendix B we present full details of the calculation for Eq. (60) explicitly for $j = 0, 1, 2$.

As for the case of the perturbative solutions to Ψ_a , the series expansion for the non-linear propagator with arbitrary numbers of loops can also be constructed in a diagrammatic fashion. Assuming Gaussian initial conditions, the Feynman rules for computing the n -loop correction to the propagator, $\delta G_{ab}^{(n)}(\mathbf{k}, \eta)$ are:

1. Draw all tree diagrams corresponding to $\Psi^{(2n)}(\mathbf{k}, \eta)$ as described in §III B. Recall that these diagrams involve $2n + 1$ initial fields each.
2. For any specific tree, drop any one initial condition, labeling the incoming line thus created with the momentum \mathbf{k} (this corresponds to the functional derivative and dropping the delta function). Pair the remaining $2n$ initial fields in all possible ways into n initial power spectra, as dictated by Wick's theorem (corresponding to the ensemble averaging). Any specific tree then leads to $(2n + 1)(2n - 1)!! = (2n + 1)!!$ n -loop diagrams, not all of which need to be topologically distinct. Diagrams containing a “tadpole” as a subdiagram (i.e. a subdiagram with a single external line) may be dropped, since they are zero, as explained below.
3. Follow Steps 2–4 of §III B. When assigning the lines their momenta, ensure that the two lines emanating from an initial power spectrum carry equal and opposite momenta. Identify the various pieces of each diagram with the mathematical expressions as shown in Figs 4 and 6. (The number of independent momenta to integrate over in Step 4 will be just the number of independent loops, n .)
4. Each diagram carries the appropriate factor of 2^n inherited from the original tree diagram. As noted above, it is possible that a specific loop diagram arises more than once. Of course such a diagram needs to be computed only once, but one must take account of its multiplicity explicitly.
5. The value of $\delta G_{ab}^{(n)}(\mathbf{k}, \eta)$ is given by the sum over the values of all diagrams coming from all trees.

Fig. 7 shows all diagrams that arise in the computation of the one-loop propagator, including the symmetry factor computed in Step 4 above. Only the first two diagrams give non-vanishing contributions. The last diagram contains a tadpole (marked with the dashed box) and this gives zero contribution, since for each individual tadpole momentum conservation implies: $\alpha(\mathbf{k}, -\mathbf{k}) = \beta(\mathbf{k}, -\mathbf{k}) = 0$. Hence, diagrams containing tadpoles vanish.

The power of the above graphical approach is that if one inspects the non-vanishing one-loop diagrams and uses the Feynman rules, then one can immediately write down the perturbative correction, as in Eq. (62).

D. Perturbative representation of the power spectrum

A perturbative expansion for the non-linear power spectrum may be obtained through insertion of the non-linear fields $\Psi_a^{(n)}$ (c.f. Eq. (45)) into Eq. (53), whereupon

$$P_{ab}(\mathbf{k}, \eta) = \sum_{l=0}^{\infty} \delta P_{ab}^{(l)}(\mathbf{k}, \eta) . \quad (63)$$

On assuming Gaussian initial conditions, then from Wick's theorem we find that only those products of fields that involve an even number of initial conditions contribute to the non-linear power spectrum. Consequently we may write,

$$\delta P_{ab}^{(l)}(\mathbf{k}, \eta) \delta^D(\mathbf{k} + \mathbf{k}') = \sum_{j=0}^{2l} \left\langle \Psi_a^{(j)}(\mathbf{k}, \eta) \Psi_b^{(2l-j)}(\mathbf{k}', \eta) \right\rangle. \quad (64)$$

On taking all contributions to the power spectrum matrix up to one-loop, $l = 1$, we have:

$$P_{ab} = \delta P_{ab}^{(0)} + \delta P_{ab}^{(1)}; \quad (65)$$

where the linear theory contribution (assuming large-scale growing mode initial conditions) is given by:

$$\begin{aligned} \delta P_{ab}^{(0)}(\mathbf{k}, \eta) \delta^D(\mathbf{k} + \mathbf{k}') &= \left\langle \Psi_a^{(0)}(\mathbf{k}, \eta) \Psi_b^{(0)}(\mathbf{k}', \eta) \right\rangle; \\ &= g_{aa'}(\eta) T_{a'}(k) g_{bb'}(\eta) T_{b'}(k) \mathcal{P}_0(k) \delta^D(\mathbf{k} + \mathbf{k}'). \end{aligned} \quad (66)$$

We may also write the above expression using conventional matrix notation:

$$\mathbf{P}^{(0)}(\mathbf{k}, \eta) = \mathbf{g}(\eta) \mathbf{T}(k) \mathbf{T}^T(k) \mathbf{g}^T(\eta) \mathcal{P}_0(k). \quad (67)$$

The one-loop corrections to the power spectrum are written:

$$\delta P_{ab}^{(1)}(\mathbf{k}, \eta) \delta^D(\mathbf{k} + \mathbf{k}') = \left\langle \Psi_a^{(0)}(\mathbf{k}, \eta) \Psi_b^{(2)}(\mathbf{k}', \eta) \right\rangle + \left\langle \Psi_a^{(1)}(\mathbf{k}, \eta) \Psi_b^{(1)}(\mathbf{k}', \eta) \right\rangle + \left\langle \Psi_a^{(2)}(\mathbf{k}, \eta) \Psi_b^{(0)}(\mathbf{k}', \eta) \right\rangle. \quad (68)$$

Consider the sum of the first and last terms, we shall call these the “reducible” contributions and denote the sum of these terms: $\delta P_{ab,R}^{(1)}$. It was shown by [26] that the non-linear propagator plays the role of a Green's function in the two-point sense, $\langle \Psi_a \phi_b^{(0)} \rangle = G_{ac} \langle \phi_c^{(0)} \phi_b^{(0)} \rangle$, and furthermore that this property holds order-by-order: $\langle \Psi_a^{(2n)} \phi_b^{(0)} \rangle = \delta G_{ac}^{(n)} \langle \phi_c^{(0)} \phi_b^{(0)} \rangle$. On applying the above relations, it is straightforward to see that we must have

$$\begin{aligned} \delta P_{ab,R}^{(1)}(\mathbf{k}, \eta) \delta^D(\mathbf{k} + \mathbf{k}') &= \left[\left\langle \Psi_a^{(0)}(\mathbf{k}, \eta) \Psi_b^{(2)}(\mathbf{k}', \eta) \right\rangle + \left\langle \Psi_a^{(2)}(\mathbf{k}, \eta) \Psi_b^{(0)}(\mathbf{k}', \eta) \right\rangle \right] \\ &= \left[g_{ac}(\eta) \delta G_{bd}^{(1)}(\mathbf{k}', \eta) \mathcal{P}_{cd}^{(0)}(\mathbf{k}') + \delta G_{ac}^{(1)}(\mathbf{k}, \eta) g_{bd}(\eta) \mathcal{P}_{cd}^{(0)}(\mathbf{k}) \right] \delta^D(\mathbf{k} + \mathbf{k}'). \end{aligned} \quad (69)$$

Specializing to growing mode initial conditions, and using momentum conservation, we find

$$\delta P_{ab,R}^{(1)}(\mathbf{k}, \eta) = \left[g_{ac}(\eta) \delta G_{bd}^{(1)}(\mathbf{k}, \eta) + \delta G_{ac}^{(1)}(\mathbf{k}, \eta) g_{bd}(\eta) \right] T_c(k) T_d(k) \mathcal{P}_0(k). \quad (70)$$

In particular, we can write this in conventional matrix notation as

$$\delta \mathbf{P}_R^{(1)}(\mathbf{k}, \eta) = \left[\mathbf{g}(\eta) \mathbf{T}(k) \mathbf{T}^T(k) [\delta \mathbf{G}^{(1)}]^T(\mathbf{k}, \eta) + \delta \mathbf{G}^{(1)}(\mathbf{k}, \eta) \mathbf{T}(k) \mathbf{T}^T(k) \mathbf{g}^T(\eta) \right] \mathcal{P}_0(k). \quad (71)$$

Adding Eqs (67) and (71), we see that the sum $[\mathbf{P}^{(0)}(\mathbf{k}, \eta) + \delta \mathbf{P}_R^{(1)}(\mathbf{k}, \eta)]$ is nothing but the one-loop truncation of the all-order expression

$$\mathbf{P}_R(\mathbf{k}, \eta) = \mathbf{G}(\mathbf{k}, \eta) \mathbf{T}(k) \mathbf{T}^T(k) \mathbf{G}^T(\mathbf{k}, \eta) \mathcal{P}_0(k). \quad (72)$$

The all-order reducible contribution collects all corrections to $\mathbf{P}(\mathbf{k}, \eta)$ that are proportional to the initial power spectrum at the same scale k .

Turning now to the second term in Eq. (68), conventionally called the “mode-coupling” contribution, we find that it can be written [1]:

$$\begin{aligned} \delta P_{ab,MC}^{(1)}(\mathbf{k}, \eta) &= 2 \int_0^\eta d\eta' \int_0^\eta d\eta'' \int d^3\mathbf{k}_1 g_{ac}(\eta - \eta') \bar{\gamma}_{cde}^{(s)}(\mathbf{k}_1, \mathbf{k} - \mathbf{k}_1) g_{dd'}(\eta') g_{ee'}(\eta') \\ &\quad \times g_{bf}(\eta - \eta'') \bar{\gamma}_{fgh}^{(s)}(-\mathbf{k}_1, \mathbf{k}_1 - \mathbf{k}) g_{gg'}(\eta'') g_{hh'}(\eta'') \mathcal{P}_{d'g'}^{(0)}(k_1) \mathcal{P}_{e'h'}^{(0)}(|\mathbf{k} - \mathbf{k}_1|). \end{aligned} \quad (73)$$

The mode-coupling piece includes corrections coming from modes other than k in the initial power spectrum. In particular, we see from Eq. (73) that the one-loop mode-coupling correction involves the convolution of two initial

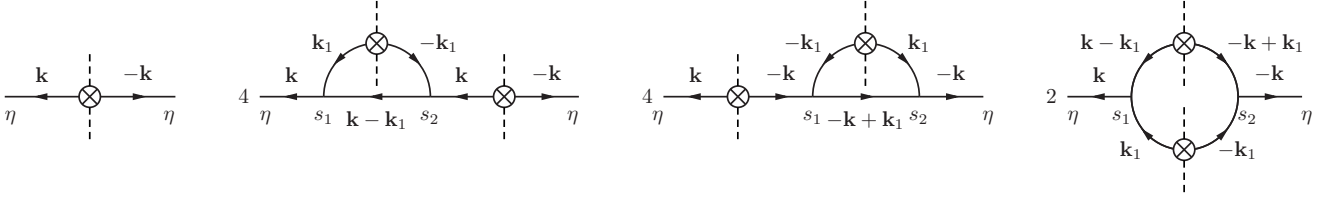


FIG. 8: The non-zero diagrams for the one-loop power spectrum $P^{(1)}(\mathbf{k}, \eta)$. The dashed lines indicate the points at which the two trees were glued together. The first diagram represents Eq. (66); the second and third graphs are the two reducible contributions in Eq. (71); and the fourth graph represents the mode-coupling term of Eq. (73).

power spectra with a specific kernel. At higher loop orders, the mode-coupling pieces involve convolutions of more than two initial powers.

The upshot is that for growing mode initial conditions, we can write the full power spectrum as

$$\mathbf{P}(\mathbf{k}, \eta) = \mathbf{G}(\mathbf{k}, \eta) \mathbf{T}(k) \mathbf{T}^T(k) \mathbf{G}^T(\mathbf{k}, \eta) \mathcal{P}_0(k) + \mathbf{P}_{\text{MC}}(\mathbf{k}, \eta). \quad (74)$$

At this point we may extend our diagrammatic description: assuming Gaussian initial conditions, the Feynman rules for computing the n -loop correction to the power spectrum, $\delta P_{ab}^{(n)}(\mathbf{k}, \eta)$ are:

1. Draw the sum of all tree diagrams corresponding to $\Psi^{(j)}(\mathbf{k}, \eta)$, and the sum of diagrams corresponding to $\Psi^{(2n-j)}(\mathbf{k}', \eta)$ as described in §III B, including the arrows on the lines.
2. Formally “multiply” these two sums using distributivity. It is convenient to draw one set of diagrams flipped around the vertical axis, so that after the pairing of diagrams for $\Psi^{(j)}(\mathbf{k}, \eta)$ with those for $\Psi^{(2n-j)}(\mathbf{k}, \eta)$, their initial conditions face each other. Next, pair the $2n + 2$ initial fields into $n + 1$ initial power spectra (some pairings may lead to the same loop diagram). Disregard diagrams that contain a tadpole as a subdiagram. (This includes disconnected diagrams in particular.)
3. Follow Step 3 of §IV C.
4. Each diagram carries the appropriate factor of 2^{r+s} inherited from the two original tree diagrams. As noted above, it is possible that a specific loop diagram arises more than once. Such a diagram needs to be computed only once, but its multiplicity must be taken into account.
5. The value of $\delta P_{ab}^{(n)}(\mathbf{k}, \eta)$ is given by the sum over the values of these diagrams for all $j = 0, \dots, 2n$.

Fig. 8 shows all non-zero diagrams for the power spectrum up to one-loop order, including the symmetry factor computed in Step 4 above. In particular, notice how Eq. (69) is very simple to write down by inspecting the second and third graphs. The last diagram corresponds to the mode-coupling piece. Evidently Eq. (73) may be written down immediately by inspecting this graph.

V. ONE-LOOP CORRECTIONS TO THE POWER SPECTRUM

A. The non-linear propagator

In §IV, we defined the non-linear propagator $G_{ab}(\mathbf{k}, \eta)$ as the ensemble average of the functional derivative of the full solution $\Psi_a(\mathbf{k}, \eta)$ by the initial condition $\phi_b^{(0)}(\mathbf{k}')$, without the delta function for momentum conservation (c.f. Eq. (58)). It was shown to have a perturbative expansion (c.f. Eqs (59) and (60)) and terms up to one-loop level were computed in Appendix B. Here we further develop the one-loop expression for the case of $N = 2$ fluids.

To begin, let us reconsider Eq. (62), we may expand all of the linear propagators, $g_{ab}(\eta)$, using Eq. (27) to obtain,

$$\begin{aligned} \delta G_{aa'}^{(1)}(\mathbf{k}, \eta) &= 4 \int_0^\eta d\eta' \sum_{l_1} g_{ab, l_1} e^{l_1(\eta - \eta')} \int d^3 \mathbf{k}_1 \bar{\gamma}_{bcd}^{(s)}(\mathbf{k}_1, \mathbf{k} - \mathbf{k}_1) \sum_{l_2} g_{cc', l_2} e^{l_2 \eta'} \int_0^{\eta'} d\eta'' \sum_{l_3} g_{de, l_3} e^{l_3(\eta' - \eta'')} \\ &\quad \times \bar{\gamma}_{efg}^{(s)}(-\mathbf{k}_1, \mathbf{k}') \sum_{l_4} g_{ff', l_4} e^{l_4 \eta''} \sum_{l_5} g_{ga', l_5} e^{l_5 \eta''} \mathcal{P}_{c'f'}^{(0)}(k_1). \end{aligned} \quad (75)$$

On rearranging the above expression we find,

$$\begin{aligned} \delta G_{aa'}^{(1)}(\mathbf{k}, \eta) &= 4 \sum_{l_1, \dots, l_5} e^{l_1 \eta} \int_0^\eta d\eta' e^{(l_2+l_3-l_1)\eta'} \int_0^{\eta'} d\eta'' e^{(l_4+l_5-l_3)\eta''} \\ &\times g_{ab, l_1} \int d^3 \mathbf{k}_1 \bar{\gamma}_{bcd}^{(s)}(\mathbf{k}_1, \mathbf{k} - \mathbf{k}_1) g_{cc', l_2} g_{de, l_3} \bar{\gamma}_{efg}^{(s)}(-\mathbf{k}_1, \mathbf{k}') g_{ff', l_4} g_{ga', l_5} \mathcal{P}_{c'f'}^{(0)}(k_1) . \end{aligned} \quad (76)$$

Considering the integrals over η' and η'' , these may be conveniently evaluated using the algebraic function $I_2(l_2, l_1, \eta)$ (c.f. Eq. (50)). Thus our final expression for the one-loop propagator takes the form:

$$\begin{aligned} \delta G_{aa'}^{(1)}(\mathbf{k}, \eta) &= 4 \sum_{l_1, \dots, l_5} e^{l_1 \eta} I_2(l_2 + l_3 - l_1, l_4 + l_5 - l_3; \eta) \\ &\times g_{ab, l_1} \int d^3 \mathbf{k}_1 \bar{\gamma}_{bcd}^{(s)}(\mathbf{k}_1, \mathbf{k} - \mathbf{k}_1) g_{cc', l_2} g_{de, l_3} \bar{\gamma}_{efg}^{(s)}(-\mathbf{k}_1, \mathbf{k}) g_{ff', l_4} g_{ga', l_5} \mathcal{P}_{c'f'}^{(0)}(k_1) . \end{aligned} \quad (77)$$

This expression may be reorganized so that the time dependent algebraic functions, the constant coefficient matrices $g_{ab, l}$ and the k -dependent matrices are grouped together. Further, if we take large-scale growing mode initial conditions, $u_a = u_a^{(1)} = (1, 1, 1, 1)$, then we find that the propagator may be written,

$$\begin{aligned} \delta G_{aa'}^{(1)}(\mathbf{k}, \eta) &= 4 \sum_{l_1, \dots, l_5} e^{l_1 \eta} I_2(l_2 + l_3 - l_1, l_4 + l_5 - l_3; \eta) g_{ab, l_1} g_{cc', l_2} g_{de, l_3} g_{ff', l_4} g_{ga', l_5} \\ &\times \int d^3 \mathbf{k}_1 \bar{\gamma}_{bcd}^{(s)}(\mathbf{k}_1, \mathbf{k} - \mathbf{k}_1) \bar{\gamma}_{efg}^{(s)}(-\mathbf{k}_1, \mathbf{k}) T_{c'}(k_1) T_{f'}(k_1) \mathcal{P}_0(k_1) . \end{aligned} \quad (78)$$

In Appendix D 1 we show that the integral over the product of vertex matrices and the power spectrum matrix leads to five linearly independent functions of k for each independent product $T_i(k_1)T_j(k_1)$. Hence, it is possible to write the propagator,

$$\delta G_{ab}^{(1)}(\mathbf{k}, \eta) = \sum_{n=1}^5 [f_n^{\delta^c \delta^c}(k) A_{ab, n}^{\delta^c \delta^c}(\eta) + f_n^{\delta^c \delta^b}(k) A_{ab, n}^{\delta^c \delta^b}(\eta) + f_n^{\delta^b \delta^b}(k) A_{ab, n}^{\delta^b \delta^b}(\eta)] , \quad (79)$$

where the summation in n runs over the set of independent integrals $f_n^{\delta^i \delta^j}(k)$ that are defined in Appendix D 1. The complete results for the $A_{ab, n}^{\delta^c \delta^c}(\eta)$, $A_{ab, n}^{\delta^c \delta^b}(\eta)$ and $A_{ab, n}^{\delta^b \delta^b}(\eta)$ functions are too lengthy to reproduce here, but their general structure is the following:

$$A_{ab, n}^{\delta^i \delta^j}(\eta) = \sum_l P_{ab, n, l}^{\delta^i \delta^j}(w_2) e^{l\eta} + Q_{ab, n}^{\delta^i \delta^j}(w_2) \eta , \quad (80)$$

where the summation in l (in this equation only) runs over the set $\{3, 2, 3/2, 1, 0, -1/2, -1, -3/2, -2, -5/2\}$, and the $P_{ab, n, l}^{\delta^i \delta^j}(w_2)$ and $Q_{ab, n}^{\delta^i \delta^j}(w_2)$ functions multiplying each η -structure are at most third order polynomials in w_2 (we used $w_1 = 1 - w_2$).

B. Mode-coupling power spectrum

Consider next the mode-coupling contribution to the power spectrum. At the one-loop level, it is given by Eq. (73). We may develop this expression further by again expanding all of the linear propagators using Eq. (27) to obtain,

$$\begin{aligned} \delta P_{ab, \text{MC}}^{(1)}(\mathbf{k}, \eta) &= 2 \int_0^\eta d\eta' \int_0^\eta d\eta'' \int d^3 \mathbf{k}_1 \sum_{l_1} g_{ac, l_1} e^{l_1(\eta - \eta')} \bar{\gamma}_{cde}^{(s)}(\mathbf{k}_1, \mathbf{k} - \mathbf{k}_1) \sum_{l_2} g_{dd', l_2} e^{l_2 \eta'} \sum_{l_3} g_{ee', l_3} e^{l_3 \eta'} \\ &\times \sum_{l_4} g_{bf, l_4} e^{l_4(\eta - \eta'')} \bar{\gamma}_{fgh}^{(s)}(-\mathbf{k}_1, \mathbf{k}_1 - \mathbf{k}) \sum_{l_5} g_{gg', l_5} e^{l_5 \eta''} \sum_{l_6} g_{hh', l_6} e^{l_6 \eta''} \mathcal{P}_{d'g'}^{(0)}(k_1) \mathcal{P}_{e'h'}^{(0)}(|\mathbf{k} - \mathbf{k}_1|) . \end{aligned} \quad (81)$$

On reorganizing this equation and collecting together all of the time dependent terms, we find

$$\begin{aligned} \delta P_{ab, \text{MC}}^{(1)}(\mathbf{k}, \eta) &= 2 \int_0^\eta d\eta' \sum_{l_1, l_2, l_3} e^{l_1 \eta} e^{(l_2+l_3-l_1)\eta'} \int_0^\eta d\eta'' \sum_{l_4, l_5, l_6} e^{l_4 \eta} e^{(l_5+l_6-l_4)\eta''} \\ &\times \int d^3 \mathbf{k}_1 g_{ac, l_1} \bar{\gamma}_{cde}^{(s)}(\mathbf{k}_1, \mathbf{k} - \mathbf{k}_1) g_{dd', l_2} g_{ee', l_3} g_{bf, l_4} \bar{\gamma}_{fgh}^{(s)}(-\mathbf{k}_1, \mathbf{k}_1 - \mathbf{k}) g_{gg', l_5} g_{hh', l_6} \mathcal{P}_{d'g'}^{(0)}(k_1) \mathcal{P}_{e'h'}^{(0)}(|\mathbf{k} - \mathbf{k}_1|) . \end{aligned} \quad (82)$$

The integrals over η' and η'' are easily performed, and the result can be conveniently written in terms of the $I_1(l, \eta)$ function introduced in Eq. (48). Hence,

$$\begin{aligned} \delta P_{ab, \text{MC}}^{(1)}(\mathbf{k}, \eta) &= 2 \sum_{l_1, l_2, l_3} e^{l_1 \eta} I_1(l_2 + l_3 - l_1; \eta) \sum_{l_4, l_5, l_6} e^{l_4 \eta} I_1(l_5 + l_6 - l_4; \eta) \\ &\times \int d^3 \mathbf{k}_1 g_{ac, l_1} \bar{\gamma}_{cde}^{(s)}(\mathbf{k}_1, \mathbf{k} - \mathbf{k}_1) g_{dd', l_2} g_{ee', l_3} g_{bf, l_4} \bar{\gamma}_{fgh}^{(s)}(-\mathbf{k}_1, \mathbf{k}_1 - \mathbf{k}) g_{gg', l_5} g_{hh', l_6} \mathcal{P}_{d'g'}^{(0)}(k_1) \mathcal{P}_{e'h'}^{(0)}(|\mathbf{k} - \mathbf{k}_1|), \end{aligned} \quad (83)$$

which is our final expression for the mode-coupling contribution to the one-loop power spectrum. Upon setting large-scale growing mode initial conditions, $u_a = u_a^{(1)} = (1, 1, 1, 1)$, the above expression may be written as,

$$\begin{aligned} \delta P_{ab, \text{MC}}^{(1)}(\mathbf{k}, \eta) &= 2 \int d^3 \mathbf{k}_1 \mathcal{P}_0(k_1) \mathcal{P}_0(|\mathbf{k} - \mathbf{k}_1|) \\ &\times \sum_{l_1, l_2, l_3} e^{l_1 \eta} I_1(l_2 + l_3 - l_1; \eta) g_{ac, l_1} \bar{\gamma}_{cde}^{(s)}(\mathbf{k}_1, \mathbf{k} - \mathbf{k}_1) g_{dd', l_2} g_{ee', l_3} T_{d'}(k_1) T_{e'}(|\mathbf{k} - \mathbf{k}_1|) \\ &\times \sum_{l_4, l_5, l_6} e^{l_4 \eta} I_1(l_5 + l_6 - l_4; \eta) g_{bf, l_4} \bar{\gamma}_{fgh}^{(s)}(-\mathbf{k}_1, \mathbf{k}_1 - \mathbf{k}) g_{gg', l_5} g_{hh', l_6} T_{g'}(k_1) T_{h'}(|\mathbf{k} - \mathbf{k}_1|). \end{aligned} \quad (84)$$

In Appendix D 2 we show that the integration over the vertex matrices and power spectrum matrices leads to four linearly independent functions of k for each independent product $T_i(k_1) T_j(k_1) T_k(|\mathbf{k} - \mathbf{k}_1|) T_l(|\mathbf{k} - \mathbf{k}_1|)$ if $(ij) = (kl)$, and six independent functions otherwise. Furthermore, if $(ij) \neq (kl)$, then merely exchanging $(ij) \leftrightarrow (kl)$ does not lead to new independent integrals. Thus, the mode-coupling correction to the one-loop power spectrum can be written:

$$\begin{aligned} \delta P_{ab, \text{MC}}^{(1)}(\mathbf{k}, \eta) &= \sum_{n=1}^4 [f_n^{\delta^c \delta^c \delta^c \delta^c}(k) A_{ab, n}^{\delta^c \delta^c \delta^c \delta^c}(\eta) + f_n^{\delta^c \delta^b \delta^c \delta^b}(k) A_{ab, n}^{\delta^c \delta^b \delta^c \delta^b}(\eta) + f_n^{\delta^b \delta^b \delta^b \delta^b}(k) A_{ab, n}^{\delta^b \delta^b \delta^b \delta^b}(\eta)] \\ &+ \sum_{n=1}^6 [f_n^{\delta^c \delta^c \delta^c \delta^b}(k) A_{ab, n}^{\delta^c \delta^c \delta^c \delta^b}(\eta) + f_n^{\delta^c \delta^c \delta^b \delta^b}(k) A_{ab, n}^{\delta^c \delta^c \delta^b \delta^b}(\eta) + f_n^{\delta^c \delta^b \delta^b \delta^b}(k) A_{ab, n}^{\delta^c \delta^b \delta^b \delta^b}(\eta)], \end{aligned} \quad (85)$$

where the independent integrals $f_n^{\delta^i \delta^j \delta^k \delta^l}(k)$ are defined in Appendix D 2. The full results for the $A_{ab, n}^{\delta^i \delta^j \delta^k \delta^l}(\eta)$ coefficients are too lengthy to reproduce here, but their general structure is the following:

$$A_{ab, n}^{\delta^i \delta^j \delta^k \delta^l}(\eta) = \sum_l P_{ab, n, l}^{\delta^i \delta^j \delta^k \delta^l}(w_2) e^{l \eta}, \quad (86)$$

with $l \in \{4, 3, 5/2, 2, 3/1, 1, 1/2, 0, -1/2, -1, -3/2, -2, -5/2, -3\}$ (in this equation only), and $P_{ab, n, l}^{\delta^i \delta^j \delta^k \delta^l}(w_2)$ an (at most) fourth order polynomial in w_2 (we used $w_1 = 1 - w_2$).

VI. RESULTS: NON-LINEAR EVOLUTION OF CDM AND BARYON FLUID

A. Propagator

In Fig. 9 we present the evolution of the initial CDM (left panel) and baryon (right panel) density fluctuations under the action of the non-linear propagator, up to the one-loop level in the perturbation series. To show the effects of the non-linearity on the dynamics, we have divided through by the linearly evolved initial fields. We see that, for both CDM and baryons, on very large scales ($k < 0.01 h \text{ Mpc}^{-1}$), the modes retain memory of their initial configurations. However, on smaller scales the propagator drops away from unity as memory is rapidly lost. The non-linear decay scale of the propagator can be represented as the point where $G_{ia}^{(1)} \phi_a^{(0)} / g_{ib} \phi_b^{(0)} = e^{-1/2}$ with $i \in \{1, 3\}$ for CDM and baryon density perturbations. We notice that the decay scale becomes smaller as redshift increases, and that for both fluid species is essentially the same for all epochs. We also notice that the propagator eventually crosses zero, this is unphysical behaviour and signifies the breakdown of the validity of the one-loop expression.

B. Power spectra of CDM and baryons

Fig. 10 presents the results for the linear and non-linear evolution of the power spectra in the 2-component fluid model. The left and right panels show results for the CDM and the baryons, respectively. As expected from our

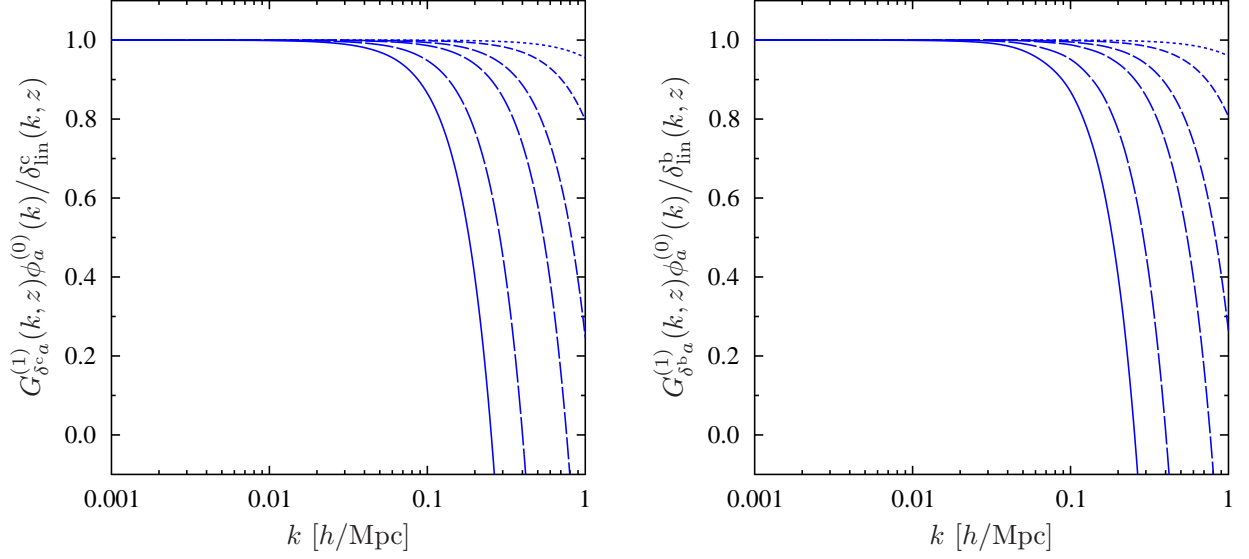


FIG. 9: Evolution of the initial density perturbations in the CDM plus baryon fluid under the action of the non-linear propagator up to one-loop level, as a function of spatial wavenumber k . Left and right panels present results for the CDM and baryon fluctuations, respectively. The linear evolution of the initial perturbation in each species has been scaled out, hence all lines approach unity on large scales. Solid through to dashed lines show results for redshifts $z = \{0, 1.0, 3.0, 5.0, 10.0, 20.0\}$.

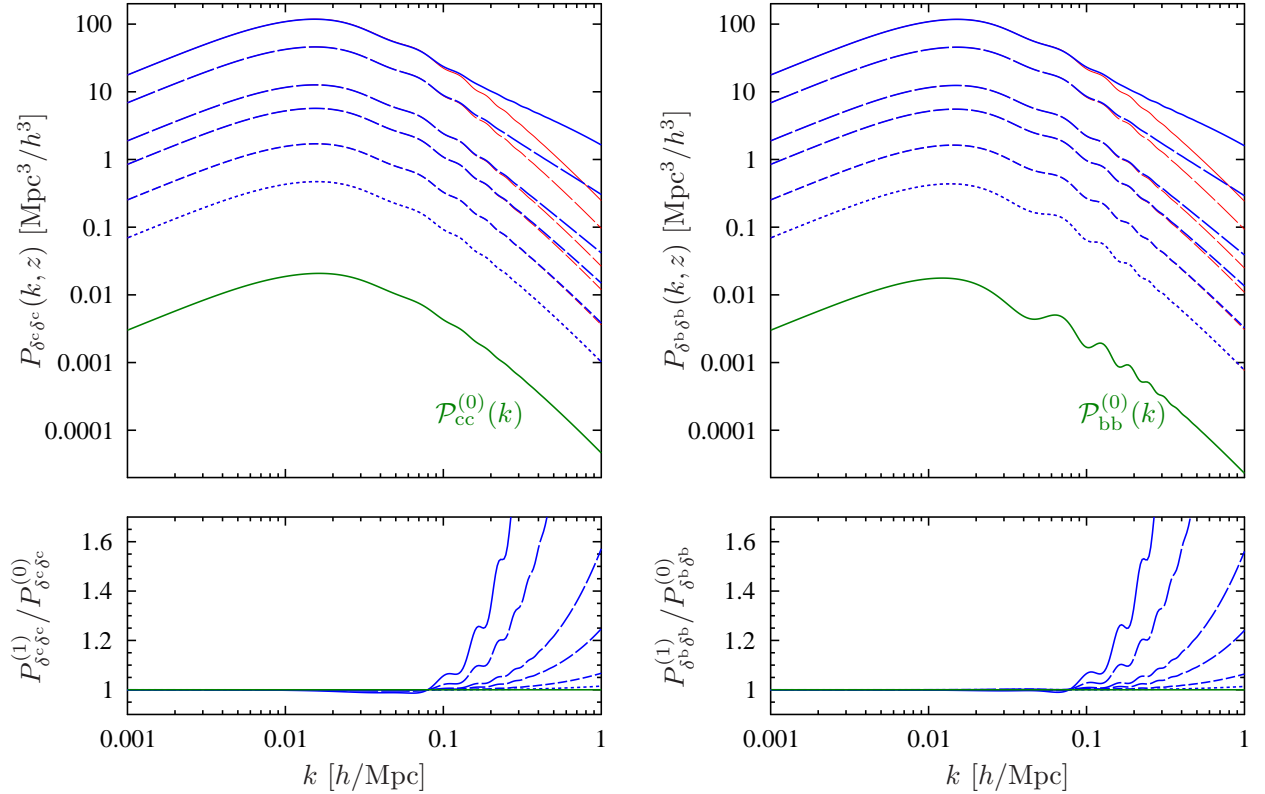


FIG. 10: Comparison of the linear and one-loop non-linear power spectrum for the CDM and baryons. *Top panels*: the absolute power as function of wavenumber. Left panels, show results for CDM, and right for the baryons. Red lines represent linear theory, and blue ones non-linear theory. The solid through to dashed lines show results for redshifts $z = \{0, 1.0, 3.0, 5.0, 10.0, 20.0\}$. Lowest solid green line shows the initial power spectrum. *Bottom panels*: show the ratio of the one-loop non-linear to linear theory power spectrum.

discussion in §II F and Fig. 2, we see that the initial CDM power spectrum ($z_i = 100$) is very smooth, whereas that for the baryon distribution is highly oscillatory (green solid lines labeled $\mathcal{P}_{cc}^{(0)}$ and $\mathcal{P}_{bb}^{(0)}$ in the plot). As the two fluids evolve under gravity the power grows, and in linear theory (red lines) larger amplitude BAO are induced in the CDM spectrum, whilst those in the baryon distribution are slowly damped.

The figure also shows how these results change when the non-linear evolution of the density fields is turned on. The non-linear power spectra are represented as blue lines, and we have included all terms up to one-loop level (c.f. Eq. (74)). At $z = 0$ and on very large scales ($k < 0.02 h \text{ Mpc}^{-1}$), the linear and non-linear calculations appear to agree well (solid lines). However, on smaller scales the agreement begins to breakdown. To investigate this in more detail, we take the ratio of the two spectra, and this is plotted in the lower panels of Fig. 2. From this we clearly see that there is a small suppression of power on scales of the order $k \sim 0.07 h \text{ Mpc}^{-1}$, this is known as the pre-virialization feature [44]. This is followed by a strong non-linear amplification at smaller scales. Interestingly, the relative non-linear boost at $z = 0$ appears to possess almost identical structure for both CDM and baryons. If we consider earlier times $z > 0$ (in the plots denoted by increasingly dashed line styles), then, besides the non-linear boosts being reduced, we note that the curves still maintain the same relative structure. As we will show in §VII, this can be attributed to the fact that the structure of the leading in η , one-loop corrections, take the same form for both CDM and baryons.

C. Comparison of the exact 2-component fluid with the approximate 1-component fluid

We now explore how our exact 2-component fluid results differ from those that would have been obtained had we used the 1-component fluid approach, along with the approximate recipe as was described in §I. In order to concentrate solely on the approximations introduced by using the 1-component fluid approach, we slightly modify the procedure for obtaining the initial power spectrum, from that set out in §I:

- 1'. Fix the cosmological model, specifying Ω_c and Ω_b , and hence f^b . Solve for the evolution of all perturbed species using the linearized coupled Einstein–Boltzmann equations. Obtain transfer functions for the CDM and baryons at some large redshift say $z = 100$.
- 2'. Use these transfer functions to generate the linear power spectrum matrix in the 2-component fluid theory, at the present day: i.e. $P_{ab}(k, z = 0) \approx g_{aa'}(z = 0)T_{a'}(k)g_{bb'}(z = 0)T_{b'}(k)Ak^n$. Using this power spectrum matrix, define the present day matter power spectrum as

$$P_{\bar{\delta}\bar{\delta}}(\mathbf{k}, z = 0) = (1 - f^b)^2 P_{\delta^c \delta^c}(\mathbf{k}, z = 0) + 2(1 - f^b)f^b P_{\delta^c \delta^b}(\mathbf{k}, z = 0) + (f^b)^2 P_{\delta^b \delta^b}(\mathbf{k}, z = 0). \quad (87)$$

One could further make the approximation that at the present day $\bar{\delta} = (1 - f_b)\delta^c + f_b\delta^b \approx \delta^c$, hence approximating the matter power spectrum as

$$P_{\bar{\delta}_A \bar{\delta}_A}(\mathbf{k}, z = 0) \approx P_{\delta^c \delta^c}(\mathbf{k}, z = 0). \quad (88)$$

The rest of the steps are unchanged from those discussed in §I. We shall refer to the initial conditions obtained using Eq. (87) as the “exact”, and those produced using Eq. (88) as the “approximate” 1-component fluid initial conditions, respectively.

Figs 11 and 12, present the ratio of the exact linear and non-linear CDM (Fig. 11) and baryon (Fig. 12) power spectra, with the power spectrum obtained from modeling CDM and baryons as an effective single matter fluid. The left and right panels show results obtained using the exact and approximate initial conditions for the 1-component fluid calculation. In all cases, the non-linear evolution is followed using the RPT framework, including all terms up to the one-loop level. For the case of CDM, we clearly see that at high redshift the approximation is rather poor, there being significantly more amplitude in the exact $N = 2$ model than the effective $N = 1$ model. We also note that there are strong BAO features in the ratio, and these increase with increasing redshift. These features are due to the fact that the $z = 0$ transfer function is used to model the initial conditions of the $N = 1$ matter fluid, and therefore can suppress power and artificially enhance the BAO. At early stages in the evolution, the systematic errors are between $\sim 4 - 5\%$ at $z = 20$, and between $\sim 2 - 3\%$ at $z = 10$. However, at later times the approximation is much better, and by $z = 3$ the errors are $< 1\%$, and by $z = 0$ are $< 0.5\%$.

On the other hand, the case for the baryons is worse. We see that the exact $N = 2$ results show less power than the approximate $N = 1$ counterpart and that this suppression increases with increasing redshift. Again we notice that there are BAO features in the residual, and the oscillation amplitude is much more significant. At early stages in the evolution the systematic errors are large: at $z = 20$ they are $\sim 25\%$, and by $z = 10$ are $\sim 15\%$. At later times the approximation is still quite poor: at $z = 3$ the errors are of the order $\sim 5\%$, and by $z = 0$ are still between $\sim 2 - 3\%$.

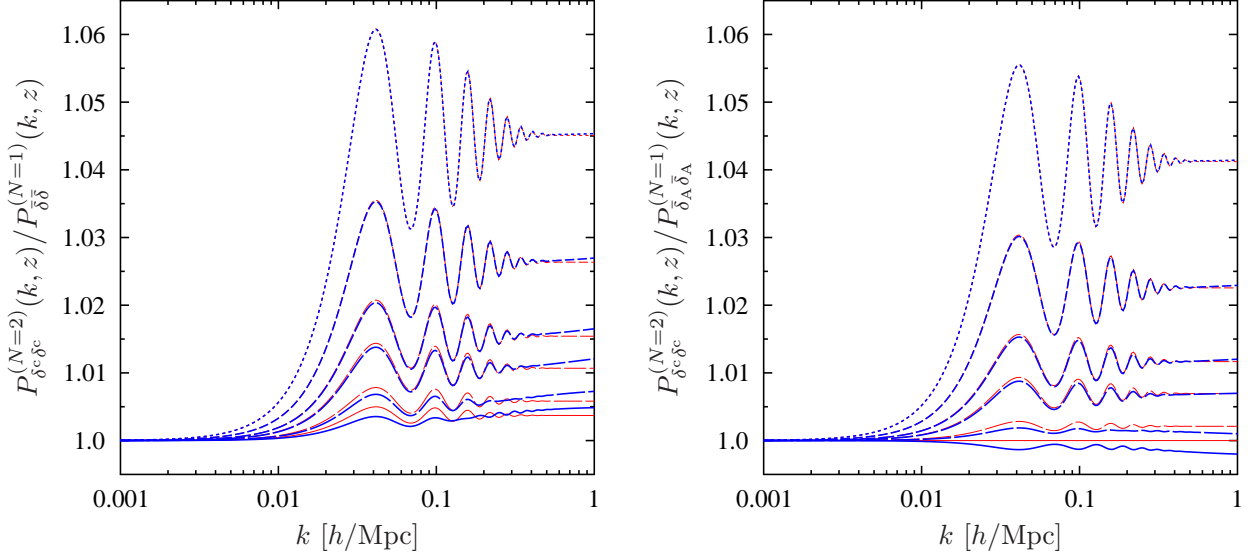


FIG. 11: Ratio of the CDM power spectrum obtained from the CDM and baryon 2-component fluid model, to the total matter spectrum obtained from the 1-component fluid approximation, as a function of wavenumber. Red lines show the ratio of power spectra in linear theory, while blue lines show the ratio of one-loop non-linear power spectra. *Left and right panels:* show results for the exact and approximate 1-component fluid initial conditions, respectively. Again, the solid through to dashed lines show results for redshifts $z = \{0, 1.0, 3.0, 5.0, 10.0, 20.0\}$.

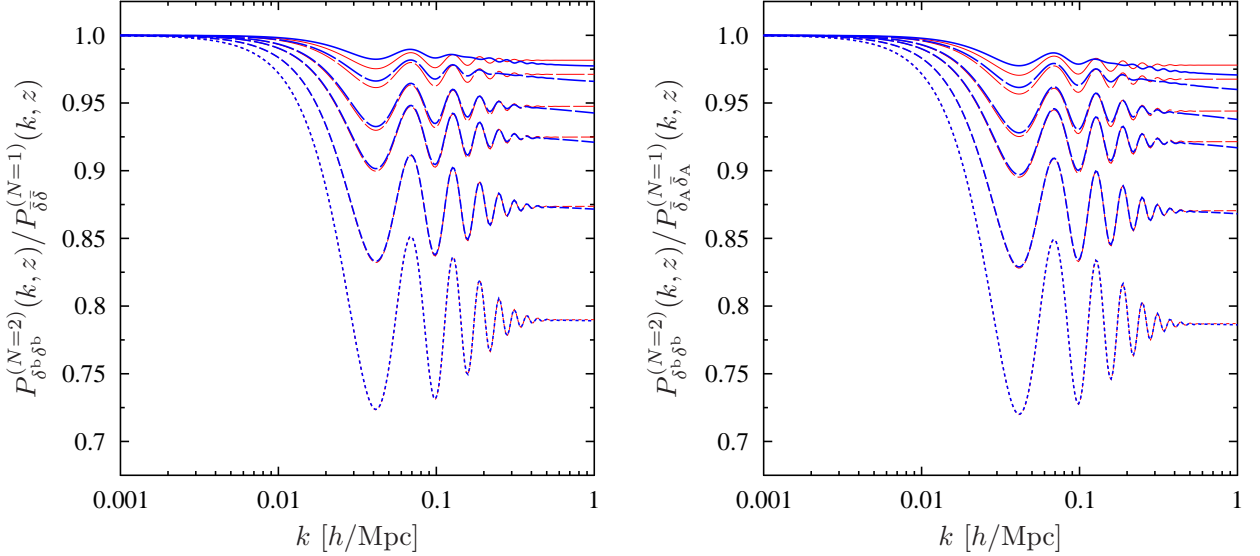


FIG. 12: Ratio of the baryon power spectrum obtained from the CDM and baryon 2-component fluid model, to the total matter spectrum obtained from the 1-component fluid approximation, as a function of wavenumber. Red lines show the ratio of power spectra in linear theory, while blue lines show the ratio of one-loop non-linear power spectra. *Left and right panels:* show results for the exact and approximate 1-component fluid initial conditions, respectively. Again, the solid through to dashed lines show results for redshifts $z = \{0, 1.0, 3.0, 5.0, 10.0, 20.0\}$.

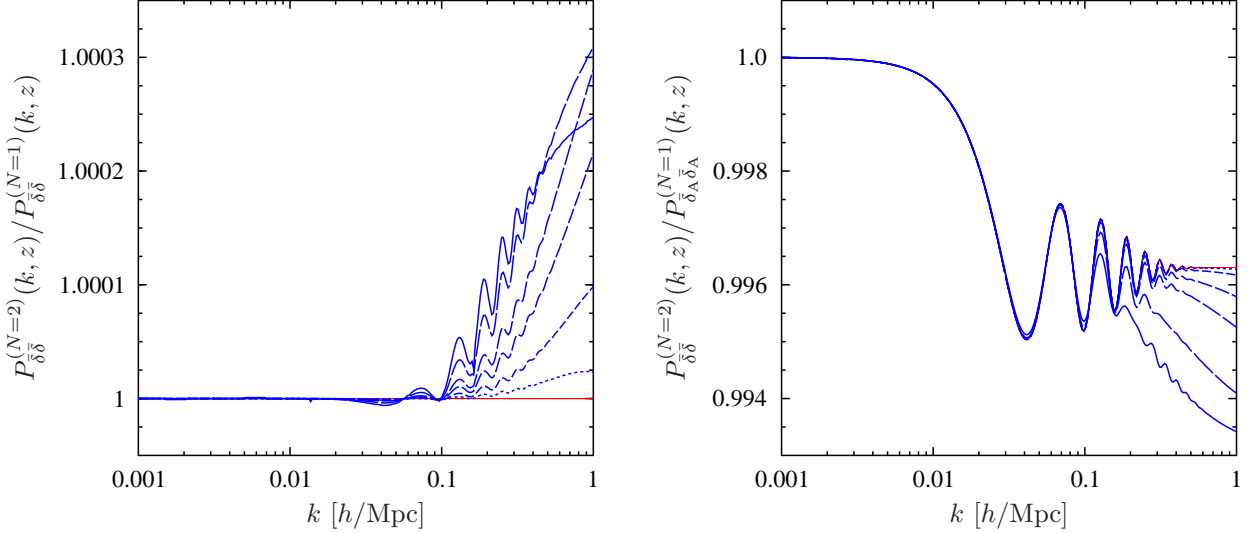


FIG. 13: Ratio of the total matter power spectrum obtained from the 2-component fluid model for CDM plus baryons, to that obtained from the 1-component fluid approximation, as a function of wavenumber. Again, red lines show the ratio of power spectra in linear theory, and blue lines the ratio of one-loop non-linear power spectra. The solid through to dashed lines show results for redshifts $z = \{0, 1.0, 3.0, 5.0, 10.0, 20.0\}$. See end of §VID for an explanation as to why the linear theory ratios are independent of time

D. Impact on total matter power spectrum

Since some cosmological probes are only sensitive to the total mass distribution, such as weak gravitational lensing, it is interesting to ask, what is the error between the exact $N = 2$ and the approximate $N = 1$ fluid dynamics, incurred when modeling the total matter power spectrum. Recall that the total matter power spectrum is defined as,

$$P_{\delta\delta}(\mathbf{k}, z) = (1 - f^b)^2 P_{\delta^c\delta^c}(\mathbf{k}, z) + 2(1 - f^b)f^b P_{\delta^c\delta^b}(\mathbf{k}, z) + (f^b)^2 P_{\delta^b\delta^b}(\mathbf{k}, z). \quad (89)$$

The results obtained by using the exact and approximate initial conditions for the 1-component fluid model are plotted in the left and right panels of Fig. 13 respectively. We see that the single-fluid approximation based on exact initial conditions is excellent, being accurate to $< 0.03\%$ for all times and scales considered. As we will show in §VII, this spectacular success can be attributed to the fact that the leading in η , one-loop corrections, depend only on the total mass distribution.

Using the approximate initial conditions for the single-fluid calculation still leads to very good agreement with the full 2-component fluid result on large scales $k \sim 0.2 h \text{ Mpc}^{-1}$, with $< 0.5\%$ accuracy for all the times considered. On smaller scales the approximation becomes worse, being of order $\sim 0.7\%$ at $k \sim 1.0 h \text{ Mpc}^{-1}$. However, this departure is unlikely to be accurate, since we can not trust the PT results on these small scales. This owes to the fact that the *missing* higher order loop corrections become increasingly more important. Nevertheless, this point is rather academic, since using the exact initial conditions will give better than 1% precision for the non-linear matter power spectrum down to scales of the order $k \sim 1.0 h \text{ Mpc}^{-1}$, as required by future weak lensing surveys, such as Euclid.

Finally, we note that one can easily show that the *linear* mass power spectrum simply scales with the square of the linear growth factor, even in the 2-component fluid theory. Hence, the ratio of the 2-component fluid linear mass power spectrum to the 1-component fluid model is constant in time. Furthermore, this constant is simply unity, if the 1-component fluid model is set up with exact initial conditions.

VII. APPROXIMATE DESCRIPTION OF THE MULTI-FLUID DYNAMICS

Given that the full expressions for the one-loop corrections to the power spectrum are quite formidable and time consuming to compute, it is of use to attempt to develop an approximate description of these expressions. We present this below. Our approximation scheme is based on insights concerning the late-time behaviour of the one-loop power spectrum, and it is valid for growing mode initial conditions and, although here we present the case of a 2-component fluid, can be generalized for N -component matter fluids.

A. Approximate form of the reducible correction

To begin, we recall that the one-loop reducible correction to the power spectrum reads (c.f. Eq. (69))

$$\delta P_{ab,R}^{(1)}(\mathbf{k}, \eta) = \left[g_{ac}(\eta) \delta G_{bd}^{(1)}(\mathbf{k}, \eta) + \delta G_{ac}^{(1)}(\mathbf{k}, \eta) g_{bd}(\eta) \right] \mathcal{P}_{cd}^{(0)}(k). \quad (90)$$

In the limit of late times, $\eta \rightarrow \infty$, we can discard all but the fastest growing modes of the linear propagator, g_{ab} , and one-loop correction to the propagator, $\delta G_{ab}^{(1)}$. For the linear propagator we have simply $g_{ab}(\eta) \rightarrow g_{ab,1} e^\eta$, while for the one-loop correction we find

$$\delta G_{ab}^{(1)}(\mathbf{k}, \eta) \rightarrow \frac{1}{5} \begin{bmatrix} 3w_1 f(k) & 2w_1 f(k) & 3w_2 f(k) & 2w_2 f(k) \\ 3w_1 g(k) & 2w_1 g(k) & 3w_2 g(k) & 2w_2 g(k) \\ 3w_1 f(k) & 2w_1 f(k) & 3w_2 f(k) & 2w_2 f(k) \\ 3w_1 g(k) & 2w_1 g(k) & 3w_2 g(k) & 2w_2 g(k) \end{bmatrix} e^{3\eta}, \quad (91)$$

where we have

$$f(k) = \int \frac{d^3 \mathbf{k}_1}{504 k^3 k_1^5} \left[6k^7 k_1 - 79k^5 k_1^3 + 50k^3 k_1^5 - 21k k_1^7 + \frac{3}{4}(k^2 - k_1^2)^3 (2k^2 + 7k_1^2) \ln \frac{|k - k_1|^2}{|k + k_1|^2} \right] \mathcal{P}_{\bar{\delta}\bar{\delta}}^{(0)}(k_1), \quad (92)$$

$$g(k) = \int \frac{d^3 \mathbf{k}_1}{168 k^3 k_1^5} \left[6k^7 k_1 - 41k^5 k_1^3 + 2k^3 k_1^5 - 3k k_1^7 + \frac{3}{4}(k^2 - k_1^2)^3 (2k^2 + k_1^2) \ln \frac{|k - k_1|^2}{|k + k_1|^2} \right] \mathcal{P}_{\bar{\delta}\bar{\delta}}^{(0)}(k_1). \quad (93)$$

These are just the f and g functions of [26], and $\mathcal{P}_{\bar{\delta}\bar{\delta}}^{(0)}(k)$ is the initial power spectrum of the total matter fluctuation, $\bar{\delta}(k) = w_1 \delta_1(k) + w_2 \delta_2(k)$:

$$\mathcal{P}_{\bar{\delta}\bar{\delta}}^{(0)}(k) = w_1^2 \mathcal{P}_{11}^{(0)}(k) + 2w_1 w_2 \mathcal{P}_{12}^{(0)}(k) + w_2^2 \mathcal{P}_{22}^{(0)}(k) = [w_1 T_1(k) + w_2 T_2(k)]^2 \mathcal{P}_0(k), \quad (94)$$

where we have assumed growing mode initial conditions. Upon evaluating Eq. (90) with the approximate form of the propagators as given above, we obtain

$$\delta P_{ab,R}^{(1)}(\mathbf{k}, \eta) \rightarrow \begin{bmatrix} 2f(k) & f(k) + g(k) & 2f(k) & f(k) + g(k) \\ f(k) + g(k) & 2g(k) & f(k) + g(k) & 2g(k) \\ 2f(k) & f(k) + g(k) & 2f(k) & f(k) + g(k) \\ f(k) + g(k) & 2g(k) & f(k) + g(k) & 2g(k) \end{bmatrix} \mathcal{P}_{\bar{\delta}\bar{\delta}}^{(0)}(k) e^{4\eta}. \quad (95)$$

For early times on the other hand, as $\eta \rightarrow 0$ we have simply that $\delta P_{ab,R}^{(1)}(\mathbf{k}, \eta) \rightarrow 0$. In fact, explicit computation shows that in this limit, the reducible correction vanishes as $\delta P_{ab,R}^{(1)}(\mathbf{k}, \eta) \rightarrow \propto (e^\eta - 1)^2$. Since the vanishing of $\delta P_{ab,R}^{(1)}(\mathbf{k}, \eta)$ as $\eta \rightarrow 0$ is required on physical grounds, we would like to implement it even in the approximate description. To do so, we will simply change the time dependence of Eq. (95) as $e^{4\eta} \rightarrow e^{2\eta}(e^\eta - 1)^2$. Thus we define the approximate one-loop reducible correction to the power spectrum as

$$\delta P_{ab,R,A}^{(1)}(\mathbf{k}, \eta) \equiv \begin{bmatrix} 2f(k) & f(k) + g(k) & 2f(k) & f(k) + g(k) \\ f(k) + g(k) & 2g(k) & f(k) + g(k) & 2g(k) \\ 2f(k) & f(k) + g(k) & 2f(k) & f(k) + g(k) \\ f(k) + g(k) & 2g(k) & f(k) + g(k) & 2g(k) \end{bmatrix} \mathcal{P}_{\bar{\delta}\bar{\delta}}^{(0)}(k) e^{2\eta} (e^\eta - 1)^2. \quad (96)$$

Needless to say, the fastest growing mode is not affected by this substitution.

B. Approximate form of the mode-coupling correction

Keeping only the fastest growing mode of the one-loop mode-coupling correction to the power spectrum, we find

$$\delta P_{ab,MC}^{(1)}(\mathbf{k}, \eta) \rightarrow \begin{bmatrix} 2F(k) & H(k) & 2F(k) & H(k) \\ H(k) & 2G(k) & H(k) & 2G(k) \\ 2F(k) & H(k) & 2F(k) & H(k) \\ H(k) & 2G(k) & H(k) & 2G(k) \end{bmatrix} e^{4\eta}, \quad (97)$$

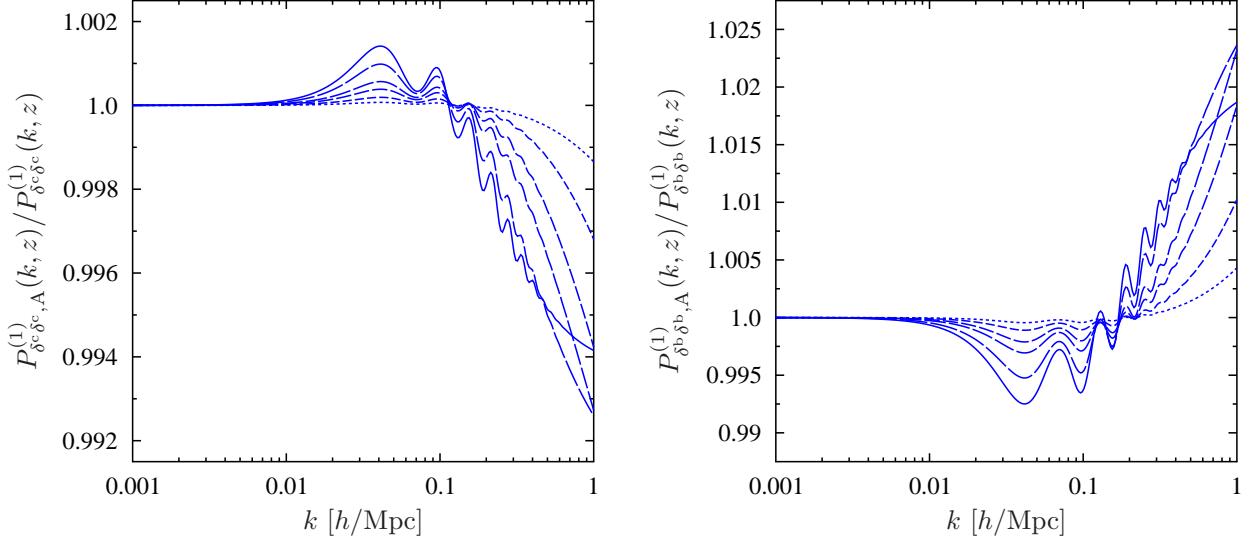


FIG. 14: Ratio of the approximate to exact one-loop non-linear matter power spectra for CDM (*left panel*) and baryons (*right panel*) in the 2-component fluid model for CDM plus baryons. As before, the solid through to dashed lines show results for redshifts $z = \{0, 1.0, 3.0, 5.0, 10.0, 20.0\}$. Approximations are good to better than 1% up to $k \approx 0.2 h \text{ Mpc}^{-1}$.

where we have defined

$$F(k) = \int d^3 \mathbf{k}_1 \frac{k^4 [7kx + k_1 (3 - 10x^2)]^2}{196k_1^2 (k^2 - 2kk_1x + k_1^2)^2} \mathcal{P}_{\delta\delta}^{(0)}(k_1) \mathcal{P}_{\delta\delta}^{(0)} \left(\sqrt{k^2 - 2kk_1x + k_1^2} \right), \quad (98)$$

$$G(k) = \int d^3 \mathbf{k}_1 \frac{k^4 [7kx - k_1 (1 + 6x^2)]^2}{196k_1^2 (k^2 - 2kk_1x + k_1^2)^2} \mathcal{P}_{\delta\delta}^{(0)}(k_1) \mathcal{P}_{\delta\delta}^{(0)} \left(\sqrt{k^2 - 2kk_1x + k_1^2} \right), \quad (99)$$

$$H(k) = \int d^3 \mathbf{k}_1 \frac{k^4 [(60x^4 - 8x^2 - 3)k_1^2 - 14kk_1x(8x^2 - 1) + 49k^2x^2]}{98k_1^2 (k^2 - 2kk_1x + k_1^2)^2} \mathcal{P}_{\delta\delta}^{(0)}(k_1) \mathcal{P}_{\delta\delta}^{(0)} \left(\sqrt{k^2 - 2kk_1x + k_1^2} \right), \quad (100)$$

where x is the cosine of the angle between \mathbf{k} and \mathbf{k}_1 , i.e. $\mathbf{k} \cdot \mathbf{k}_1 = kk_1x$.

For early times, the situation is completely analogous to the case of the reducible correction: as $\eta \rightarrow 0$ we have that $\delta P_{ab, \text{MC}}^{(1)}(\mathbf{k}, \eta) \rightarrow 0$ and in fact, $\delta P_{ab, \text{MC}}^{(1)}(\mathbf{k}, \eta) \rightarrow \propto (e^\eta - 1)^2$ in this limit. So again we implement the vanishing of the mode-coupling correction as $\eta \rightarrow 0$ by simply changing the time dependence of Eq. (97) as $e^{4\eta} \rightarrow e^{2\eta}(e^\eta - 1)^2$. Then the approximate one-loop mode-coupling correction to the power spectrum is defined as

$$\delta P_{ab, \text{MC}, A}^{(1)}(\mathbf{k}, \eta) \equiv \begin{bmatrix} 2F(k) & H(k) & 2F(k) & H(k) \\ H(k) & 2G(k) & H(k) & 2G(k) \\ 2F(k) & H(k) & 2F(k) & H(k) \\ H(k) & 2G(k) & H(k) & 2G(k) \end{bmatrix} e^{2\eta}(e^\eta - 1)^2. \quad (101)$$

Clearly the fastest growing mode is not affected by this substitution.

C. Comparison of the approximate and exact 2-component fluid models

Fig. 14 shows the ratio of the approximate non-linear CDM (*left panel*) and baryon (*right panel*) power spectra with the exact 2-component fluid non-linear power spectra:

$$\frac{P_{ab, A}^{(1)}(k, z)}{P_{ab}^{(1)}(k, z)} \equiv \frac{P_{ab}^{(0)}(k, z) + \delta P_{ab, R, A}^{(1)} + \delta P_{ab, \text{MC}, A}^{(1)}(k, z)}{P_{ab}^{(0)}(k, z) + \delta P_{ab, R}^{(1)} + \delta P_{ab, \text{MC}}^{(1)}(k, z)}. \quad (102)$$

For the case of CDM, the agreement is very good, being $< 0.2\%$ for $k < 0.2 h \text{ Mpc}^{-1}$ (i.e. on scales large enough for one-loop PT to be trusted), and for all times considered. The approximation performs worse for baryons, however, the agreement is still quite good, being $< 0.7\%$, on scales of up to $k \sim 0.2 h \text{ Mpc}^{-1}$, again for all considered times.

We note in passing that the success of the approximation – which was based on the late time behaviour of the one-loop correction – for relatively early times (say $z = 10$ – 20) is simply a consequence of the fact that at early times the one-loop correction to the power spectrum is small. Hence, even if the approximation of the one-loop correction itself is not very accurate at such times, this does not influence the fact that the full non-linear power spectrum is still well approximated. Clearly, if all of the $\delta P^{(1)}$ s are small compared to $P^{(0)}$ in Eq. (102), then the ratio is close to one, irrespective of whether the individual approximations $\delta P^{(1)} \approx \delta P_A^{(1)}$ are particularly good or not.

We thus conclude that the one-loop corrections to the power spectrum for both CDM and baryons are very well-modeled by the leading late time terms, for all scales and times considered. Incidentally, this observation explains two phenomena we encountered earlier. Firstly, as noted in §VIB, the structure of the non-linear to linear power spectra for the CDM and baryons (see bottom panels of Fig. 10) are almost identical. This is because the leading late time corrections in Eqs (96) and (101) for both CDM and baryons are seen to take *precisely the same form*. Secondly, the spectacular success of the single-fluid approximation in modeling the total mass power spectrum, noted in §VID (see Fig. 13), is due to the fact the leading late time terms depend only on the average initial field, and not on the two fields separately. Thus, treating the *total* 2-component fluid as an effective 1-component fluid is *exact at the level of the leading non-linear corrections*.

Finally, this approximate theory is of great practical advantage, since it reduces the number of numerical integrals to be evaluated by roughly a factor of 10 for the case of the 2-component fluid, so giving an order of magnitude speed up in computational time. Further, the approximate theory can be represented by a compact set of equations.

VIII. SUMMARY AND CONCLUSIONS

In this paper we have generalized the matrix based RPT formalism of Crocce and Scoccimarro [1] to the problem of dealing with N -component fluids, each of which evolves from a distinct set of initial conditions and contributes to the matter-density and velocity fields.

In §II we showed that, for N -component fluids, the essential structure of the RPT framework remained the same as for the $N = 1$ case – that is, the equations of motion could be solved in exactly the same way. However, the details of the building blocks of the theory did change: i.e. the vertex, propagator and initial conditions. For $N = 2$ the vertex matrix offered no surprises. The linear propagator was more interesting, and we showed that besides the usual growing and decaying modes $\{D_+ \propto e^\eta, D_-^{(1)} \propto e^{-3\eta/2}\}$, there were two additional eigenvalues: a static and decaying mode $\{D_{\text{stat}} \propto \text{const}, D_-^{(2)} \propto e^{-\eta/2}\}$. Interestingly, in going to $N > 2$ no further time dependence was gained. Unlike the 1-component fluid case, it was no longer possible to choose pure growing modes, unless all of the fluids evolved from identical initial conditions. However, we showed that one can still set up the initial conditions to possess pure large-scale growing modes. All our results were obtained for this specific choice of initial conditions.

In §III it was shown that the equations of motion for the N -component fluid case could be solved using a power series solution and that the solutions could be recovered order by order. A graphical representation of the solutions was also described.

In §IV we discussed the statistics of the fields: in particular the covariance matrix of the N -component fluid perturbations, and the fully non-linear propagator. This latter quantity can be understood to be the statistic that provides information on the memory of the evolved field to the initial conditions. It also possesses a perturbative expansion and we gave expressions up to one-loop order. A diagrammatic representation was also discussed.

As for the case of the 1-component fluid RPT, we then showed that for the N -component fluid RPT the full non-linear power spectrum also possessed a series expansion, and that the series could be grouped into two sub-series, “reducible” and “mode-coupling”. It was shown that the reducible terms were proportional to the initial power spectrum and non-linear propagators. Again we gave complete details for the series up to the one-loop level in the expansions. A diagrammatic description was also discussed.

In §V we developed further the one-loop expressions for the propagator and the mode-coupling contribution to the power spectrum. These expressions were then given for the explicit case of a 2-component fluid.

In §VI we applied the formalism to the problem of modeling the non-linear evolution of a CDM and baryon fluid in the Λ CDM paradigm. This enabled us to test the validity of the approximation of treating CDM and baryons as an effective 1-component fluid evolving from a single set of initial conditions, as is currently standard practice.

For the case of CDM, it was shown that the approximation was very good for $z < 3$, with the exact and approximate CDM power spectra differing by $< 1\%$. However, for higher redshifts the approximation became progressively worse, it being of the order $\sim 3\%$ at $z = 10$, with the power in the exact theory being amplified and having weaker BAO features than the approximate theory.

For the case of baryons the situation was worse: at $z = 20$ the exact and approximate spectra differed by $\sim 25\%$, and at $z = 10$ by $\sim 15\%$. At later times the approximation was still quite poor, and at $z = 3$ the errors were of the

order $\sim 5\%$, and by $z = 0$ were still between $\sim 2 - 3\%$. The power in the exact theory was suppressed in amplitude but possessed stronger BAO than the corresponding power for the approximate theory.

These conclusions remained essentially unaffected, when the so-called approximate 1-component fluid initial conditions were employed for the effective 1-component fluid computation.

Lastly, we computed the total non-linear matter power spectrum and found that the exact and approximate theory agreed to within $< 0.03\%$, when the so-called exact 1-component fluid initial conditions were used. Employing the approximate 1-component fluid initial conditions on the other hand leads to an agreement to within $< 0.5\%$ on scales where the perturbation theory was valid $k < 0.2 h \text{ Mpc}^{-1}$ and for all times of interest. Deviations on the order of $\sim 0.7\%$ were found on smaller scales with this approximation.

Our main conclusions therefore are:

- For theoretical modeling of the low-redshift CDM distribution, the approximate 1-component fluid treatment provides a good approximation. For higher redshift studies, such as those that probe the epoch of reionization, or attempt to model the first objects that form (stars/haloes), then one must be careful to use the appropriate CDM transfer function for the redshift of interest. Otherwise, systematic errors will be present at the level of several percent.
- For theoretical modeling of baryons in the Universe, a 1-component fluid treatment leads to significant $> 1\%$ errors at all times. This implies that cosmological probes that are primarily sensitive to the distributions of baryons in the universe, such as: 21 cm radiation from neutral hydrogen, or the Lyman alpha forest absorption lines in high redshift quasars, can not be modeled using dark matter only simulations at high precision. Instead the baryons must be modeled using a 2-component fluid system of CDM and baryons, with the initial distributions being specified by the linear Einstein–Boltzmann solutions. The correct treatment of CDM and baryon initial conditions may also affect how galaxies form.
- Observational probes for cosmology that are sensitive to the total mass distribution, such as weak gravitational lensing, can be accurately interpreted using an effective single CDM plus baryon fluid. Thus current modeling technology is good enough for high precision work, but it is highly desirable to use the exact prescription when specifying the initial conditions for the effective single fluid.

Acknowledgments

We acknowledge Ravi Sheth for providing comments on an early draft. We thank Martin Crocce, Zhaoming Ma, Roman Scoccimarro, Uros Seljak, and Romain Teyssier for useful discussions. GS acknowledges support from the Hungarian Scientific Research Fund grant OKTA K-60432 and the Swiss National Science Foundation under contract 200020-117602. RES acknowledges support from a Marie Curie Reintegration Grant and partial support from the Swiss National Foundation under contract 200021-116696/1 and WCU grant R32-2008-000-10130-0.

-
- [1] M. Crocce and R. Scoccimarro, PRD **73**, 063519 (2006), arXiv:astro-ph/0509418.
 - [2] P. J. Peebles and B. Ratra, Reviews of Modern Physics **75**, 559 (2003), arXiv:astro-ph/0207347.
 - [3] D. N. Spergel, R. Bean, O. Doré, M. R. Nolta, C. L. Bennett, J. Dunkley, G. Hinshaw, N. Jarosik, E. Komatsu, L. Page, et al., ApJS **170**, 377 (2007), arXiv:astro-ph/0603449.
 - [4] E. Komatsu, J. Dunkley, M. R. Nolta, C. L. Bennett, B. Gold, G. Hinshaw, N. Jarosik, D. Larson, M. Limon, L. Page, et al., ApJS **180**, 330 (2009), 0803.0547.
 - [5] C.-P. Ma and E. Bertschinger, ApJ **455**, 7 (1995), arXiv:astro-ph/9506072.
 - [6] U. Seljak and M. Zaldarriaga, ApJ **469**, 437 (1996), arXiv:astro-ph/9603033.
 - [7] F. Bernardeau, S. Colombi, E. Gaztañaga, and R. Scoccimarro, Phys. Rep. **367**, 1 (2002), arXiv:astro-ph/0112551.
 - [8] E. Bertschinger, ApJS **137**, 1 (2001), arXiv:astro-ph/0103301.
 - [9] G. Efstathiou, M. Davis, S. D. M. White, and C. S. Frenk, ApJS **57**, 241 (1985).
 - [10] P. A. Thomas and H. M. P. Couchman, MNRAS **257**, 11 (1992).
 - [11] H. M. P. Couchman, P. A. Thomas, and F. R. Pearce, ApJ **452**, 797 (1995), arXiv:astro-ph/9409058.
 - [12] N. Sugiyama, ApJS **100**, 281 (1995), arXiv:astro-ph/9412025.
 - [13] D. J. Eisenstein and W. Hu, ApJ **496**, 605 (1998), arXiv:astro-ph/9709112.
 - [14] A. Meiksin, M. White, and J. A. Peacock, MNRAS **304**, 851 (1999), arXiv:astro-ph/9812214.
 - [15] F. R. Pearce, A. Jenkins, C. S. Frenk, S. D. M. White, P. A. Thomas, H. M. P. Couchman, J. A. Peacock, and G. Efstathiou, MNRAS **326**, 649 (2001), arXiv:astro-ph/0010587.

- [16] R. Teyssier, *A&A* **385**, 337 (2002), arXiv:astro-ph/0111367.
- [17] V. Springel, *MNRAS* **364**, 1105 (2005), arXiv:astro-ph/0505010.
- [18] V. Springel, *ArXiv e-prints* (2009), 0901.4107.
- [19] A. Albrecht, G. Bernstein, R. Cahn, W. L. Freedman, J. Hewitt, W. Hu, J. Huth, M. Kamionkowski, E. W. Kolb, L. Knox, et al., *ArXiv Astrophysics e-prints* (2006), arXiv:astro-ph/0609591.
- [20] J. A. Peacock, P. Schneider, G. Efstathiou, J. R. Ellis, B. Leibundgut, S. J. Lilly, and Y. Mellier, *Tech. Rep.* (2006).
- [21] P. Zhang, U.-L. Pen, and H. Trac, *MNRAS* **355**, 451 (2004), arXiv:astro-ph/0402115.
- [22] I. T. Iliev, G. Mellema, U.-L. Pen, H. Merz, P. R. Shapiro, and M. A. Alvarez, *MNRAS* **369**, 1625 (2006), arXiv:astro-ph/0512187.
- [23] S. R. Furlanetto, S. P. Oh, and F. H. Briggs, *Phys. Rep.* **433**, 181 (2006), arXiv:astro-ph/0608032.
- [24] A. Pillepich, C. Porciani, and S. Matarrese, *ApJ* **662**, 1 (2007), arXiv:astro-ph/0611126.
- [25] R. A. C. Croft, D. H. Weinberg, N. Katz, and L. Hernquist, *ApJ* **495**, 44 (1998), arXiv:astro-ph/9708018.
- [26] M. Crocce and R. Scoccimarro, *PRD* **73**, 063520 (2006), arXiv:astro-ph/0509419.
- [27] M. Crocce and R. Scoccimarro, *PRD* **77**, 023533 (2008), arXiv:0704.2783.
- [28] M. Shoji and E. Komatsu, *ApJ* **700**, 705 (2009), 0903.2669.
- [29] S. Matarrese and M. Pietroni, *Journal of Cosmology and Astro-Particle Physics* **6**, 26 (2007), arXiv:astro-ph/0703563.
- [30] S. Matarrese and M. Pietroni, *Modern Physics Letters A* **23**, 25 (2008), arXiv:astro-ph/0702653.
- [31] F. Bernardeau, M. Crocce, and R. Scoccimarro, *PRD* **78**, 103521 (2008), 0806.2334.
- [32] M. Pietroni, *Journal of Cosmology and Astro-Particle Physics* **10**, 36 (2008), 0806.0971.
- [33] T. Matsubara, *PRD* **78**, 083519 (2008), 0807.1733.
- [34] Y. Y. Y. Wong, *Journal of Cosmology and Astro-Particle Physics* **10**, 35 (2008), 0809.0693.
- [35] S. Saito, M. Takada, and A. Taruya, *Physical Review Letters* **100**, 191301 (2008), 0801.0607.
- [36] K. Ichiki, M. Takada, and T. Takahashi, *PRD* **79**, 023520 (2009), 0810.4921.
- [37] J. Brandbyge, S. Hannestad, T. Haugbølle, and B. Thomsen, *Journal of Cosmology and Astro-Particle Physics* **8**, 20 (2008), 0802.3700.
- [38] J. Brandbyge and S. Hannestad, *Journal of Cosmology and Astro-Particle Physics* **5**, 2 (2009), 0812.3149.
- [39] J. Brandbyge and S. Hannestad, *ArXiv e-prints* (2009), 0908.1969.
- [40] R. Scoccimarro, S. Colombi, J. N. Fry, J. A. Frieman, E. Hivon, and A. Melott, *ApJ* **496**, 586 (1998), arXiv:astro-ph/9704075.
- [41] P. J. E. Peebles, *The large-scale structure of the universe* (Research supported by the National Science Foundation. Princeton, N.J., Princeton University Press, 1980. 435 p., 1980).
- [42] S. Dodelson, *Modern cosmology* (Modern cosmology / Scott Dodelson. Amsterdam (Netherlands): Academic Press. ISBN 0-12-219141-2, 2003, XIII + 440 p., 2003).
- [43] S. M. Carroll, W. H. Press, and E. L. Turner, *Annual Reviews of Astronomy & Astrophysics* **30**, 499 (1992).
- [44] R. E. Smith, R. Scoccimarro, and R. K. Sheth, *PRD* **75**, 063512 (2007), arXiv:astro-ph/0609547.
- [45] It appears to us that what may be implemented in the RPT framework is not so much what would usually be understood as the “perturbative renormalization” of the theory, but rather a “resummation” of the perturbative series, in some specific approximation (the “high- k ” limit). We will continue to use the acronym RPT to refer to the method, but would suggest that it is more properly read as *resummed*, and not *renormalized* perturbation theory.

APPENDIX A: A RELATION INVOLVING THE CONFORMAL EXPANSION RATE

We prove that $d\mathcal{H}/d\tau = -\mathcal{H}^2 [\Omega_m(a)/2 - \Omega_\Lambda(a)]$. To begin, we recall that for a homogeneous and isotropic universe, the Einstein field equations reduce to:

$$\frac{3\ddot{a}}{a} = -4\pi G(3p + \rho); \quad \dot{a}^2 + K = \frac{8\pi G\rho a^2}{3}, \quad (\text{A1})$$

where dots denote differentiation with respect to cosmological time t . Then for the Λ CDM model with matter density $\rho = \rho_m + \rho_\Lambda$ and pressure $p = p_\Lambda = -\rho_\Lambda$, we find

$$\frac{\ddot{a}}{a} = -\frac{4\pi G\rho_m}{3} + \frac{8\pi G\rho_\Lambda}{3} = -H^2(a) \left[\frac{\Omega_m(a)}{2} - \Omega_\Lambda(a) \right]. \quad (\text{A2})$$

Consider now,

$$\frac{d\mathcal{H}}{d\tau} = \frac{d}{d\tau}(aH) = \frac{dt}{d\tau} \frac{d}{dt}(a\dot{a}) = a\ddot{a}. \quad (\text{A3})$$

The last two equations together give the desired result

$$\frac{d\mathcal{H}}{d\tau} = -\mathcal{H}^2 \left[\frac{\Omega_m(a)}{2} - \Omega_\Lambda(a) \right]. \quad (\text{A4})$$

APPENDIX B: CALCULATING THE PROPAGATOR

1. The non-linear propagator

In this appendix we provide explicit details of the calculation of the propagator for the PT solutions up to third order in the expansion for $\Psi_a^{(n)}$. To begin, recall that the propagator is defined through Eq. (58), as

$$G_{ab}(\mathbf{k}, \eta) \delta^D(\mathbf{k} - \mathbf{k}') \equiv \left\langle \frac{\delta \Psi_a(\mathbf{k}, \eta)[\phi^{(0)}]}{\delta \phi_b^{(0)}(\mathbf{k}')} \right\rangle. \quad (\text{B1})$$

If we insert the series expansion for $\Psi_a^{(n)}$ as given by Eq. (41), then we obtain a series expansion for the propagator.

$$G_{ab}(\mathbf{k}, \eta) \delta^D(\mathbf{k} - \mathbf{k}') = \sum_{n=0} \left\langle \frac{\delta \Psi_a^{(n)}(\mathbf{k}, \eta)[\phi^{(0)}]}{\delta \phi_b^{(0)}(\mathbf{k}')} \right\rangle. \quad (\text{B2})$$

The next step is to calculate the functional derivatives of the perturbative solutions. Functionals are essentially functions that depend on the full shape of another function over a certain domain. We shall denote functionals using the notation, $F[y(x)]$, and this has the specific meaning,

$$F[y(x)] = \int_a^b dx g(y(x)). \quad (\text{B3})$$

where $g(y)$ is some arbitrary continuous function. Functional derivatives may be taken using the relation,

$$dF \equiv \int_a^b dx \left. \frac{\delta F}{\delta y(x)} \right|_{y^0(x)} \delta y(x), \quad (\text{B4})$$

where in the above we identify $\delta F / \delta y(x)|_{y^0(x)}$ as the functional derivative about the function, $y^0(x)$.

2. Propagator for solutions: $n = \{0, 1, 2\}$

To see how we may use Eq. (B4), let us explicitly apply it to the solutions $\Psi^{(n)}$, for $n = \{0, 1, 2\}$.

- Solution for $n = 0$:

For the linear theory solution we have, $\Psi_a^{(0)}(\mathbf{k}, \eta) = g_{ab}(\eta) \phi_b^{(0)}(\mathbf{k})$. This is not in the form of Eq. (B3), but we can easily write it in such a form using the Dirac delta function,

$$\Psi_a^{(0)}(\mathbf{k}, \eta) [\phi_b^{(0)}(\mathbf{k}')] = \int d^3 \mathbf{k}' \delta^D(\mathbf{k} - \mathbf{k}') g_{ab}(\eta) \phi_b^{(0)}(\mathbf{k}'). \quad (\text{B5})$$

Now consider a small change $\delta \phi_b^{(0)}(\mathbf{k}')$ to the initial conditions $\phi_b^{(0)}(\mathbf{k}')$, whereupon we have

$$\begin{aligned} \Psi_a^{(0)}(\mathbf{k}, \eta) [\phi_b^{(0)}(\mathbf{k}') + \delta \phi_b^{(0)}(\mathbf{k}')] &= \int d^3 \mathbf{k}' \delta^D(\mathbf{k} - \mathbf{k}') g_{ab}(\eta) [\phi_b^{(0)}(\mathbf{k}') + \delta \phi_b^{(0)}(\mathbf{k}')] ; \\ &= \Psi_a^{(0)}(\mathbf{k}, \eta) [\phi_b^{(0)}(\mathbf{k}')] + \int d^3 \mathbf{k}' \delta^D(\mathbf{k} - \mathbf{k}') g_{aa'}(\eta) \delta \phi_b^{(0)}(\mathbf{k}'). \end{aligned} \quad (\text{B6})$$

Taking the first term on the right-hand-side over to the left, we find

$$d\Psi_a^{(0)}(\mathbf{k}, \eta) [\phi_b^{(0)}(\mathbf{k}')] = \int d^3 \mathbf{k}' \delta^D(\mathbf{k} - \mathbf{k}') g_{ab}(\eta) \delta \phi_b^{(0)}(\mathbf{k}'). \quad (\text{B7})$$

and on comparing the above with our definition from Eq. (B4), we identify the functional derivative as,

$$\frac{\delta \Psi_a^{(0)}(\mathbf{k}, \eta)}{\delta \phi_b^{(0)}(\mathbf{k}')} = \delta^D(\mathbf{k} - \mathbf{k}') g_{ab}(\eta). \quad (\text{B8})$$

Finally, we are interested in the ensemble average evolution of the mode, and since there are no initial fields remaining there is no stochasticity left in the relation and we simply have,

$$\left\langle \frac{\delta \Psi_a^{(0)}(\mathbf{k}, \eta)}{\delta \phi_b^{(0)}(\mathbf{k}')} \right\rangle = \delta^D(\mathbf{k} - \mathbf{k}') g_{ab}(\eta) . \quad (\text{B9})$$

- Solution for $n = 1$:

Let us now turn to the more complicated situation of computing the functional derivatives of the first order solution. The first order solution is a functional of the form,

$$\Psi_a^{(1)}(\mathbf{k}, \eta) [\phi_{c'}^{(0)}(\mathbf{k}_1), \phi_{d'}^{(0)}(\mathbf{k}_2)] = \int_0^\eta d\eta' g_{ab}(\eta - \eta') \int d^3\mathbf{k}_1 d^3\mathbf{k}_2 \gamma_{bcd}^{(s)}(\mathbf{k}, \mathbf{k}_1, \mathbf{k}_2) g_{cc'}(\eta') \phi_{c'}^{(0)}(\mathbf{k}_1) g_{dd'}(\eta') \phi_{d'}^{(0)}(\mathbf{k}_2) . \quad (\text{B10})$$

Repeating the procedure of above, we consider a small change $\delta \phi_{a'}^{(0)}(\mathbf{k})$ to the initial conditions $\phi_{a'}^{(0)}(\mathbf{k})$, whereupon we have

$$\begin{aligned} d\Psi_a^{(1)}(\mathbf{k}, \eta) [\phi_{c'}^{(0)}, \phi_{d'}^{(0)}] &= \int_0^\eta d\eta' g_{ab}(\eta - \eta') \int d^3\mathbf{k}_1 d^3\mathbf{k}_2 \gamma_{bcd}^{(s)}(\mathbf{k}, \mathbf{k}_1, \mathbf{k}_2) g_{cc'}(\eta') g_{dd'}(\eta') \\ &\times \left[\delta \phi_{c'}^{(0)}(\mathbf{k}_1) \phi_{d'}^{(0)}(\mathbf{k}_2) + \phi_{c'}^{(0)}(\mathbf{k}_1) \delta \phi_{d'}^{(0)}(\mathbf{k}_2) \right] ; \quad (\text{B11}) \\ &= 2 \int_0^\eta d\eta' g_{ab}(\eta - \eta') \int d^3\mathbf{k}_1 d^3\mathbf{k}_2 \gamma_{bcd}^{(s)}(\mathbf{k}, \mathbf{k}_1, \mathbf{k}_2) g_{cc'}(\eta') \phi_{c'}^{(0)}(\mathbf{k}_1) g_{dd'}(\eta') \delta \phi_{d'}^{(0)}(\mathbf{k}_2) , \quad (\text{B12}) \end{aligned}$$

where the last equality follows from the fact that owing to the symmetry of the vertex matrix $\gamma_{bcd}^{(s)}(\mathbf{k}, \mathbf{k}_1, \mathbf{k}_2)$, the solutions are symmetric to changes $\{\mathbf{k}_1, \mathbf{k}_2\} \rightarrow \{\mathbf{k}_2, \mathbf{k}_1\}$ and $\{c, d\} \rightarrow \{d, c\}$.

We would like to take the functional derivative with respect to the arbitrary initial condition $\delta \phi_{a'}^{(0)}(\mathbf{k}')$, and so we use the relation

$$\delta \phi_a^{(0)}(\mathbf{k}_i) = \int d^3\mathbf{k}_j \delta^D(\mathbf{k}_i - \mathbf{k}_j) \delta_{ab}^K \delta \phi_b^{(0)}(\mathbf{k}_j) , \quad (\text{B13})$$

to rewrite the initial conditions in terms of the field that we vary. Hence, Eq. (B12), becomes

$$\begin{aligned} d\Psi_a^{(1)}(\mathbf{k}, \eta) [\phi_{c'}^{(0)}(\mathbf{k}_1), \phi_{d'}^{(0)}(\mathbf{k}_2)] &= \int_0^\eta d\eta' g_{ab}(\eta - \eta') \int d^3\mathbf{k}_1 d^3\mathbf{k}_2 \gamma_{bcd}^{(s)}(\mathbf{k}, \mathbf{k}_1, \mathbf{k}_2) g_{cc'}(\eta') \phi_{c'}^{(0)}(\mathbf{k}_1) g_{dd'}(\eta') \\ &\times \int d^3\mathbf{k}' \delta^D(\mathbf{k}_1 - \mathbf{k}') \delta_{d'a'}^K \delta \phi_{a'}^{(0)}(\mathbf{k}') . \quad (\text{B14}) \end{aligned}$$

On comparing the above expression with Eq. (B4), we identify the functional derivative as

$$\frac{\delta \Psi_a^{(1)}(\mathbf{k}, \eta)}{\delta \phi_{a'}^{(0)}(\mathbf{k}')} = \delta^D(\mathbf{k}_1 - \mathbf{k}') \int_0^\eta d\eta' g_{ab}(\eta - \eta') \int d^3\mathbf{k}_1 d^3\mathbf{k}_2 \gamma_{bcd}^{(s)}(\mathbf{k}, \mathbf{k}_1, \mathbf{k}_2) g_{cc'}(\eta') \phi_{c'}^{(0)}(\mathbf{k}_1) g_{da'}(\eta') . \quad (\text{B15})$$

On taking the ensemble average we have $\langle \phi_{c'}^{(0)}(\mathbf{k}_1) \rangle = 0$, and hence

$$\left\langle \frac{\delta \Psi_a^{(1)}(\mathbf{k}, \eta)}{\delta \phi_{a'}^{(0)}(\mathbf{k}')} \right\rangle = 0 . \quad (\text{B16})$$

One direct corollary of this result is that, the propagator for the perturbative solutions which involve an even number of initial conditions is zero. Hence, only odd powers of $\phi^{(0)}$ contribute.

- Solution for $n = 2$:

Based on the previous calculation, we expect that the first non-zero contribution to the non-linear propagator is $n = 2$, since it involves three initial conditions. This can be computed as follows. The solution is a functional of the form,

$$\begin{aligned}\Psi_a^{(2)}(\mathbf{k}, \eta)[\phi_{c'}^{(0)}(\mathbf{k}_1), \phi_{f'}^{(0)}(\mathbf{k}_3), \phi_{g'}^{(0)}(\mathbf{k}_4)] &= 2 \int_0^\eta d\eta' g_{ab}(\eta - \eta') \int d^3\mathbf{k}_1 d^3\mathbf{k}_2 \gamma_{bcd}^{(s)}(\mathbf{k}, \mathbf{k}_1, \mathbf{k}_2) \Psi_c^{(0)}(\mathbf{k}_1, \eta') \Psi_d^{(1)}(\mathbf{k}_2, \eta'), \\ &= 2 \int_0^\eta d\eta' g_{ab}(\eta - \eta') \int d^3\mathbf{k}_1 d^3\mathbf{k}_2 \gamma_{bcd}^{(s)}(\mathbf{k}, \mathbf{k}_1, \mathbf{k}_2) g_{cc'}(\eta') \phi_{c'}^{(0)}(\mathbf{k}_1) \\ &\quad \times \int_0^{\eta'} d\eta'' g_{de}(\eta' - \eta'') \int d^3\mathbf{k}_3 d^3\mathbf{k}_4 \gamma_{efg}^{(s)}(\mathbf{k}_2, \mathbf{k}_3, \mathbf{k}_4) \\ &\quad \times g_{ee'}(\eta'') \phi_{e'}^{(0)}(\mathbf{k}_3) g_{ff'}(\eta'') \phi_{f'}^{(0)}(\mathbf{k}_4),\end{aligned}\tag{B17}$$

where the factor of two comes from the fact that the first equation is symmetric to interchanging, $\{c, d\} \rightarrow \{d, c\}$ and $\{\mathbf{k}_1, \mathbf{k}_2\} \rightarrow \{\mathbf{k}_2, \mathbf{k}_1\}$. Repeating the procedure of above, we now consider a small change $\delta\phi_{a'}^{(0)}(\mathbf{k}')$ to the initial conditions $\phi_{a'}^{(0)}(\mathbf{k}')$, whereupon

$$\begin{aligned}d\Psi_a^{(2)}(\mathbf{k}, \eta)[\phi_{c'}^{(0)}(\mathbf{k}_1), \phi_{f'}^{(0)}(\mathbf{k}_3), \phi_{g'}^{(0)}(\mathbf{k}_4)] &= 2 \int_0^\eta d\eta' g_{ab}(\eta - \eta') \int d^3\mathbf{k}_1 d^3\mathbf{k}_2 \gamma_{bcd}^{(s)}(\mathbf{k}, \mathbf{k}_1, \mathbf{k}_2) g_{cc'}(\eta') \int_0^{\eta'} d\eta'' g_{de}(\eta' - \eta'') \\ &\quad \times \int d^3\mathbf{k}_3 d^3\mathbf{k}_4 \gamma_{efg}^{(s)}(\mathbf{k}_2, \mathbf{k}_3, \mathbf{k}_4) g_{ff'}(\eta'') g_{gg'}(\eta'') \left[\delta\phi_{c'}^{(0)}(\mathbf{k}_1) \phi_{f'}^{(0)}(\mathbf{k}_3) \phi_{g'}^{(0)}(\mathbf{k}_4) \right. \\ &\quad \left. + \phi_{c'}^{(0)}(\mathbf{k}_1) \delta\phi_{f'}^{(0)}(\mathbf{k}_3) \phi_{g'}^{(0)}(\mathbf{k}_4) + \phi_{c'}^{(0)}(\mathbf{k}_1) \phi_{f'}^{(0)}(\mathbf{k}_3) \delta\phi_{g'}^{(0)}(\mathbf{k}_4) \right].\end{aligned}\tag{B18}$$

We notice that the last two terms are symmetric to changes $\{\mathbf{k}_3, \mathbf{k}_4\} \rightarrow \{\mathbf{k}_4, \mathbf{k}_3\}$ and $\{f, g\} \rightarrow \{g, f\}$ and this gives us a factor of 2. Next we use Eq. (B13) to repeatedly rewrite the perturbations $\delta\phi^{(0)}$ in terms of the arbitrary initial field $\delta\phi_{a'}^{(0)}(\mathbf{k}')$. Hence,

$$\begin{aligned}d\Psi_a^{(2)}(\mathbf{k}, \eta) &= 2 \int_0^\eta d\eta' g_{ab}(\eta - \eta') \int d^3\mathbf{k}_1 d^3\mathbf{k}_2 \gamma_{bcd}^{(s)}(\mathbf{k}, \mathbf{k}_1, \mathbf{k}_2) g_{cc'}(\eta') \int_0^{\eta'} d\eta'' g_{de}(\eta' - \eta'') \\ &\quad \times \int d^3\mathbf{k}_3 d^3\mathbf{k}_4 \gamma_{efg}^{(s)}(\mathbf{k}_2, \mathbf{k}_3, \mathbf{k}_4) g_{ff'}(\eta'') g_{gg'}(\eta'') \\ &\quad \times \int d^3\mathbf{k}' \left[\delta^D(\mathbf{k}_1 - \mathbf{k}') \delta_{c'a'}^K \phi_{f'}^{(0)}(\mathbf{k}_3) \phi_{g'}^{(0)}(\mathbf{k}_4) + 2\phi_{c'}^{(0)}(\mathbf{k}_1) \phi_{f'}^{(0)}(\mathbf{k}_3) \delta^D(\mathbf{k}_4 - \mathbf{k}') \delta_{g'a'}^K \right] \delta\phi_{a'}^{(0)}(\mathbf{k}').\end{aligned}\tag{B19}$$

On comparing the above with our definition for the functional derivative as given by Eq. (B4), we may make the following identification:

$$\begin{aligned}\frac{\delta\Psi_a^{(2)}(\mathbf{k}, \eta)}{\delta\phi_{a'}^{(0)}(\mathbf{k}')} &= 2 \int_0^\eta d\eta' g_{ab}(\eta - \eta') \int d^3\mathbf{k}_1 d^3\mathbf{k}_2 \gamma_{bcd}^{(s)}(\mathbf{k}, \mathbf{k}_1, \mathbf{k}_2) g_{cc'}(\eta') \int_0^{\eta'} d\eta'' g_{de}(\eta' - \eta'') \\ &\quad \times \int d^3\mathbf{k}_3 d^3\mathbf{k}_4 \gamma_{efg}^{(s)}(\mathbf{k}_2, \mathbf{k}_3, \mathbf{k}_4) g_{ff'}(\eta'') g_{gg'}(\eta'') \\ &\quad \times \left[\delta^D(\mathbf{k}_1 - \mathbf{k}') \delta_{c'a'}^K \phi_{f'}^{(0)}(\mathbf{k}_3) \phi_{g'}^{(0)}(\mathbf{k}_4) + 2\phi_{c'}^{(0)}(\mathbf{k}_1) \phi_{f'}^{(0)}(\mathbf{k}_3) \delta^D(\mathbf{k}_4 - \mathbf{k}') \delta_{g'a'}^K \right].\end{aligned}\tag{B20}$$

Finally, we take the ensemble average and find that the term in square brackets becomes,

$$\begin{aligned}&\rightarrow \left[\delta^D(\mathbf{k}_1 - \mathbf{k}') \delta_{c'a'}^K \left\langle \phi_{f'}^{(0)}(\mathbf{k}_3) \phi_{g'}^{(0)}(\mathbf{k}_4) \right\rangle + 2 \left\langle \phi_{c'}^{(0)}(\mathbf{k}_1) \phi_{f'}^{(0)}(\mathbf{k}_3) \right\rangle \delta^D(\mathbf{k}_4 - \mathbf{k}') \delta_{g'a'}^K \right]; \\ &\rightarrow \left[\delta^D(\mathbf{k}_1 - \mathbf{k}') \delta_{c'a'}^K \mathcal{P}_{f'g'}^{(0)}(\mathbf{k}_3) \delta^D(\mathbf{k}_3 + \mathbf{k}_4) + 2\mathcal{P}_{c'f'}^{(0)}(\mathbf{k}_1) \delta^D(\mathbf{k}_1 + \mathbf{k}_3) \delta^D(\mathbf{k}_4 - \mathbf{k}') \delta_{g'a'}^K \right].\end{aligned}\tag{B21}$$

Consider the first term in this bracket, we note that it contains a $\delta^D(\mathbf{k}_3 + \mathbf{k}_4)$. If we integrate this first term over \mathbf{k}_4 then the resulting expression involves $\gamma_{efg}^{(s)}(\mathbf{k}_2, \mathbf{k}_3, -\mathbf{k}_3)$, which from momentum conservation means that waves with equal and opposite momenta enter the interaction and so completely cancel and no wave exits. Thus, the above expression reduces to

$$\begin{aligned}\left\langle \frac{\delta\Psi_a^{(2)}(\mathbf{k}, \eta)}{\delta\phi_{a'}^{(0)}(\mathbf{k}')} \right\rangle &= 4 \int_0^\eta d\eta' g_{ab}(\eta - \eta') \int d^3\mathbf{k}_1 d^3\mathbf{k}_2 \bar{\gamma}_{bcd}^{(s)}(\mathbf{k}_1, \mathbf{k}_2) \delta^D(\mathbf{k} - \mathbf{k}_1 - \mathbf{k}_2) g_{cc'}(\eta') \int_0^{\eta'} d\eta'' g_{de}(\eta' - \eta'') \\ &\quad \times \int d^3\mathbf{k}_3 d^3\mathbf{k}_4 \bar{\gamma}_{efg}^{(s)}(\mathbf{k}_3, \mathbf{k}_4) \delta^D(\mathbf{k}_2 - \mathbf{k}_3 - \mathbf{k}_4) g_{ff'}(\eta'') g_{ga'}(\eta'') \mathcal{P}_{c'f'}^{(0)}(\mathbf{k}_1) \delta^D(\mathbf{k}_1 + \mathbf{k}_3) \delta^D(\mathbf{k}_4 - \mathbf{k}').\end{aligned}\tag{B22}$$

If we integrate over \mathbf{k}_4 , then \mathbf{k}_3 , and finally over \mathbf{k}_2 , then we obtain the desired expression,

$$\begin{aligned} \left\langle \frac{\delta\Psi_a^{(2)}(\mathbf{k}, \eta)}{\delta\phi_{a'}^{(0)}(\mathbf{k}')} \right\rangle &= \delta^D(\mathbf{k} - \mathbf{k}') \times 4 \int_0^\eta d\eta' g_{ab}(\eta - \eta') \int d^3\mathbf{k}_1 \bar{\gamma}_{bcd}^{(s)}(\mathbf{k}_1, \mathbf{k} - \mathbf{k}_1) g_{cc'}(\eta') \int_0^{\eta'} d\eta'' g_{de}(\eta' - \eta'') \\ &\times \bar{\gamma}_{efg}^{(s)}(-\mathbf{k}_1, \mathbf{k}') g_{ff'}(\eta'') g_{ga'}(\eta'') \mathcal{P}_{c'f'}^{(0)}(\mathbf{k}_1) . \end{aligned} \quad (\text{B23})$$

Finally, if we assume large-scale growing mode initial conditions $u_a = (1, 1, \dots, 1, 1)$, then we find the first non-zero perturbative correction to the propagator is given by:

$$\begin{aligned} \delta G_{aa'}^{(1)}(\mathbf{k}, \eta) &= 4 \int_0^\eta d\eta' g_{ab}(\eta - \eta') \int d^3\mathbf{k}_1 \bar{\gamma}_{bcd}^{(s)}(\mathbf{k}_1, \mathbf{k} - \mathbf{k}_1) g_{cc'}(\eta') T_{c'}(k_1) \int_0^{\eta'} d\eta'' g_{de}(\eta' - \eta'') \\ &\times \bar{\gamma}_{efg}^{(s)}(-\mathbf{k}_1, \mathbf{k}') g_{ff'}(\eta'') T_{f'}(k_1) g_{ga'}(\eta'') \mathcal{P}_0(\mathbf{k}_1) . \end{aligned} \quad (\text{B24})$$

APPENDIX C: CALCULATING THE MODE-COUPLING POWER SPECTRUM

In this appendix, we present details of the computation of the mode-coupling contribution to the one-loop power spectrum given by Eq. (73). In Eq. (68) we identified this term as,

$$\begin{aligned} \left\langle \Psi_a^{(1)}(\mathbf{k}) \Psi_{a'}^{(1)}(\mathbf{k}') \right\rangle &= \left\langle \int_0^\eta d\eta_1 g_{ab}(\eta - \eta_1) \int d^3\mathbf{k}_1 d^3\mathbf{k}_2 \gamma_{bcd}^{(s)}(\mathbf{k}, \mathbf{k}_1, \mathbf{k}_2) g_{ce}(\eta_1) g_{df}(\eta_1) \phi_e^{(0)}(\mathbf{k}_1) \phi_f^{(0)}(\mathbf{k}_2) \right. \\ &\times \left. \int_0^\eta d\eta_2 g_{a'b'}(\eta - \eta_2) \int d^3\mathbf{k}_3 d^3\mathbf{k}_4 g_{a'b'}(\eta_2) \gamma_{b'c'd'}^{(s)}(\mathbf{k}', \mathbf{k}_3, \mathbf{k}_4) g_{c'e'}(\eta_2) g_{d'f'}(\eta_2) \phi_{e'}^{(0)}(\mathbf{k}_3) \phi_{f'}^{(0)}(\mathbf{k}_4) \right\rangle , \\ &= \int \prod_{i=1}^4 d^3\mathbf{k}_i \int_0^\eta d\eta_2 g_{a'b'}(\eta - \eta_2) \gamma_{b'c'd'}^{(s)}(\mathbf{k}', \mathbf{k}_3, \mathbf{k}_4) g_{c'e'}(\eta_2) g_{d'f'}(\eta_2) \\ &\times \int_0^\eta d\eta_1 g_{ab}(\eta - \eta_1) \gamma_{bcd}^{(s)}(\mathbf{k}, \mathbf{k}_1, \mathbf{k}_2) g_{ce}(\eta_1) g_{df}(\eta_1) \left\langle \phi_e^{(0)}(\mathbf{k}_1) \phi_f^{(0)}(\mathbf{k}_2) \phi_{e'}^{(0)}(\mathbf{k}_3) \phi_{f'}^{(0)}(\mathbf{k}_4) \right\rangle . \end{aligned} \quad (\text{C1})$$

On assuming Gaussian initial conditions we may use Wick's theorem to rewrite the product of initial fields,

$$\begin{aligned} \left\langle \phi_e^{(0)}(\mathbf{k}_1) \phi_f^{(0)}(\mathbf{k}_2) \phi_{e'}^{(0)}(\mathbf{k}_3) \phi_{f'}^{(0)}(\mathbf{k}_4) \right\rangle &= [\mathcal{P}_{ef}(\mathbf{k}_1) \delta^D(\mathbf{k}_1 + \mathbf{k}_2) \mathcal{P}_{e'f'}(\mathbf{k}_3) \delta^D(\mathbf{k}_3 + \mathbf{k}_4) \\ &+ \mathcal{P}_{ee'}(\mathbf{k}_1) \delta^D(\mathbf{k}_1 + \mathbf{k}_3) \mathcal{P}_{ff'}(\mathbf{k}_2) \delta^D(\mathbf{k}_2 + \mathbf{k}_4) \\ &+ \mathcal{P}_{ef'}(\mathbf{k}_1) \delta^D(\mathbf{k}_1 + \mathbf{k}_4) \mathcal{P}_{fe'}(\mathbf{k}_2) \delta^D(\mathbf{k}_2 + \mathbf{k}_3)] . \end{aligned} \quad (\text{C2})$$

We notice that the first term in this structure involves Dirac delta functions with $\delta^D(\mathbf{k}_1 + \mathbf{k}_2)$ and $\delta^D(\mathbf{k}_3 + \mathbf{k}_4)$, if we were to perform any of the k -integrals, this would lead to a vertex matrix $\gamma_{bcd}^{(s)}(\mathbf{k}, \mathbf{k}_1, -\mathbf{k}_1) = 0$. Thus from momentum conservation the first term vanishes. The next two terms are non-zero, but are symmetric to relabelings, and so give a factor of 2. Thus we have,

$$\begin{aligned} \left\langle \Psi_a^{(1)}(\mathbf{k}) \Psi_{a'}^{(1)}(\mathbf{k}') \right\rangle &= 2 \int_0^\eta d\eta_1 g_{ab}(\eta - \eta_1) g_{ce}(\eta_1) g_{df}(\eta_1) \int_0^\eta d\eta_2 g_{a'b'}(\eta - \eta_2) g_{c'e'}(\eta_2) g_{d'f'}(\eta_2) \\ &\times \int \prod_{i=1}^4 d^3\mathbf{k}_i \gamma_{bcd}^{(s)}(\mathbf{k}, \mathbf{k}_1, \mathbf{k}_2) \gamma_{b'c'd'}^{(s)}(\mathbf{k}', \mathbf{k}_3, \mathbf{k}_4) \mathcal{P}_{ee'}(\mathbf{k}_1) \delta^D(\mathbf{k}_1 + \mathbf{k}_3) \mathcal{P}_{ff'}(\mathbf{k}_2) \delta^D(\mathbf{k}_2 + \mathbf{k}_4) . \end{aligned} \quad (\text{C3})$$

Considering the k -space integrals, if we perform the \mathbf{k}_4 and \mathbf{k}_3 integrals then we arrive at,

$$\rightarrow \int d^3\mathbf{k}_1 d^3\mathbf{k}_2 \gamma_{bcd}^{(s)}(\mathbf{k}, \mathbf{k}_1, \mathbf{k}_2) \gamma_{b'c'd'}^{(s)}(\mathbf{k}', -\mathbf{k}_1, -\mathbf{k}_2) \mathcal{P}_{ee'}(\mathbf{k}_1) \mathcal{P}_{ff'}(\mathbf{k}_2) . \quad (\text{C4})$$

If we now use $\gamma_{abc}^{(s)}(\mathbf{k}, \mathbf{k}_1, \mathbf{k}_2) = \bar{\gamma}_{abc}^{(s)}(\mathbf{k}_1, \mathbf{k}_2) \delta^D(\mathbf{k} - \mathbf{k}_1 - \mathbf{k}_2)$ to factor out the Dirac delta functions from the vertex matrices, then we find

$$\begin{aligned} \left\langle \Psi_a^{(1)}(\mathbf{k}) \Psi_{a'}^{(1)}(\mathbf{k}') \right\rangle &= 2 \int_0^\eta d\eta_1 g_{ab}(\eta - \eta_1) g_{ce}(\eta_1) g_{df}(\eta_1) \int_0^\eta d\eta_2 g_{a'b'}(\eta - \eta_2) g_{c'e'}(\eta_2) g_{d'f'}(\eta_2) \\ &\times \int d^3\mathbf{k}_1 d^3\mathbf{k}_2 \bar{\gamma}_{bcd}^{(s)}(\mathbf{k}_1, \mathbf{k}_2) \delta^D(\mathbf{k} - \mathbf{k}_1 - \mathbf{k}_2) \bar{\gamma}_{b'c'd'}^{(s)}(-\mathbf{k}_1, -\mathbf{k}_2) \delta^D(\mathbf{k}' + \mathbf{k}_1 + \mathbf{k}_2) \mathcal{P}_{ee'}(\mathbf{k}_1) \mathcal{P}_{ff'}(\mathbf{k}_2) . \end{aligned} \quad (\text{C5})$$

On computing the integral over \mathbf{k}_2 and factoring out the delta function $\delta^D(\mathbf{k} + \mathbf{k}')$, we find that our general expression for the one-loop mode-coupling contribution to the power spectrum is given by, (c.f. Eq. (73)) and see also [1])

$$\begin{aligned} \delta P_{aa',\text{MC}}^{(1)}(\mathbf{k}, \eta) &= 2 \int d^3\mathbf{k}_1 \int_0^\eta d\eta_1 \int_0^\eta d\eta_2 g_{ab}(\eta - \eta_1) \bar{\gamma}_{bcd}^{(s)}(\mathbf{k}_1, \mathbf{k} - \mathbf{k}_1) g_{ce}(\eta_1) g_{df}(\eta_1) \\ &\times g_{a'b'}(\eta - \eta_2) \bar{\gamma}_{b'c'd'}^{(s)}(-\mathbf{k}_1, \mathbf{k}_1 - \mathbf{k}) g_{c'e'}(\eta_2) g_{d'f'}(\eta_2) \mathcal{P}_{ee'}(\mathbf{k}_1) \mathcal{P}_{ff'}(|\mathbf{k} - \mathbf{k}_1|). \end{aligned} \quad (\text{C6})$$

Finally, on choosing large-scale growing mode initial conditions, $u_a^{(1)} = (1, \dots, 1)$, the above expression reduces to

$$\begin{aligned} \delta P_{aa',\text{MC}}^{(1)}(\mathbf{k}, \eta) &= 2 \int d^3\mathbf{k}_1 \mathcal{P}_0(k_1) \mathcal{P}_0(|\mathbf{k} - \mathbf{k}_1|) \\ &\times \int_0^\eta d\eta_1 g_{ab}(\eta - \eta_1) \bar{\gamma}_{bcd}^{(s)}(\mathbf{k}_1, \mathbf{k} - \mathbf{k}_1) g_{ce}(\eta_1) T_e(k_1) g_{df}(\eta_1) T_f(|\mathbf{k} - \mathbf{k}_1|) \\ &\times \int_0^\eta d\eta_2 g_{a'b'}(\eta - \eta_2) \bar{\gamma}_{b'c'd'}^{(s)}(-\mathbf{k}_1, \mathbf{k}_1 - \mathbf{k}) g_{c'e'}(\eta_2) T_{e'}(k_1) g_{d'f'}(\eta_2) T_{f'}(|\mathbf{k} - \mathbf{k}_1|). \end{aligned} \quad (\text{C7})$$

APPENDIX D: SOME MOMENTUM INTEGRALS

1. Momentum integrals arising in computing $\delta G_{ab}^{(1)}(\mathbf{k}, \eta)$

When computing $\delta G_{ab}^{(1)}(\mathbf{k}, \eta)$, we encounter the momentum integral

$$\int d^3\mathbf{k}_1 \bar{\gamma}_{bcd}^{(s)}(\mathbf{k}_1, \mathbf{k} - \mathbf{k}_1) \bar{\gamma}_{efg}^{(s)}(-\mathbf{k}_1, \mathbf{k}) \mathcal{P}_{cf'}^{(0)}(k_1). \quad (\text{D1})$$

Since all non-zero matrix elements of $\bar{\gamma}_{abc}^{(s)}(\mathbf{k}_1, \mathbf{k}_2)$ are either $\alpha(\mathbf{k}_1, \mathbf{k}_2)/2$, $\alpha(\mathbf{k}_2, \mathbf{k}_1)/2$ or $\beta(\mathbf{k}_1, \mathbf{k}_2)$, we see that only nine distinct types of integrals can arise in the computation. These are

$$I_1^{\delta^i \delta^j}(k) = \int d^3\mathbf{k}_1 \alpha(\mathbf{k}_1, \mathbf{k} - \mathbf{k}_1) \alpha(-\mathbf{k}_1, \mathbf{k}) \mathcal{P}_{ij}^{(0)}(k_1) = -\frac{1}{3} k^2 \int d^3\mathbf{k}_1 \frac{1}{k_1^2} \mathcal{P}_{ij}^{(0)}(k_1), \quad (\text{D2})$$

$$I_2^{\delta^i \delta^j}(k) = \int d^3\mathbf{k}_1 \alpha(\mathbf{k}_1, \mathbf{k} - \mathbf{k}_1) \alpha(\mathbf{k}, -\mathbf{k}_1) \mathcal{P}_{ij}^{(0)}(k_1) = -\frac{1}{3} \int d^3\mathbf{k}_1 \mathcal{P}_{ij}^{(0)}(k_1), \quad (\text{D3})$$

$$I_3^{\delta^i \delta^j}(k) = \int d^3\mathbf{k}_1 \alpha(\mathbf{k} - \mathbf{k}_1, \mathbf{k}_1) \alpha(-\mathbf{k}_1, \mathbf{k}) \mathcal{P}_{ij}^{(0)}(k_1) = \int d^3\mathbf{k}_1 \left[\frac{k^2 + k_1^2}{4k_1^2} + \frac{(k^2 - k_1^2)^2}{16kk_1^3} \ln \frac{|k - k_1|^2}{|k + k_1|^2} \right] \mathcal{P}_{ij}^{(0)}(k_1), \quad (\text{D4})$$

$$I_4^{\delta^i \delta^j}(k) = \int d^3\mathbf{k}_1 \alpha(\mathbf{k} - \mathbf{k}_1, \mathbf{k}_1) \alpha(\mathbf{k}, -\mathbf{k}_1) \mathcal{P}_{ij}^{(0)}(k_1) = \int d^3\mathbf{k}_1 \left[\frac{3k^2 - k_1^2}{4k^2} - \frac{(k^2 - k_1^2)^2}{16k^3k_1} \ln \frac{|k - k_1|^2}{|k + k_1|^2} \right] \mathcal{P}_{ij}^{(0)}(k_1), \quad (\text{D5})$$

$$I_5^{\delta^i \delta^j}(k) = \int d^3\mathbf{k}_1 \beta(\mathbf{k}_1, \mathbf{k} - \mathbf{k}_1) \alpha(-\mathbf{k}_1, \mathbf{k}) \mathcal{P}_{ij}^{(0)}(k_1) = \int d^3\mathbf{k}_1 \left[\frac{k^2(k^2 - 3k_1^2)}{8k_1^4} + \frac{k(k^2 - k_1^2)^2}{32k_1^5} \ln \frac{|k - k_1|^2}{|k + k_1|^2} \right] \mathcal{P}_{ij}^{(0)}(k_1), \quad (\text{D6})$$

$$I_6^{\delta^i \delta^j}(k) = \int d^3\mathbf{k}_1 \alpha(\mathbf{k}_1, \mathbf{k} - \mathbf{k}_1) \beta(-\mathbf{k}_1, \mathbf{k}) \mathcal{P}_{ij}^{(0)}(k_1) = -\frac{1}{6} \int d^3\mathbf{k}_1 \left[1 + \frac{k^2}{k_1^2} \right] \mathcal{P}_{ij}^{(0)}(k_1), \quad (\text{D7})$$

$$I_7^{\delta^i \delta^j}(k) = \int d^3\mathbf{k}_1 \alpha(\mathbf{k} - \mathbf{k}_1, \mathbf{k}_1) \beta(-\mathbf{k}_1, \mathbf{k}) \mathcal{P}_{ij}^{(0)}(k_1) = \frac{1}{6} \int d^3\mathbf{k}_1 \mathcal{P}_{ij}^{(0)}(k_1), \quad (\text{D8})$$

$$I_8^{\delta^i \delta^j}(k) = \int d^3\mathbf{k}_1 \beta(\mathbf{k}_1, \mathbf{k} - \mathbf{k}_1) \alpha(\mathbf{k}, -\mathbf{k}_1) \mathcal{P}_{ij}^{(0)}(k_1) = - \int d^3\mathbf{k}_1 \left[\frac{k^2 + k_1^2}{8k_1^2} + \frac{(k^2 - k_1^2)^2}{32kk_1^3} \ln \frac{|k - k_1|^2}{|k + k_1|^2} \right] \mathcal{P}_{ij}^{(0)}(k_1), \quad (\text{D9})$$

$$I_9^{\delta^i \delta^j}(k) = \int d^3\mathbf{k}_1 \beta(\mathbf{k}_1, \mathbf{k} - \mathbf{k}_1) \beta(-\mathbf{k}_1, \mathbf{k}) \mathcal{P}_{ij}^{(0)}(k_1) = -\frac{1}{12} k^2 \int d^3\mathbf{k}_1 \frac{1}{k_1^2} \mathcal{P}_{ij}^{(0)}(k_1). \quad (\text{D10})$$

However, only five of the above integrals are independent (for any given i and j), and we have the following relations

$$I_6^{\delta^i \delta^j}(k) = \frac{1}{2} I_1^{\delta^i \delta^j}(k) + \frac{1}{2} I_2^{\delta^i \delta^j}(k), \quad I_7^{\delta^i \delta^j}(k) = -\frac{1}{2} I_2^{\delta^i \delta^j}(k), \quad I_8^{\delta^i \delta^j}(k) = -\frac{1}{2} I_3^{\delta^i \delta^j}(k), \quad I_9^{\delta^i \delta^j}(k) = \frac{1}{4} I_1^{\delta^i \delta^j}(k). \quad (\text{D11})$$

Then we may choose any non-degenerate linear combination of e.g. $\{I_1^{\delta^i \delta^j}(k), \dots, I_5^{\delta^i \delta^j}(k)\}$ as our set of independent integrals. In order to facilitate comparison with the known expressions for the case of a single component fluid [26], we define:

$$f_1^{\delta^i \delta^j}(k) = \frac{19}{42} I_1^{\delta^i \delta^j}(k) + \frac{1}{6} I_2^{\delta^i \delta^j}(k) + \frac{5}{42} I_3^{\delta^i \delta^j}(k) + \frac{1}{6} I_4^{\delta^i \delta^j}(k) + \frac{2}{21} I_5^{\delta^i \delta^j}(k) \quad (D12)$$

$$= \int \frac{d^3 \mathbf{k}_1}{504 k^3 k_1^5} \left[6k^7 k_1 - 79k^5 k_1^3 + 50k^3 k_1^5 - 21k k_1^7 + \frac{3}{4}(k^2 - k_1^2)^3 (2k^2 + 7k_1^2) \ln \frac{|k - k_1|^2}{|k + k_1|^2} \right] \mathcal{P}_{ij}^{(0)}(k_1)$$

$$f_2^{\delta^i \delta^j}(k) = \frac{5}{14} I_1^{\delta^i \delta^j}(k) + \frac{1}{14} I_2^{\delta^i \delta^j}(k) - \frac{1}{14} I_3^{\delta^i \delta^j}(k) + \frac{1}{14} I_4^{\delta^i \delta^j}(k) + \frac{2}{7} I_5^{\delta^i \delta^j}(k) \quad (D13)$$

$$= \int \frac{d^3 \mathbf{k}_1}{168 k^3 k_1^5} \left[6k^7 k_1 - 41k^5 k_1^3 + 2k^3 k_1^5 - 3k k_1^7 + \frac{3}{4}(k^2 - k_1^2)^3 (2k^2 + k_1^2) \ln \frac{|k - k_1|^2}{|k + k_1|^2} \right] \mathcal{P}_{ij}^{(0)}(k_1)$$

$$f_3^{\delta^i \delta^j}(k) = -\frac{1}{2} I_1^{\delta^i \delta^j}(k) - \frac{3}{2} I_2^{\delta^i \delta^j}(k) + \frac{5}{2} I_3^{\delta^i \delta^j}(k) - \frac{3}{2} I_4^{\delta^i \delta^j}(k) + 2 I_5^{\delta^i \delta^j}(k) \quad (D14)$$

$$= \int \frac{d^3 \mathbf{k}_1}{24 k^3 k_1^5} \left[6k^7 k_1 + k^5 k_1^3 + 9k k_1^7 + \frac{3}{4}(k^2 - k_1^2)^2 (2k^4 + 5k^2 k_1^2 + 3k_1^4) \ln \frac{|k - k_1|^2}{|k + k_1|^2} \right] \mathcal{P}_{ij}^{(0)}(k_1)$$

$$f_4^{\delta^i \delta^j}(k) = \frac{5}{6} I_1^{\delta^i \delta^j}(k) + \frac{3}{2} I_2^{\delta^i \delta^j}(k) - \frac{3}{2} I_3^{\delta^i \delta^j}(k) + \frac{3}{2} I_4^{\delta^i \delta^j}(k) - \frac{2}{7} I_5^{\delta^i \delta^j}(k) \quad (D15)$$

$$= \int \frac{-d^3 \mathbf{k}_1}{72 k^3 k_1^5} \left[6k^7 k_1 + 29k^5 k_1^3 - 18k^3 k_1^5 + 27k k_1^7 + \frac{3}{4}(k^2 - k_1^2)^2 (2k^4 + 9k^2 k_1^2 + 9k_1^4) \ln \frac{|k - k_1|^2}{|k + k_1|^2} \right] \mathcal{P}_{ij}^{(0)}(k_1)$$

$$f_5^{\delta^i \delta^j}(k) = I_2^{\delta^i \delta^j}(k) \quad (D16)$$

$$= \int \frac{-d^3 \mathbf{k}_1}{3} \mathcal{P}_{ij}^{(0)}(k_1),$$

as the set of independent integrals appearing in Eq. (79). Clearly the functions $\{f_1, f_2, f_3, f_4\}$ are just the $\{f, g, h, i\}$ functions of [26], while f_5 is simply a constant. This constant is formally divergent for initial power spectra that fall no faster than k^{-3} at large k . However, we regard this to be an artifact of using unsmoothed (i.e. infinitely “choppy”) initial fields to arbitrarily low spatial scales. Clearly this is unphysical. Hence, in obtaining the numerical results presented in this paper, we applied a Gaussian smoothing to all initial power spectra, with smoothing scale $R_{\text{smooth}} = 0.1 h^{-1} \text{ Mpc}$, i.e. we set $\mathcal{P}_{ij}^{(0)}(k) \rightarrow \mathcal{P}_{ij}^{(0)}(k) e^{-k^2 R_{\text{smooth}}^2}$.

Finally, for the sake of completeness, we note that the $f(k)$ and $g(k)$ functions of §VII A may be expressed with the basis integrals as

$$f(k) = w_1^2 f_1^{\delta^c \delta^c}(k) + 2w_1 2_2 f_1^{\delta^c \delta^b}(k) + w_2^2 f_1^{\delta^b \delta^b}(k), \quad (D17)$$

$$g(k) = w_1^2 f_2^{\delta^c \delta^c}(k) + 2w_1 2_2 f_2^{\delta^c \delta^b}(k) + w_2^2 f_2^{\delta^b \delta^b}(k). \quad (D18)$$

2. Momentum integrals arising in computing $\delta P_{ab, \text{MC}}^{(1)}(\mathbf{k}, \eta)$

When computing the mode-coupling piece of the one-loop power spectrum, $\delta P_{ab, \text{MC}}^{(1)}(\mathbf{k}, \eta)$, we encounter the momentum integral

$$\int d^3 \mathbf{k}_1 \bar{\gamma}_{bcd}^{(s)}(\mathbf{k}_1, \mathbf{k} - \mathbf{k}_1) \bar{\gamma}_{efg}^{(s)}(-\mathbf{k}_1, \mathbf{k}_1 - \mathbf{k}) \mathcal{P}_{ee'}^{(0)}(k_1) \mathcal{P}_{ff'}^{(0)}(|\mathbf{k} - \mathbf{k}_1|). \quad (D19)$$

Since $\alpha(-\mathbf{k}_1, -\mathbf{k}_2) = \alpha(\mathbf{k}_1, \mathbf{k}_2)$ and $\beta(-\mathbf{k}_1, -\mathbf{k}_2) = \beta(\mathbf{k}_1, \mathbf{k}_2)$, we see that only six distinct types of integrals can arise in the computation. These read

$$\begin{aligned} J_1^{\delta^i \delta^j \delta^k \delta^l}(k) &= \int d^3 \mathbf{k}_1 [\alpha(\mathbf{k}_1, \mathbf{k} - \mathbf{k}_1)]^2 \mathcal{P}_{ij}^{(0)}(k_1) \mathcal{P}_{kl}^{(0)}(|\mathbf{k} - \mathbf{k}_1|), \\ &= \int d^3 \mathbf{k}_1 \frac{k^2 x^2}{k_1^2} \mathcal{P}_{ij}^{(0)}(k_1) \mathcal{P}_{kl}^{(0)}\left(\sqrt{k^2 - 2kk_1x + k_1^2}\right), \end{aligned} \quad (\text{D20})$$

$$\begin{aligned} J_2^{\delta^i \delta^j \delta^k \delta^l}(k) &= \int d^3 \mathbf{k}_1 \alpha(\mathbf{k}_1, \mathbf{k} - \mathbf{k}_1) \alpha(\mathbf{k} - \mathbf{k}_1, \mathbf{k}_1) \mathcal{P}_{ij}^{(0)}(k_1) \mathcal{P}_{kl}^{(0)}(|\mathbf{k} - \mathbf{k}_1|), \\ &= \int d^3 \mathbf{k}_1 \frac{k^2 x(k - k_1 x)}{k_1(k^2 - 2kk_1x + k_1^2)} \mathcal{P}_{ij}^{(0)}(k_1) \mathcal{P}_{kl}^{(0)}\left(\sqrt{k^2 - 2kk_1x + k_1^2}\right), \end{aligned} \quad (\text{D21})$$

$$\begin{aligned} J_3^{\delta^i \delta^j \delta^k \delta^l}(k) &= \int d^3 \mathbf{k}_1 \alpha(\mathbf{k}_1, \mathbf{k} - \mathbf{k}_1) \beta(\mathbf{k}_1, \mathbf{k} - \mathbf{k}_1) \mathcal{P}_{ij}^{(0)}(k_1) \mathcal{P}_{kl}^{(0)}(|\mathbf{k} - \mathbf{k}_1|), \\ &= \int d^3 \mathbf{k}_1 \frac{k^3 x(kx - k_1)}{2k_1^2(k^2 - 2kk_1x + k_1^2)} \mathcal{P}_{ij}^{(0)}(k_1) \mathcal{P}_{kl}^{(0)}\left(\sqrt{k^2 - 2kk_1x + k_1^2}\right), \end{aligned} \quad (\text{D22})$$

$$\begin{aligned} J_4^{\delta^i \delta^j \delta^k \delta^l}(k) &= \int d^3 \mathbf{k}_1 [\beta(\mathbf{k}_1, \mathbf{k} - \mathbf{k}_1)]^2 \mathcal{P}_{ij}^{(0)}(k_1) \mathcal{P}_{kl}^{(0)}(|\mathbf{k} - \mathbf{k}_1|), \\ &= \int d^3 \mathbf{k}_1 \frac{k^4(k_1 - kx)^2}{4k_1^2(k^2 - 2kk_1x + k_1^2)^2} \mathcal{P}_{ij}^{(0)}(k_1) \mathcal{P}_{kl}^{(0)}\left(\sqrt{k^2 - 2kk_1x + k_1^2}\right), \end{aligned} \quad (\text{D23})$$

$$\begin{aligned} J_5^{\delta^i \delta^j \delta^k \delta^l}(k) &= \int d^3 \mathbf{k}_1 [\alpha(\mathbf{k} - \mathbf{k}_1, \mathbf{k}_1)]^2 \mathcal{P}_{ij}^{(0)}(k_1) \mathcal{P}_{kl}^{(0)}(|\mathbf{k} - \mathbf{k}_1|), \\ &= \int d^3 \mathbf{k}_1 \frac{k^2(k - k_1x)^2}{(k^2 - 2kk_1x + k_1^2)^2} \mathcal{P}_{ij}^{(0)}(k_1) \mathcal{P}_{kl}^{(0)}\left(\sqrt{k^2 - 2kk_1x + k_1^2}\right), \end{aligned} \quad (\text{D24})$$

$$\begin{aligned} J_6^{\delta^i \delta^j \delta^k \delta^l}(k) &= \int d^3 \mathbf{k}_1 \alpha(\mathbf{k} - \mathbf{k}_1, \mathbf{k}_1) \beta(\mathbf{k}_1, \mathbf{k} - \mathbf{k}_1) \mathcal{P}_{ij}^{(0)}(k_1) \mathcal{P}_{kl}^{(0)}(|\mathbf{k} - \mathbf{k}_1|), \\ &= \int d^3 \mathbf{k}_1 \frac{k^3 [xk^2 - k_1(x^2 + 1)k + k_1^2x]}{2k_1(k^2 - 2kk_1x + k_1^2)^2} \mathcal{P}_{ij}^{(0)}(k_1) \mathcal{P}_{kl}^{(0)}\left(\sqrt{k^2 - 2kk_1x + k_1^2}\right). \end{aligned} \quad (\text{D25})$$

However, not all of these integrals are independent, since changing the variable of integration as $\mathbf{k}_1 \rightarrow \mathbf{k}'_1 = \mathbf{k} - \mathbf{k}_1$ merely exchanges $J_1^{\delta^i \delta^j \delta^k \delta^l}(k)$ with $J_5^{\delta^k \delta^l \delta^i \delta^j}(k)$ and $J_3^{\delta^i \delta^j \delta^k \delta^l}(k)$ with $J_6^{\delta^k \delta^l \delta^i \delta^j}(k)$. Thus, for $(ij) = (kl)$, J_5 and J_6 are not independent integrals:

$$J_5^{\delta^i \delta^j \delta^i \delta^j}(k) = J_1^{\delta^i \delta^j \delta^i \delta^j}(k), \quad J_6^{\delta^i \delta^j \delta^i \delta^j}(k) = J_3^{\delta^i \delta^j \delta^i \delta^j}(k). \quad (\text{D26})$$

On the other hand, if $(ij) \neq (kl)$, then we find that we may express each $J_n^{\delta^i \delta^j \delta^k \delta^l}(k)$ with some $J_m^{\delta^i \delta^j \delta^k \delta^l}(k)$:

$$\begin{aligned} J_1^{\delta^i \delta^l \delta^i \delta^j}(k) &= J_5^{\delta^i \delta^j \delta^k \delta^l}(k), \quad J_2^{\delta^k \delta^l \delta^i \delta^j}(k) = J_2^{\delta^i \delta^j \delta^k \delta^l}(k), \quad J_3^{\delta^k \delta^l \delta^i \delta^j}(k) = J_6^{\delta^i \delta^j \delta^k \delta^l}(k) \\ J_4^{\delta^k \delta^l \delta^i \delta^j}(k) &= J_4^{\delta^i \delta^j \delta^k \delta^l}(k), \quad J_5^{\delta^k \delta^l \delta^i \delta^j}(k) = J_1^{\delta^i \delta^j \delta^k \delta^l}(k), \quad J_6^{\delta^k \delta^l \delta^i \delta^j}(k) = J_3^{\delta^i \delta^j \delta^k \delta^l}(k). \end{aligned} \quad (\text{D27})$$

Thus, we may define

$$f_n^{\delta^i \delta^j \delta^i \delta^j}(k) = J_n^{\delta^i \delta^j \delta^i \delta^j}(k), \quad n = 1, \dots, 4, \quad (ij) = \{(cc), (cb), (bb)\}, \quad (\text{D28})$$

$$f_n^{\delta^i \delta^j \delta^k \delta^l}(k) = J_n^{\delta^i \delta^j \delta^k \delta^l}(k), \quad n = 1, \dots, 6, \quad (ij)(kl) = \{(cc)(cb), (cc)(bb), (cb)(bb)\} \quad (\text{D29})$$

as the set of independent integrals appearing in Eq. (85).

Finally, for the sake of completeness, we note that the $F(k)$, $G(k)$ and $H(k)$ functions of §VII B may be expressed with these basis integrals as

$$F(k) = \frac{25}{196} J_1^{\bar{\delta}\bar{\delta}\bar{\delta}\bar{\delta}}(k) + \frac{25}{98} J_2^{\bar{\delta}\bar{\delta}\bar{\delta}\bar{\delta}}(k) + \frac{10}{49} J_3^{\bar{\delta}\bar{\delta}\bar{\delta}\bar{\delta}}(k) + \frac{4}{49} J_4^{\bar{\delta}\bar{\delta}\bar{\delta}\bar{\delta}}(k) + \frac{25}{196} J_5^{\bar{\delta}\bar{\delta}\bar{\delta}\bar{\delta}}(k) + \frac{10}{49} J_6^{\bar{\delta}\bar{\delta}\bar{\delta}\bar{\delta}}(k), \quad (\text{D30})$$

$$G(k) = \frac{9}{196} J_1^{\bar{\delta}\bar{\delta}\bar{\delta}\bar{\delta}}(k) + \frac{9}{98} J_2^{\bar{\delta}\bar{\delta}\bar{\delta}\bar{\delta}}(k) + \frac{12}{49} J_3^{\bar{\delta}\bar{\delta}\bar{\delta}\bar{\delta}}(k) + \frac{16}{49} J_4^{\bar{\delta}\bar{\delta}\bar{\delta}\bar{\delta}}(k) + \frac{9}{196} J_5^{\bar{\delta}\bar{\delta}\bar{\delta}\bar{\delta}}(k) + \frac{12}{49} J_6^{\bar{\delta}\bar{\delta}\bar{\delta}\bar{\delta}}(k), \quad (\text{D31})$$

$$H(k) = \frac{15}{98} J_1^{\bar{\delta}\bar{\delta}\bar{\delta}\bar{\delta}}(k) + \frac{15}{49} J_2^{\bar{\delta}\bar{\delta}\bar{\delta}\bar{\delta}}(k) + \frac{26}{49} J_3^{\bar{\delta}\bar{\delta}\bar{\delta}\bar{\delta}}(k) + \frac{16}{49} J_4^{\bar{\delta}\bar{\delta}\bar{\delta}\bar{\delta}}(k) + \frac{15}{98} J_5^{\bar{\delta}\bar{\delta}\bar{\delta}\bar{\delta}}(k) + \frac{26}{49} J_6^{\bar{\delta}\bar{\delta}\bar{\delta}\bar{\delta}}(k), \quad (\text{D32})$$

where

$$\begin{aligned}
J_n^{\bar{\delta}\bar{\delta}\bar{\delta}}(k) = & w_1^4 J_n^{\delta^c \delta^c \delta^c}(k) + 2w_1^3 w_2 J_n^{\delta^c \delta^c \delta^b}(k) + w_1^2 w_2^2 J_n^{\delta^c \delta^b \delta^b}(k) \\
& + 2w_1^3 w_2 J_n^{\delta^c \delta^b \delta^c}(k) + 4w_1^2 w_2^2 J_n^{\delta^c \delta^b \delta^c \delta^b}(k) + 2w_1 w_2^3 J_n^{\delta^c \delta^b \delta^b \delta^b}(k) \\
& + w_1^2 w_2^2 J_n^{\delta^b \delta^b \delta^c \delta^c}(k) + 2w_1 w_2^3 J_n^{\delta^b \delta^b \delta^c \delta^b}(k) + w_2^4 J_n^{\delta^b \delta^b \delta^b \delta^b}(k).
\end{aligned} \tag{D33}$$

In Eqs (D30)–(D32) above, we clearly have $J_5^{\bar{\delta}\bar{\delta}\bar{\delta}}(k) = J_1^{\bar{\delta}\bar{\delta}\bar{\delta}}(k)$ and $J_6^{\bar{\delta}\bar{\delta}\bar{\delta}}(k) = J_3^{\bar{\delta}\bar{\delta}\bar{\delta}}(k)$. However, to obtain the compact expressions for $F(k)$, $G(k)$ and $H(k)$ as in Eqs (98)–(100), one must substitute Eqs (D20)–(D25) as they stand into the general formulae, Eqs (D30)–(D32), disregarding the above identities.

APPENDIX E: THE LINEAR PROPAGATOR FOR $N = 3$

For $N = 3$, the propagator takes the form as in Eq. (27):

$$g_{ab}(\eta) = \sum_l e^{l\eta} g_{ab,l}, \tag{E1}$$

with $l \in \{1, 0, -1/2, -3/2\}$. The $g_{ab,l}$ are constant matrices:

$$g_{ab,1} = \frac{1}{5} \begin{bmatrix} 3w_1 & 2w_1 & 3w_2 & 2w_2 & 3w_3 & 2w_3 \\ 3w_1 & 2w_1 & 3w_2 & 2w_2 & 3w_3 & 2w_3 \\ 3w_1 & 2w_1 & 3w_2 & 2w_2 & 3w_3 & 2w_3 \\ 3w_1 & 2w_1 & 3w_2 & 2w_2 & 3w_3 & 2w_3 \\ 3w_1 & 2w_1 & 3w_2 & 2w_2 & 3w_3 & 2w_3 \\ 3w_1 & 2w_1 & 3w_2 & 2w_2 & 3w_3 & 2w_3 \end{bmatrix}, \tag{E2}$$

$$g_{ab,0} = \begin{bmatrix} 1-w_1 & 2(1-w_1) & -w_2 & -2w_2 & -w_3 & -2w_3 \\ 0 & 0 & 0 & 0 & 0 & 0 \\ -w_1 & -2w_1 & 1-w_2 & 2(1-w_2) & -w_3 & -2w_3 \\ 0 & 0 & 0 & 0 & 0 & 0 \\ -w_1 & -2w_1 & -w_2 & -2w_2 & 1-w_3 & 2(1-w_3) \\ 0 & 0 & 0 & 0 & 0 & 0 \end{bmatrix}, \tag{E3}$$

$$g_{ab,-1/2} = \begin{bmatrix} 0 & -2(1-w_1) & 0 & 2w_2 & 0 & 2w_3 \\ 0 & 1-w_1 & 0 & -w_2 & 0 & -w_3 \\ 0 & 2w_1 & 0 & -2(1-w_2) & 0 & 2w_3 \\ 0 & -w_1 & 0 & 1-w_2 & 0 & -w_3 \\ 0 & 2w_1 & 0 & 2w_2 & 0 & -2(1-w_3) \\ 0 & -w_1 & 0 & -w_2 & 0 & 1-w_3 \end{bmatrix}, \tag{E4}$$

$$g_{ab,-3/2} = \frac{1}{5} \begin{bmatrix} 2w_1 & -2w_1 & 2w_2 & -2w_2 & 2w_3 & -2w_3 \\ -3w_1 & 3w_1 & -3w_2 & 3w_2 & -3w_3 & 3w_3 \\ 2w_1 & -2w_1 & 2w_2 & -2w_2 & 2w_3 & -2w_3 \\ -3w_1 & 3w_1 & -3w_2 & 3w_2 & -3w_3 & 3w_3 \\ 2w_1 & -2w_1 & 2w_2 & -2w_2 & 2w_3 & -2w_3 \\ -3w_1 & 3w_1 & -3w_2 & 3w_2 & -3w_3 & 3w_3 \end{bmatrix}. \tag{E5}$$

The eigenvectors of the linear propagator g_{ab} are:

$$u_a^{(1)} = \begin{pmatrix} 1 \\ 1 \\ 1 \\ 1 \\ 1 \\ 1 \end{pmatrix}; u_a^{(2)} = \begin{pmatrix} 2/3 \\ -1 \\ 2/3 \\ -1 \\ 2/3 \\ -1 \end{pmatrix}; u_a^{(3,1)} = \begin{pmatrix} w_2 \\ 0 \\ -w_1 \\ 0 \\ 0 \\ 0 \end{pmatrix}; u_a^{(3,2)} = \begin{pmatrix} w_3 \\ 0 \\ 0 \\ 0 \\ -w_1 \\ 0 \end{pmatrix}; u_a^{(4,1)} = \begin{pmatrix} 2w_2 \\ -w_2 \\ -2w_1 \\ w_1 \\ 0 \\ 0 \end{pmatrix}; u_a^{(4,2)} = \begin{pmatrix} 2w_3 \\ -w_3 \\ 0 \\ 0 \\ -2w_1 \\ w_1 \end{pmatrix}. \tag{E6}$$

The eigenvectors correspond to the following eigenvalues:

$$\mathbf{u}^{(1)} : \lambda_1 = e^\eta, \quad \mathbf{u}^{(2)} : \lambda_2 = e^{-3\eta/2}, \quad \mathbf{u}^{(3,m)} : \lambda_3 = 1, \quad \mathbf{u}^{(4,m)} : \lambda_4 = e^{-\eta/2}, \quad m = 1, 2. \tag{E7}$$

APPENDIX F: THE LINEAR PROPAGATOR FOR GENERAL N

Here we compute the linear propagator, $g_{ab}(\eta) = \mathcal{L}^{-1}[\sigma_{ab}(s), s, \eta]$, for general N , where $\mathcal{L}^{-1}[f(s), s, \eta]$ denotes the inverse Laplace transform of the function $f(s)$ from the variable s to the variable η and $\sigma_{ab}(s) = (s\delta_{ab} + \Omega_{ab})^{-1}$.

We begin by noting that

$$(s\mathbf{1} + \Omega)_{(2j-1)(2k-1)} = s\delta_{jk}, \quad (s\mathbf{1} + \Omega)_{(2j)(2k-1)} = -\frac{3}{2}w_k, \quad (\text{F1})$$

$$(s\mathbf{1} + \Omega)_{(2j-1)(2k)} = -\delta_{jk}, \quad (s\mathbf{1} + \Omega)_{(2j)(2k)} = \left(\frac{1}{2} + s\right)\delta_{jk}, \quad (\text{F2})$$

with $j, k = 1, 2, \dots, N$. Now we claim that $\sigma_{ab}(s)$ may be written in the following form for general N :

$$\begin{aligned} \sigma_{(2j-1)(2k-1)}(s) &= \frac{3w_k}{s(s-1)(2s+3)} + \frac{\delta_{jk}}{s}, \\ \sigma_{(2j)(2k-1)}(s) &= \frac{3w_k}{(s-1)(2s+3)}, \\ \sigma_{(2j-1)(2k)}(s) &= \frac{6w_k}{s(s-1)(2s+1)(2s+3)} + \frac{2\delta_{jk}}{s(2s+1)}, \\ \sigma_{(2j)(2k)}(s) &= \frac{6w_k}{(s-1)(2s+1)(2s+3)} + \frac{2\delta_{jk}}{(2s+1)}, \end{aligned} \quad (\text{F3})$$

($j, k = 1, 2, \dots, N$). We prove this claim by explicit computation. We calculate

$$[\sigma(s) \cdot (s\mathbf{1} + \Omega)]_{ab} = \sum_{c=1}^{2N} \sigma_{ac}(s)(s\mathbf{1} + \Omega)_{cb} = \sum_{k=1}^N [\sigma_{a(2k-1)}(s)(s\mathbf{1} + \Omega)_{(2k-1)b} + \sigma_{a(2k)}(s)(s\mathbf{1} + \Omega)_{(2k)b}] , \quad (\text{F4})$$

where in the last expression, we have split the sum over c into two sums, corresponding to odd and even c respectively. Now we examine the four cases corresponding to a and b being odd or even separately. We find

1. $a = 2n - 1, b = 2m - 1$

$$\begin{aligned} &\sum_{k=1}^N [\sigma_{(2n-1)(2k-1)}(s)(s\mathbf{1} + \Omega)_{(2k-1)(2m-1)} + \sigma_{(2n-1)(2k)}(s)(s\mathbf{1} + \Omega)_{(2k)(2m-1)}] \\ &= \sum_{k=1}^N \left[\left(\frac{3w_k}{s(s-1)(2s+3)} + \frac{\delta_{nk}}{s} \right) (s\delta_{km}) + \left(\frac{6w_k}{s(s-1)(2s+1)(2s+3)} + \frac{2\delta_{nk}}{s(2s+1)} \right) \left(-\frac{3}{2}w_m \right) \right] \\ &= \frac{3w_m}{(s-1)(2s+3)} + \delta_{nm} - \frac{3}{2}w_m \left(\frac{6}{s(s-1)(2s+1)(2s+3)} + \frac{2}{s(2s+1)} \right) \\ &= \delta_{nm}, \end{aligned} \quad (\text{F5})$$

where we have used that $\sum_{k=1}^N w_k = 1$.

2. $a = 2n, b = 2m - 1$

$$\begin{aligned} &\sum_{k=1}^N [\sigma_{(2n)(2k-1)}(s)(s\mathbf{1} + \Omega)_{(2k-1)(2m-1)} + \sigma_{(2n)(2k)}(s)(s\mathbf{1} + \Omega)_{(2k)(2m-1)}] \\ &= \sum_{k=1}^N \left[\left(\frac{3w_k}{(s-1)(2s+3)} \right) (s\delta_{km}) + \left(\frac{6w_k}{(s-1)(2s+1)(2s+3)} + \frac{2\delta_{nk}}{(2s+1)} \right) \left(-\frac{3}{2}w_m \right) \right] \\ &= \frac{3sw_m}{(s-1)(2s+3)} - \frac{3}{2}w_m \left(\frac{6}{(s-1)(2s+1)(2s+3)} + \frac{2}{(2s+1)} \right) \\ &= 0, \end{aligned} \quad (\text{F6})$$

where we have used that $\sum_{k=1}^N w_k = 1$.

3. $a = 2n - 1, b = 2m$

$$\begin{aligned}
& \sum_{k=1}^N [\sigma_{(2n-1)(2k-1)}(s)(s\mathbf{1} + \Omega)_{(2k-1)(2m)} + \sigma_{(2n-1)(2k)}(s)(s\mathbf{1} + \Omega)_{(2k)(2m)}] \\
&= \sum_{k=1}^N \left[\left(\frac{3w_k}{s(s-1)(2s+3)} + \frac{\delta_{nk}}{s} \right) (-\delta_{km}) + \left(\frac{6w_k}{s(s-1)(2s+1)(2s+3)} + \frac{2\delta_{nk}}{s(2s+1)} \right) \left(\frac{1}{2} + s \right) \delta_{km} \right] \quad (\text{F7}) \\
&= -\frac{3w_m}{s(s-1)(2s+3)} - \frac{\delta_{nm}}{s} + \left(\frac{1}{2} + s \right) \left(\frac{6w_m}{s(s-1)(2s+1)(2s+3)} + \frac{2\delta_{nm}}{s(2s+1)} \right) \\
&= 0.
\end{aligned}$$

4. $a = 2n, b = 2m$

$$\begin{aligned}
& \sum_{k=1}^N [\sigma_{(2n)(2k-1)}(s)(s\mathbf{1} + \Omega)_{(2k-1)(2m)} + \sigma_{(2n)(2k)}(s)(s\mathbf{1} + \Omega)_{(2k)(2m)}] \\
&= \sum_{k=1}^N \left[\left(\frac{3w_k}{(s-1)(2s+3)} \right) (-\delta_{km}) + \left(\frac{6w_k}{(s-1)(2s+1)(2s+3)} + \frac{2\delta_{nk}}{(2s+1)} \right) \left(\frac{1}{2} + s \right) \delta_{km} \right] \quad (\text{F8}) \\
&= -\frac{3w_m}{(s-1)(2s+3)} + \left(\frac{1}{2} + s \right) \left(\frac{6w_m}{(s-1)(2s+1)(2s+3)} + \frac{2\delta_{nm}}{(2s+1)} \right) \\
&= \delta_{nm} . \triangleleft
\end{aligned}$$

Finally, we recognize that performing the inverse Laplace transform of Eq. (F3), we simply obtain Eq. (26).

Similar explicit computations (which however we do not reproduce) establish that for general N , the propagator has the following $2N$ eigenvalues and eigenvectors:

1. Eigenvalue $\lambda_1 = e^\eta$ with multiplicity one. The corresponding eigenvector is:

$$u_a^{(1)} = (1, 1, \dots, 1, 1)^T. \quad (\text{F9})$$

2. Eigenvalue $\lambda_2 = e^{-3\eta/2}$ with multiplicity one. The corresponding eigenvector is:

$$u_a^{(2)} = (2/3, -1, \dots, 2/3, -1)^T. \quad (\text{F10})$$

3. Eigenvalue $\lambda_3 = 1$ with multiplicity $N - 1$. The corresponding eigenvectors are:

$$u_a^{(3,m)} = (w_m, 0, \dots, 0, -w_1, 0, \dots, 0)^T = w_m \delta_{a1} - w_1 \delta_{a(2m-1)}, \quad (\text{F11})$$

($m = 2, \dots, N$), i.e. the two non-zero entries in $\mathbf{u}^{(3,m)}$ are the first and the $2m - 1$ -th.

4. Eigenvalue $\lambda_3 = e^{-\eta/2}$ with multiplicity $N - 1$. The corresponding eigenvectors are:

$$u_a^{(4,m)} = (2w_m, -w_m, 0, \dots, 0, -2w_1, w_1, 0, \dots, 0)^T = 2w_m \delta_{a1} - w_m \delta_{a2} - 2w_1 \delta_{a(2m-1)} + w_1 \delta_{a(2m)}, \quad (\text{F12})$$

($m = 2, \dots, N$), i.e. the four non-zero entries in $\mathbf{u}^{(3,m)}$ are the first and second and the $2m - 1$ -th and $2m$ -th.